SVHSER 5243

Hamilton Standard Engineering Report

FINAL REPORT – LITHIUM PEROXIDE TEST PROGRAM
CONTRACT NO. NAS 9–8159
NASA MANNED SPACECRAFT CENTER

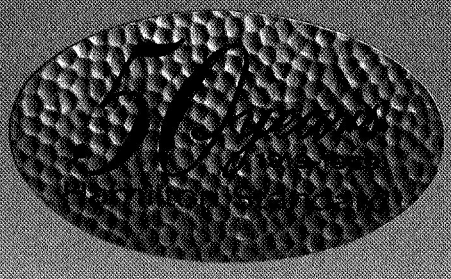

Hamilton Standard
DIVISION OF UNITED AIRCRAFT CORPORATION
WINDSOR LOCKS, CONNECTICUT 06096 • U.S.A.

NASA CR 92490

Hamilton Standard DIVISION OF UNITED AIRCRAFT CORPORATION

SVHSER 5243

HAMILTON STANDARD ENGINEERING REPORT
SVHSER 5243

FINAL REPORT
LITHIUM PEROXIDE TEST PROGRAM

CONTRACT NO. NAS 9-8159
NASA MANNED SPACECRAFT CENTER

Prepared by: R.A. Baum Jr. Date: 1-3-69
R.A. Baum Jr, Analytical Engineer

T.E. Fitzsimmons Date: 1-3-69
T.E. Fitzsimmons, Senior Analytical Engineer

K.J. Dresser Date: 3 Jan 69
K.J. Dresser, Senior Analytical Engineer

Approved by: J.S. Lovell Date: 1/6/69
J.S. Lovell, Chief, Advanced Engineering

K.L. Hower Date: 1/6/69
K.L. Hower, Manager, Special Programs

Number of Pages: 122

TABLE OF CONTENTS

LIST OF FIGURES

LIST OF FIGURES (Continued)

LIST OF FIGURES (Continued)

LIST OF TABLES

1.0 SUMMARY

The test results have shown that a carbon dioxide control and oxygen supply system utilizing lithium peroxide offers both a suit-mounted, and vehicle weight and volume advantage over other systems for an advanced portable life support system. This is shown in Figures 5-26 through 5-29 where a weight and volume comparison of this system is made with the lithium hydroxide/oxygen system. For a 4 hour mission at an average metabolic rate of 2000 Btu/hr, the lithium peroxide/oxygen system is 80 in^3 smaller and 4.3 lb. lighter. As the number of missions increases the weight and volume savings of the lithium peroxide/oxygen system becomes more significant.

The overall objective of this program was to experimentally evaluate the use of lithium peroxide to control carbon dioxide and supply oxygen for an advanced portable life support system.

During this test program, a total of 54 tests were completed. These tests were conducted to generate system design data, and to evaluate the effect upon lithium peroxide performance of variations in chemical bulk density, catalyst addition, bed temperature, bed geometry, and quantity of lithium peroxide.

Lithium peroxide in the form of low and high bulk density granules, both catalyzed with 2% nickel sulfate (to promote the release of oxygen) and uncatalyzed, was investigated during the program. The catalyzed, low bulk density material has shown the best performance. This material has demonstrated a very slow breakthrough characteristic; durations greater than two hours have been observed for the outlet partial pressure of carbon dioxide to increase from 0.5 to 4.0 mmHg.

The most critical operating parameter has been found to be the temperature of the lithium peroxide bed. Due to the high level of carbon dioxide and water vapor fed to the canister, temperatures in excess of 600°F have been measured. It has been found that high bed temperatures deter the carbon dioxide removal performance, but enhance the oxygen evolution performance due to thermal decomposition of the lithium peroxide.

2.0 INTRODUCTION

Extensive studies have been undertaken with the goal of defining the optimum concept for the next generation portable life support system to be used for space extravehicular activities. Investigation of present systems quickly reveals that the primary area for improvement lies in the expendables. "Improvement" is defined as a reduction in the suit-mounted volume, the vehicle launch weight penalty, and rechargeability optimization. In the Apollo Portable Life Support System (PLSS), for example, the expendables are made up of the oxygen supply, lithium hydroxide, water (utilized as the heat sink for sublimation to the space vacuum), and the battery power supply. Of these four expendables, the oxygen supply and carbon dioxide control systems represent a large percentage of the system volume and weight penalties. More compact and lightweight techniques of providing carbon dioxide control and oxygen supply represent an effective way to "improve" a portable life support system.

For several years, attempts have been made to accomplish the dual function of carbon dioxide control and oxygen supply within one system. This can be accomplished by developing a system which employs a superoxide, peroxide, or ozonide of potassium, sodium, or lithium. All of these chemical compounds have the capability of absorbing carbon dioxide while simultaneously releasing oxygen. Analytical studies and preliminary testing indicate that lithium peroxide (Li_2O_2) offers an excellent potential for reducing the system volume and weight while providing the dual function of carbon dioxide control and oxygen supply. Lithium peroxide has the theoretical capacity to remove 0.96 lb. of carbon dioxide per pound, while simultaneously releasing 0.35 lb. of oxygen per pound. This can occur through a variety of chemical reactions, as indicated by the following reactions.

In the presence of moisture, lithium peroxide can react directly with carbon dioxide to form lithium carbonate and release oxygen. The letters in parenthesis represent the solid, liquid, vapor and gaseous phases.

$$Li_2O_2(s) + CO_2(g) \xrightarrow{H_2O(v)} Li_2\ CO_3(s) + 1/2\ O_2(g)$$

Also, the lithium peroxide can react directly with the water vapor to form lithium hydroxide and hydrogen peroxide.

$$Li_2\ O_2(s) + 2H_2O(v) \longrightarrow 2LiOH(s) + H_2O_2(\ell)$$

and the water vapor can further react with the lithium hydroxide to form a hydrate.

$$LiOH(s) + H_2O(v) \longrightarrow LiOH \cdot H_2O(s)$$

Carbon dioxide can then be absorbed through either of the following reactions:

2.0 (Continued)

$$2LiOH(s) + CO_2(g) \longrightarrow Li_2CO_3(s) + H_2O(\ell)$$

or

$$2LiOH \cdot H_2O(s) + CO_2(g) \longrightarrow Li_2CO_3(s) + 2H_2O(\ell)$$

And oxygen is released by decomposition of the hydrogen peroxide.

$$H_2O_2(\ell) \longrightarrow H_2O(v) + 1/2\ O_2(g)$$

As pointed out by Markowitz in Reference 1, a catalyst is required to achieve the theoretical yield of oxygen by insuring decomposition of all of the hydrogen peroxide.

As a result of previous work, this contract was awarded to perform a test program to further evaluate the capabilities of lithium peroxide. The objective of this program was to generate data to permit the design of a lithium peroxide system which provides both carbon dioxide control and oxygen supply for a portable life support system having the following design conditions.

Mission duration	4 hours
Average metabolic rate	2000 Btu/hr
System pressure	3.7 psia
System flow rate	7 cfm (pure O_2)
System inlet temperature	85°F
Average inlet dew point	70°F

During the course of the program, the following variables were investigated to evaluate their effect upon lithium peroxide performance.

1. Chemical bulk density
2. Catalyst addition
3. Lithium peroxide
4. Lithium peroxide
5. Weight of lithium peroxide
6. Inlet dew point

This report will discuss the results of these tests (more than 50 tests total), the feasibility of a lithium peroxide system as sized for future mission requirements (AAP, LEO, etc.), and comparison of this system will be made with others which provide the function of carbon dioxide control and oxygen supply for a portable life support system.

3.0 PROGRAM DEFINITION

This section defines the program objectives, test objectives, program description, test conditions, test facility, test hardware, planned test sequence, and the test results.

3.1 Program Objectives

The overall objective was to evaluate the potential of lithium peroxide to remove carbon dioxide and supply oxygen for an advanced portable life support system. The specific objectives were:

- to advance the state-of-the-art in life support system technology
- to develop specific components and subsystems for incorporation into an advanced portable life support system.

3.2 Test Objectives

The following objectives were established for the test program:

- to establish the best chemical form of lithium peroxide granules to be utilized to control carbon dioxide and supply oxygen for a portable life support system
- to establish the optimum bed temperature for the design of the lithium peroxide canister
- to establish the optimum geometry for the design of the lithium peroxide canister
- to generate data to quantify all system level penalties accrued by the lithium peroxide subsystem (e.g., to establish the cooling requirement due to the heat of reaction of the chemical)
- to generate data to permit the design of a prototype lithium peroxide canister which will maintain the helmet inlet partial pressure of carbon dioxide below 0.5 mm Hg and provide the metabolic and leakage oxygen requirements for 4 hours at an average metabolic rate of 2000 Btu/hr. (2.0 mm Hg partial pressure of carbon dioxide is allowed during emergency operation at 3500 Btu/hr.).

3.3 Program Description

The program was intended to evaluate the major variables which effect the performance of lithium peroxide. Five major variables were identified and investigated during the

3.3 (Continued)

course of the program. These were:

1. Chemical bulk density
2. Catalyst addition
3. Bed temperature
4. Bed geometry
5. Weight of lithium peroxide

The effect of the variables was investigated via the following sequence of test evaluation series.

Chemical Form Evaluation

Granular lithium peroxide was procured in two distinct bulk densities, both with and without catalyst impregnation. Both were subjected to performance testing at a constant metabolic rate of 2000 Btu/hr for 4 hours. The initial portion of this test series was conducted under scale model test conditions (1/3 size lithium peroxide beds) to minimize the quantity of material needed for an initial evaluation. The two leading material forms were then subjected to a series of full size tests to verify their performance under scale model conditions. This series, which consisted of a total of 18 tests, identified the best form of chemical and was used for the remainder of the testing.

Bed Temperature/Geometry Evaluation

For this test series, canisters with internal, water cooling coils were used to control bed temperature. Three geometric configurations were subjected to tests at a constant metabolic rate of 2000 Btu/hr for 4 hours. The face areas of these canisters (defined in Section 3.6) was such that canister 2 had twice the face area of canister 1, and canister 3 was 3 times the face area of canister 1. This test series, consisting of 13 tests, identified the best canister configuration and the desired range of bed temperatures.

Chemical Weight Evaluation

Varied chemical weights between 3 and 8 pounds were subjected to tests according to the variable metabolic profile (defined in Section 3.4) for 4 hours. This metabolic profile is slightly greater than a 2000 Btu/hr average profile. These tests were conducted using the optimum canister geometry and the range of bed temperature which had previously been shown to provide the best performance. This evaluation consisted of 12 tests.

Off-Design Performance Evaluation

An off-design performance evaluation, consisting of the 9 tests defined in Section 3.7, was planned. However, only two were conducted prior to a problem area being uncovered. At this point, the program was redirected, utilizing the remaining tests to investigate the

3.3 (Continued)

problem. This problem is discussed further in Section 4.0. A total of 11 tests, including the 2 off-design tests, were conducted to conclude the test program.

3.4 Test Conditions

This section defines the test conditions employed for both the constant and variable metabolic profiles employed during the test program.

Constant Metabolic Profile	Bed Size	
	1/3 Scale	Full Scale
Total Gas Flow Rate (lb/hr)	2.8 ± 0.1	8.4 ± 0.2
Inlet Gas Temperature (°F)	85 ± 2	85 ± 2
Inlet Pressure (3.7 psia nom.)	191 ± 2 mm Hg	191 ± 2
Inlet Dew Point (°F)	70 ± 1	70 ± 1
CO_2 Flow Rate (lb/hr)	0.13 ± 0.001	0.39 ± 0.02

Variable Metabolic Profile

Metabolic Expenditure (Btu/hr)	Mission Duration (min.)
2000	45
2500	30
500	15
2000	45
2500	30
500	15
2500	60

For the variable profile tests, the total flow rate, inlet temperature, and pressure are the same as for the constant metabolic profile. The carbon dioxide flow rate and the dew point are as defined below:

		Bed Size	
		1/3 Scale	Full Scale
Metabolic Rate (Btu/hr)	Dew Point (°F)	CO_2 Flow Rate (lb/hr)	
500	55.	0.033 ± 0.005	0.098 ± 0.005
2000	70.	0.13 ± 0.01	0.39 ± 0.02
2500	80.	0.163 ± 0.01	0.488 ± 0.02

3.5 Test Facility

The testing was performed using the Li_2O_2 test rig (Rig 21) which is shown schematically in Figure 3-1 and is depicted in Figures 3-2 and 3-3. A close-up of a canister mounted in the rig is shown in Figure 3-4.

This test facility is a closed loop system having a total volume of about 1.5 ft^3 to simulate the internal volume of a space suit and portable life support system. The metabolic processes of the crewman are simulated by feeding carbon dioxide and water vapor into the system at the desired metabolic level and simultaneously bleeding gas from the system to account for the crewmen's metabolic oxygen consumption. All gas conditions into the lithium peroxide canister are identical to those which would be the effluent from a space suit for the metabolic conditions being tested. Included in the rig instrumentation are the following:

	Instrument	Accuracy
1.	O_2 Bleed Flowmeter	± 2% F.S.
2.	CO_2 Make-up Flowmeter	± 2% F.S.
3.	Diluent Make-up Flowmeter (N_2, He)	± 2% F.S.
4.	Loop Sample Flowmeter	± 2% F.S.
5.	Loop Sample Flowmeter	± 2% F.S.
6.	Loop Flow Flowmeter	± 2% F.S.
7.	Pressure Gage (Delta P_{1-2})	± 5 mm Hg
8.	Pressure Gage (P_3)	± 0.15 psi
9.	Pressure Gage (P_4)	± 0.15 psi
10.	Pressure Gage (P_6)	± 0.15 psi
11.	Pressure Gage (P_7)	± 0.15 psi
12.	Pressure Gage (P_8)	± 0.15 psi
13.	Pressure Gage (P_9)	± 0.15 psi
14.	Pressure Gage (P_{10})	± 0.15 psi
15.	Pressure Gage (P_{11})	± 0.15 psi
16.	Temperature Indicator	± 1°F
17.	Thermocouples (All)	± 1°F
18.	Dewpointer (Cambridge)	± 1°F
19.	CO_2 Analyzer (MSA Lira)	± 5%
20.	CO_2 Analyzer (MSA Lira)	± 5%
21.	Beckman O_2 Analyzer	± 0.5%
22.	Beckman O_2 Analyzer	± 0.5%
23.	Scale	± 1/16 lb.
24.	Speedmax Temperature Indicator	± 2°F
25.	Cooling Water Flowmeter	± 2% F.S.

3.6 Test Hardware

A total of 5 test canisters were used during the program. They are shown in Figures

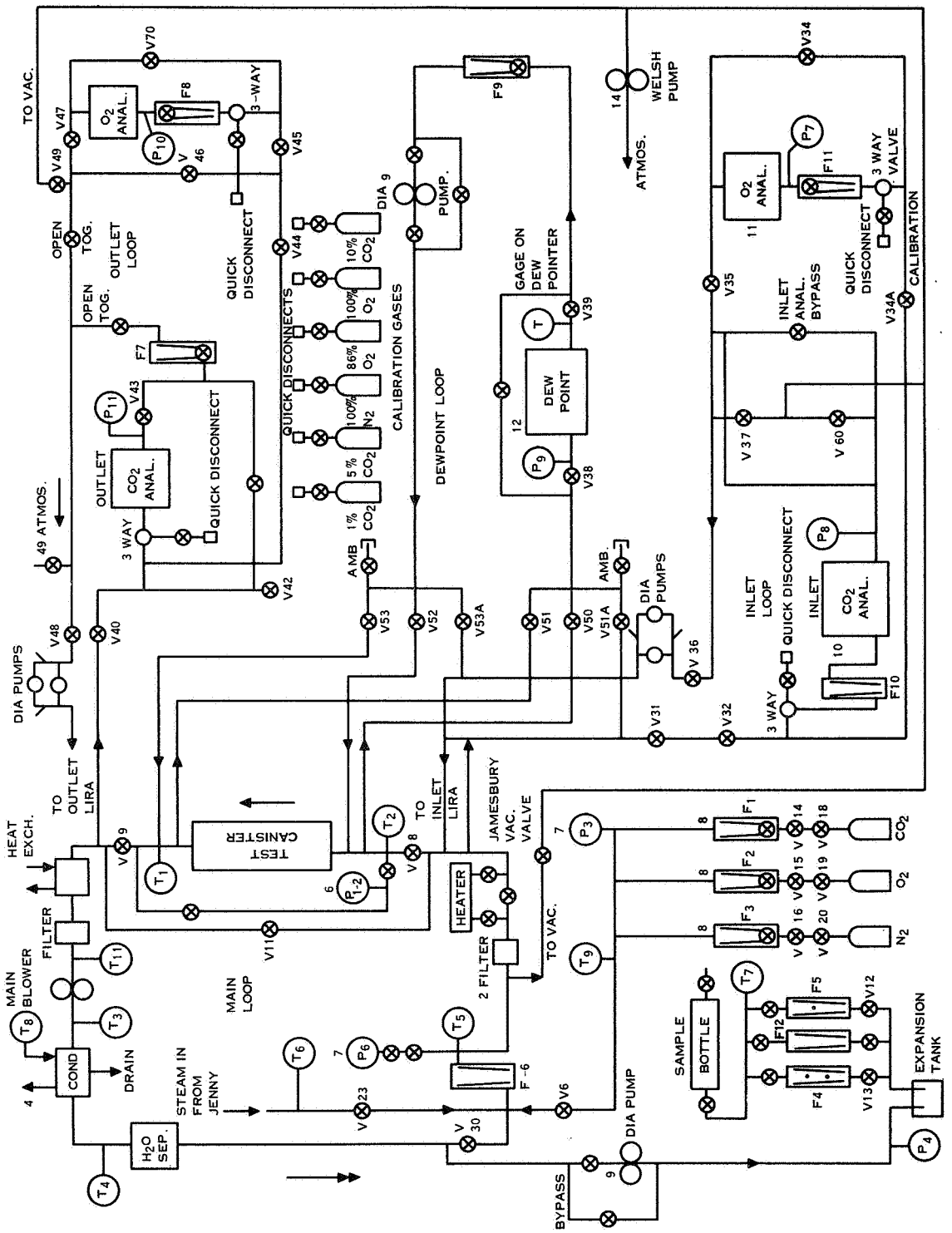

Figure 3-1. Lithium Peroxide Test Rig Schematic

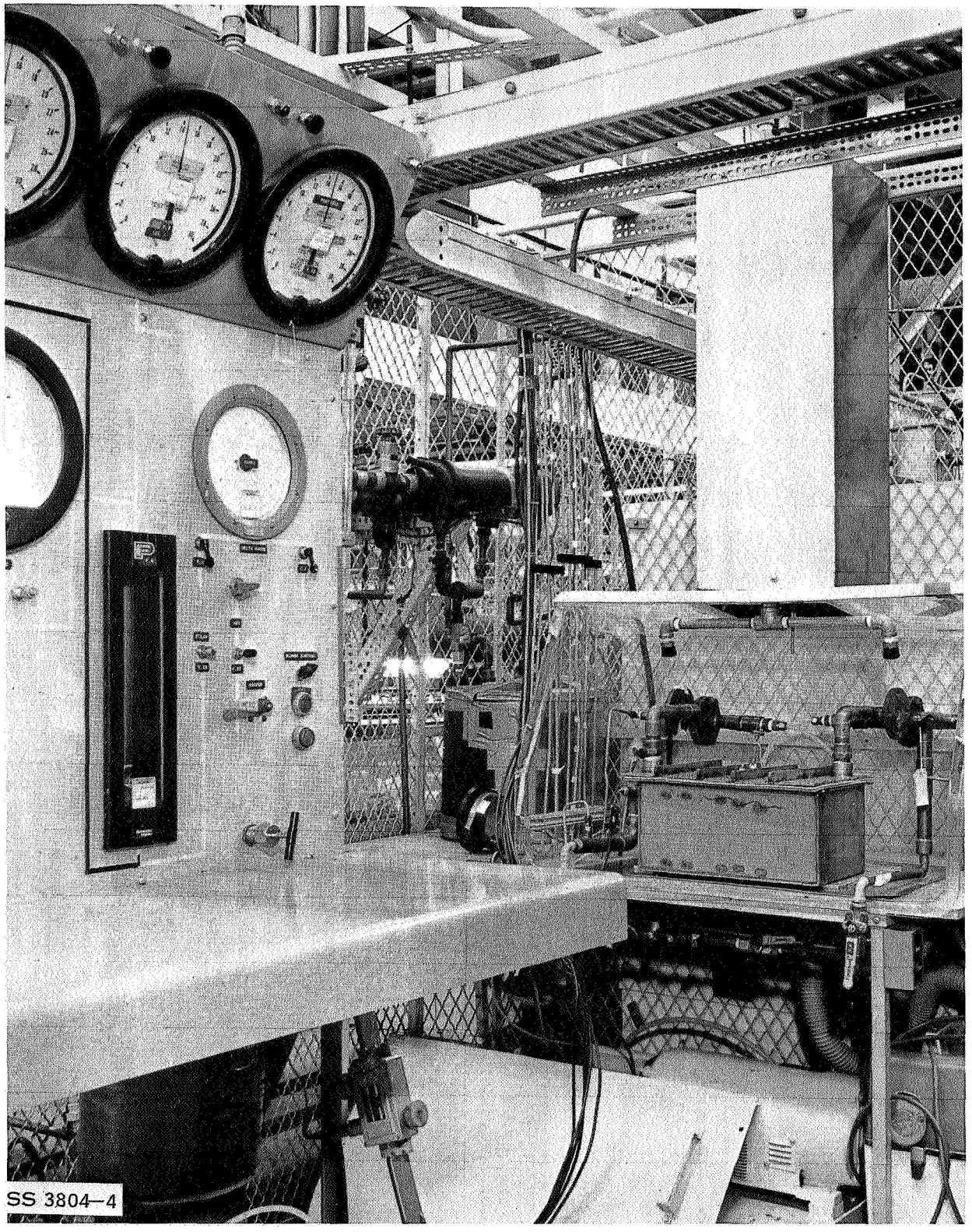

Figure 3-2. SS 3804-4 View of Flow Meter Panel and Canister in Rig.

(Same as picture in previous report)

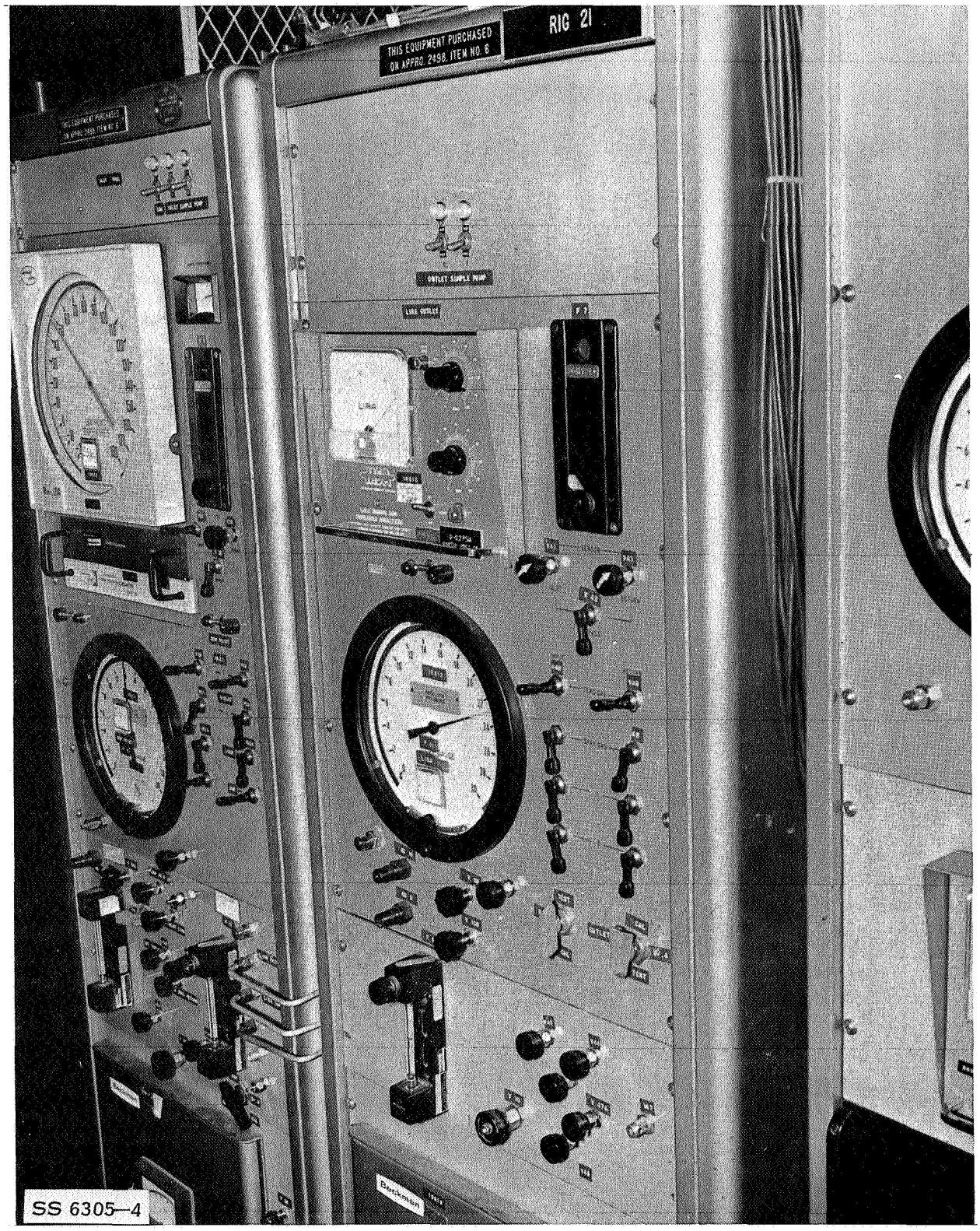

Figure 3-3. SS 6305-4 View of Inlet and Outlet Instrument Panels

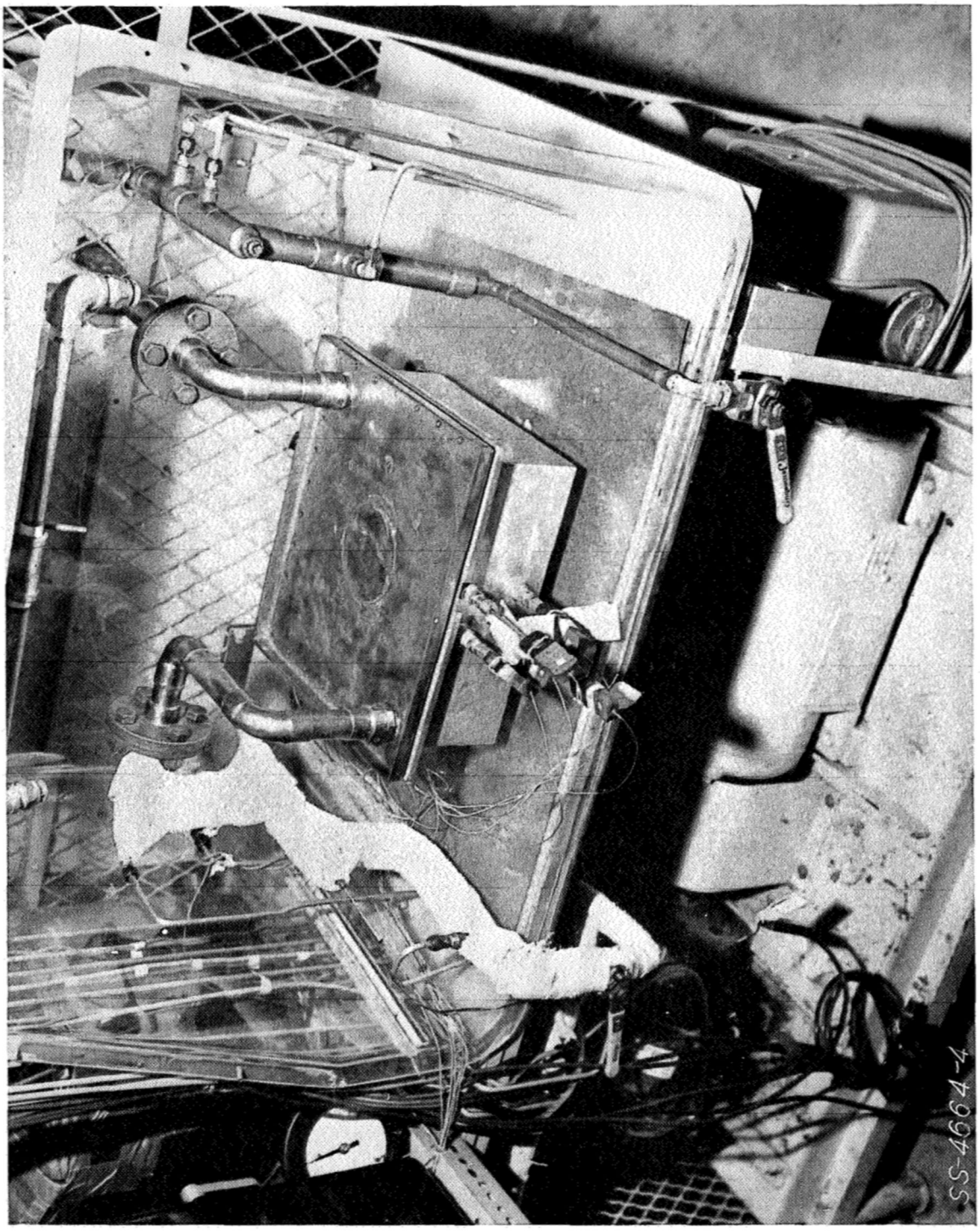

Figure 3-4. Li_2O_2 Test Canister Mounted In The Test Rig.

3.6 (Continued)

3-5 through 3-11. All were fabricated from stainless steel and employed internal cooling coils made of copper tubing. The dimensions of these canisters are defined as follows:

Scale Model Testing (1/3 Scale)

Diameter 4.5 in.; maximum length - 6.5 in.; flow area - 15.7 in^2

Full Scale Testing

Canister No. 1

Face - 3.5 in x 7.5 in; maximum length - 8 in.; flow area - 26.3 in^2

Canister No. 2

Face - 4.7 in x 9.9 in; maximum length - 8 in.; flow area - 46.5 in^2

Canister No. 3

Face - 6.6 in x 14.0 in; maximum length - 4 in; flow area - 92.5 in^2

Canister No. 4

Face - 6.6 in x 14.0 in; maximum length - 5.8 in; flow area - 92.5 in^2

3.7 Planned Test Sequence

This section defines the test sequence as originally planned.

The following designations are defined to simplify the description of each test.

a. Baseline Conditions - The metabolic profile for the test is constant at 2000 Btu/hr (conditions per Section 3.4)

b. Variable Profile - The variable metabolic profile is defined per Section 3.4

c. Canisters 1, 2, and 3 (defined in Section 3.6) are designated as C1, C2, and C3, respectively, for full scale tests.

d. BT - Lithium peroxide bed temperature

e. Subscripts a, b, c, etc. are used to define repetitive testing to the same test description

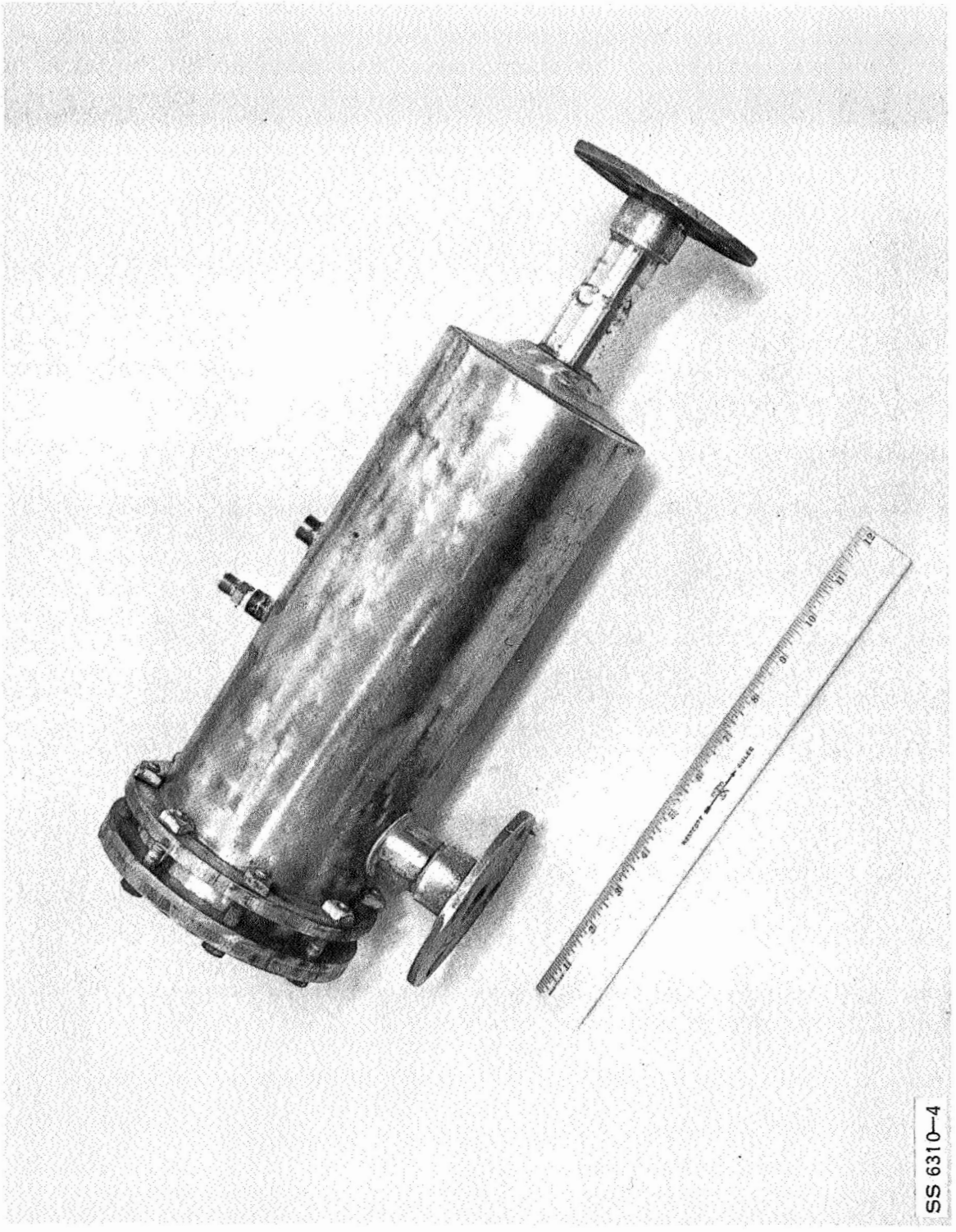

Figure 3-5. SS 6310-4 Cylindrical Canister

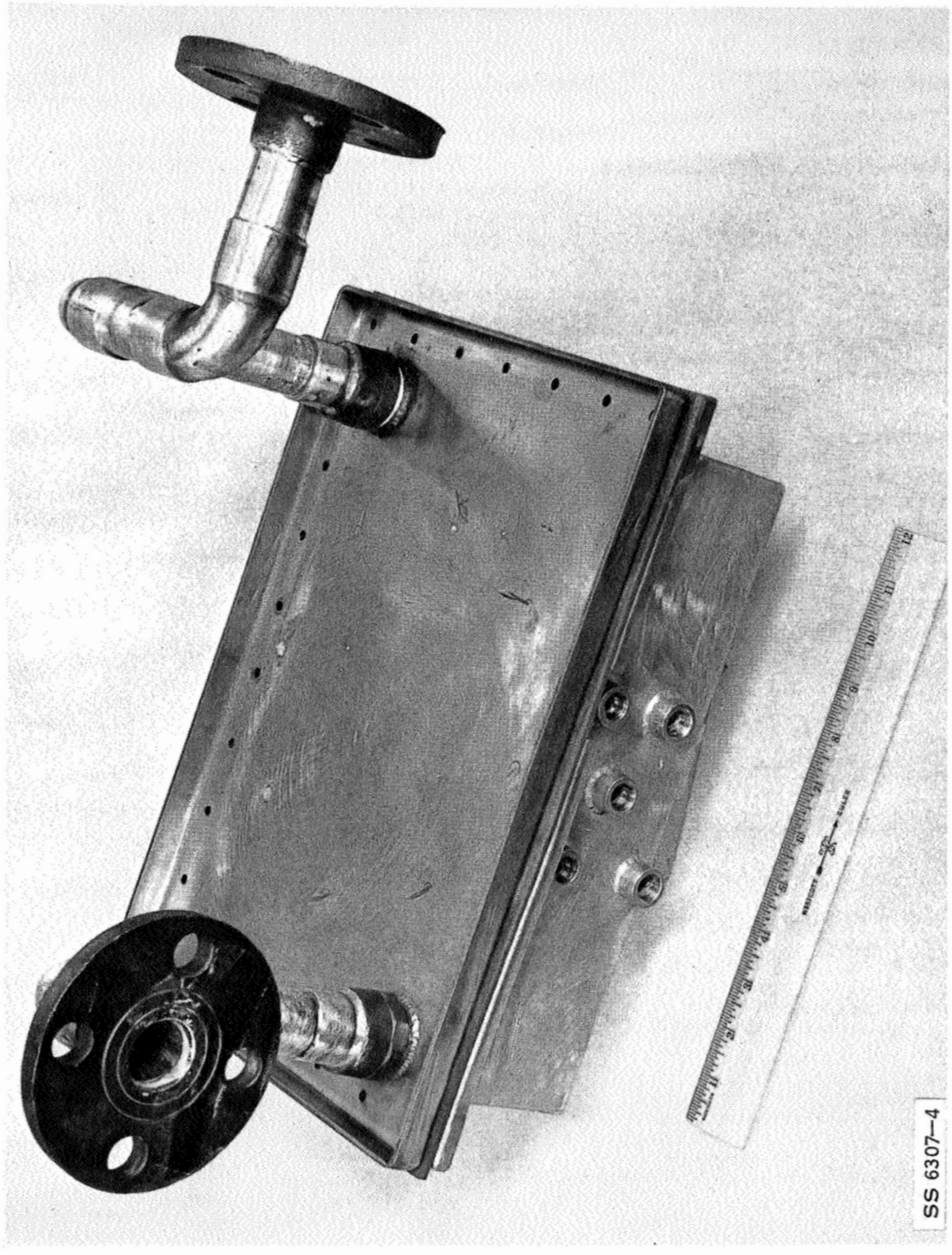

Figure 3-6. SS 6307-4 Canister #1

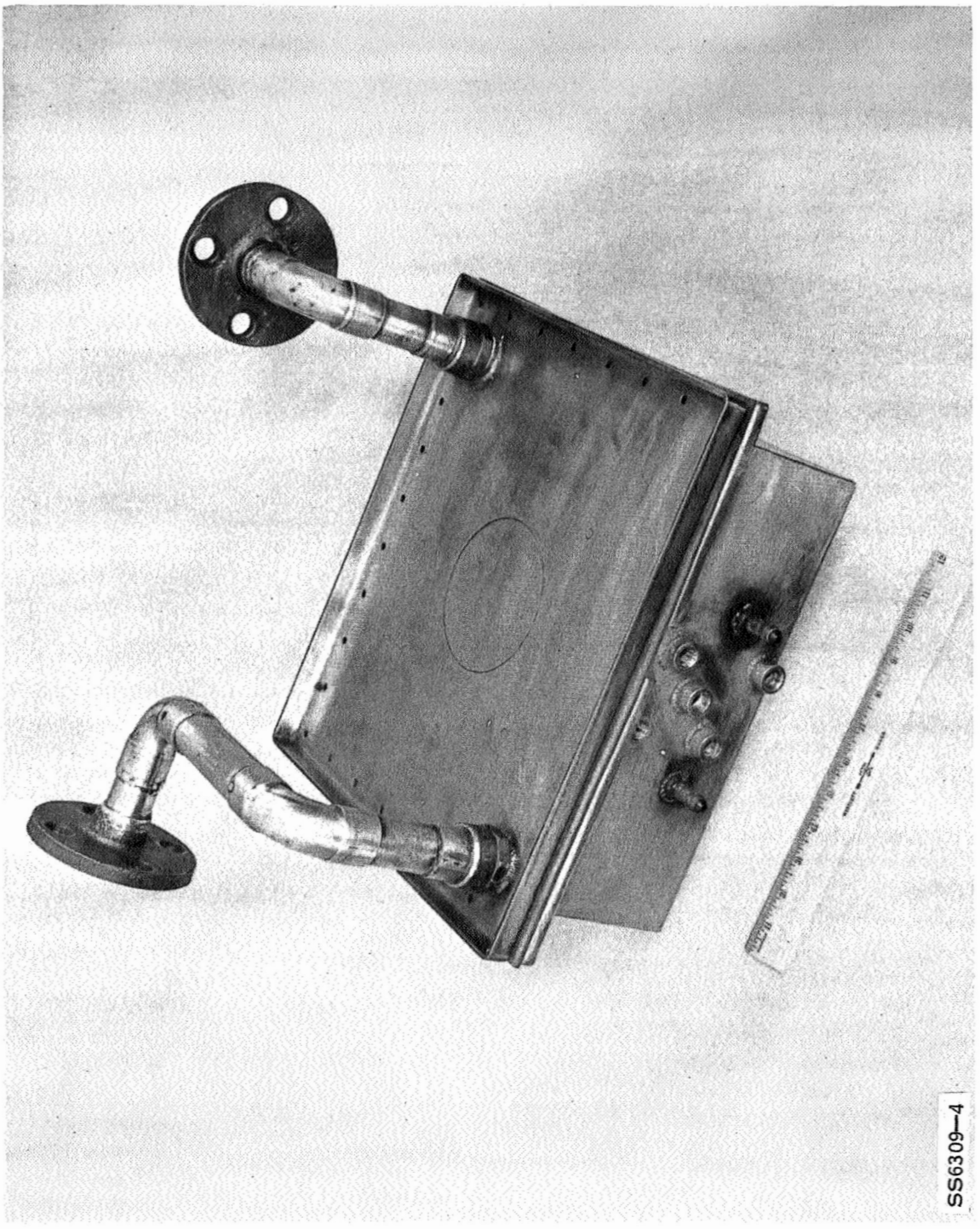

Figure 3-7. SS 6309-4 Canister #2

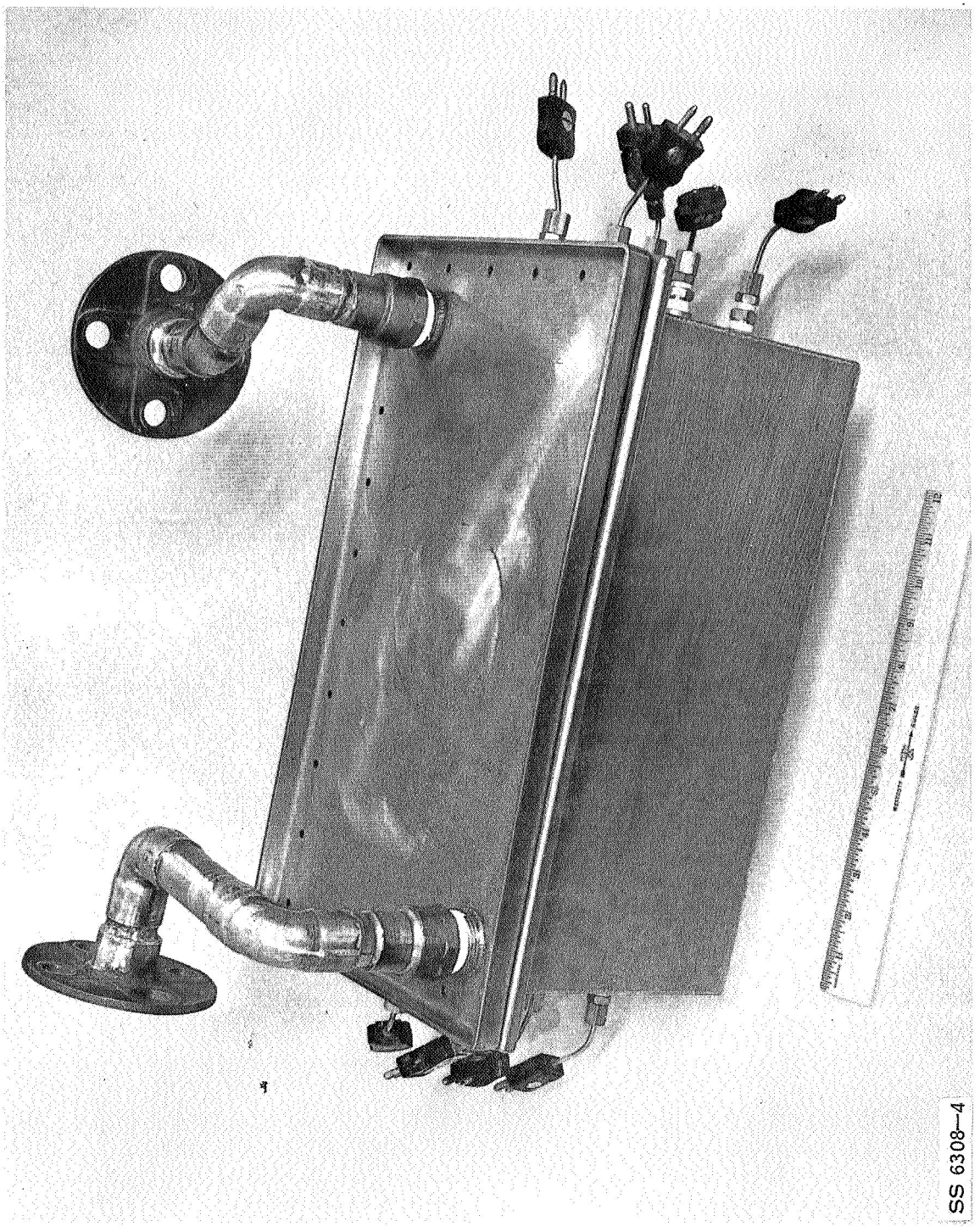

Figure 3-8. SS 6308-4 Canister #3

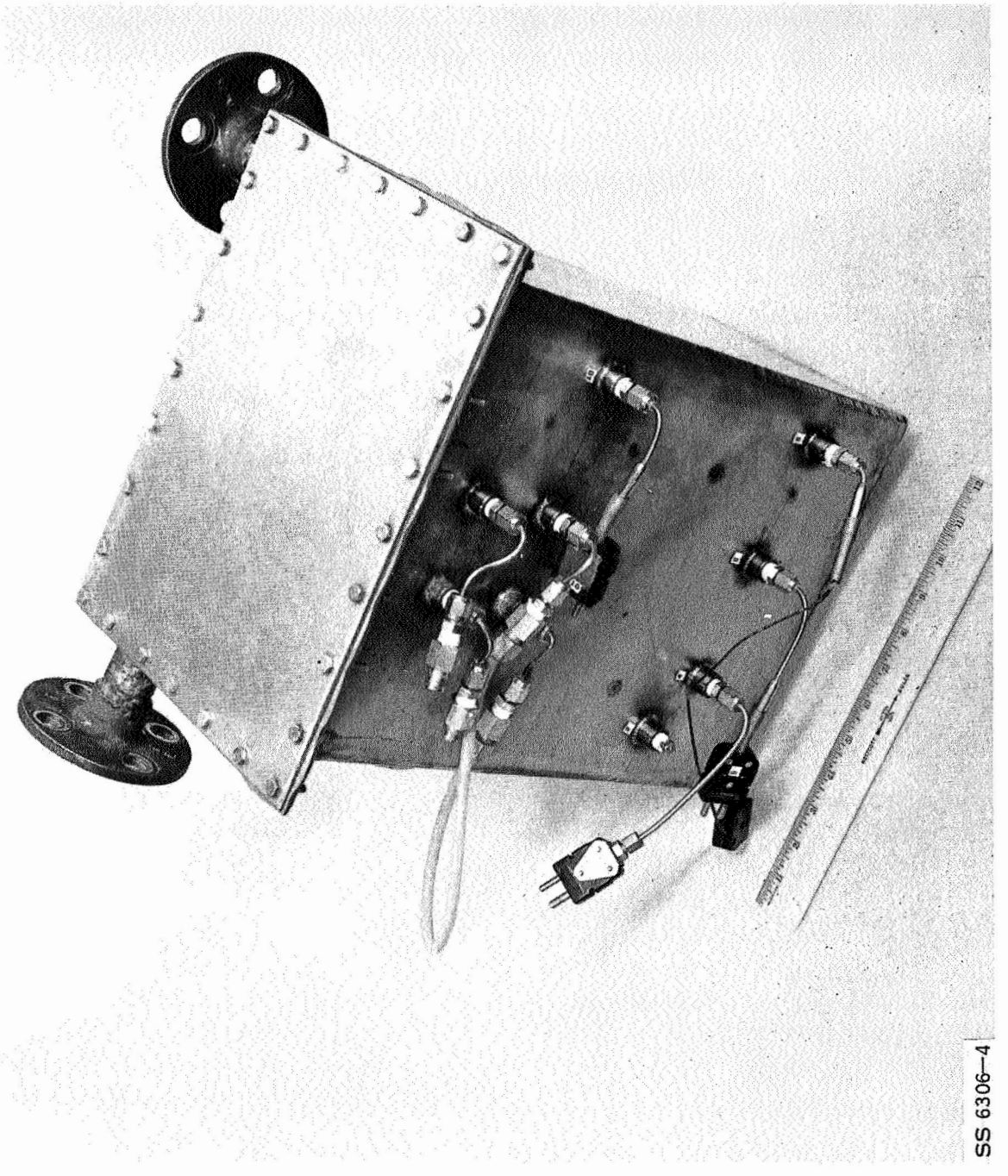

Figure 3-9. SS 6306-4 Canister #4

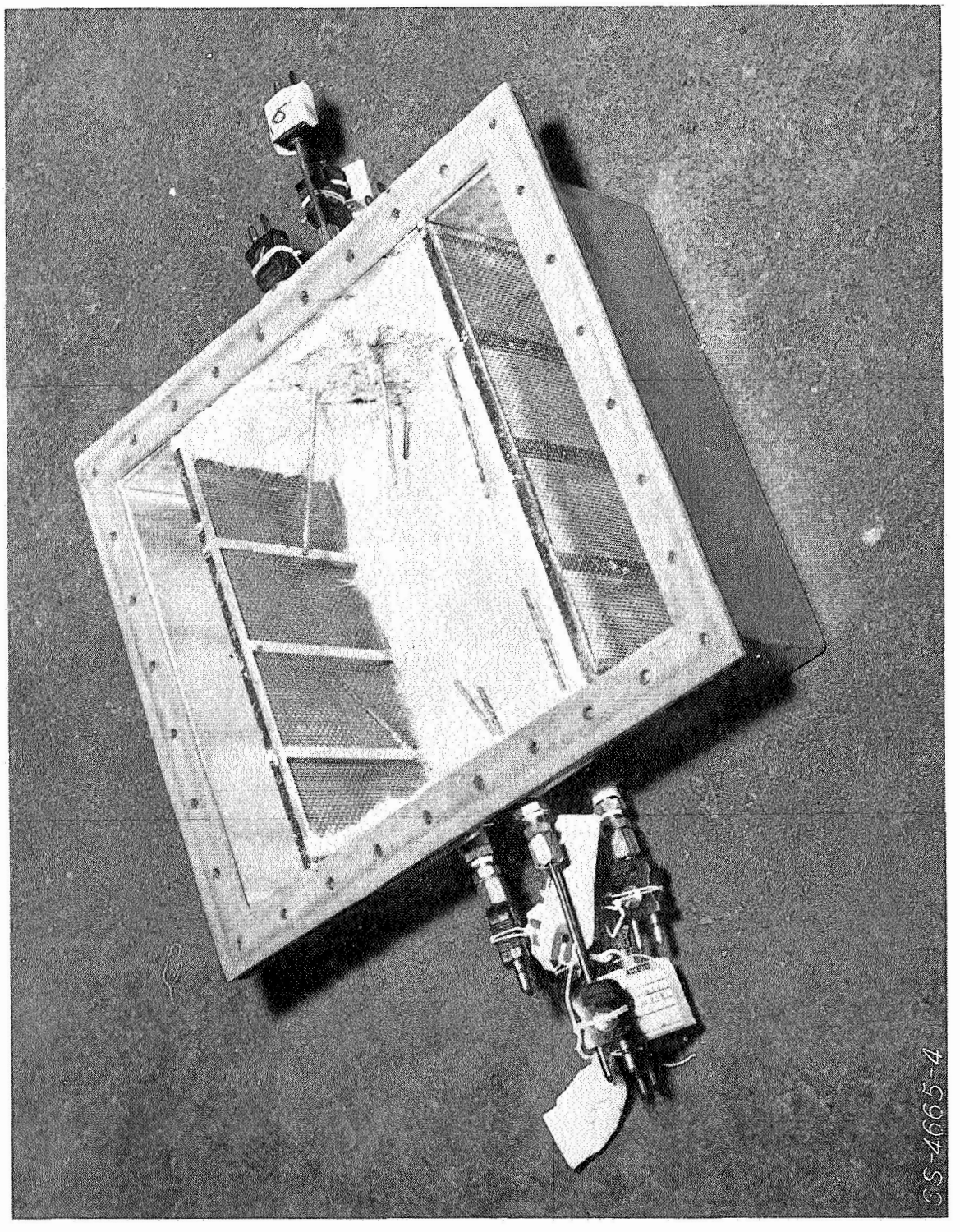

Figure 3-10. Typical View Of An Unloaded Canister.

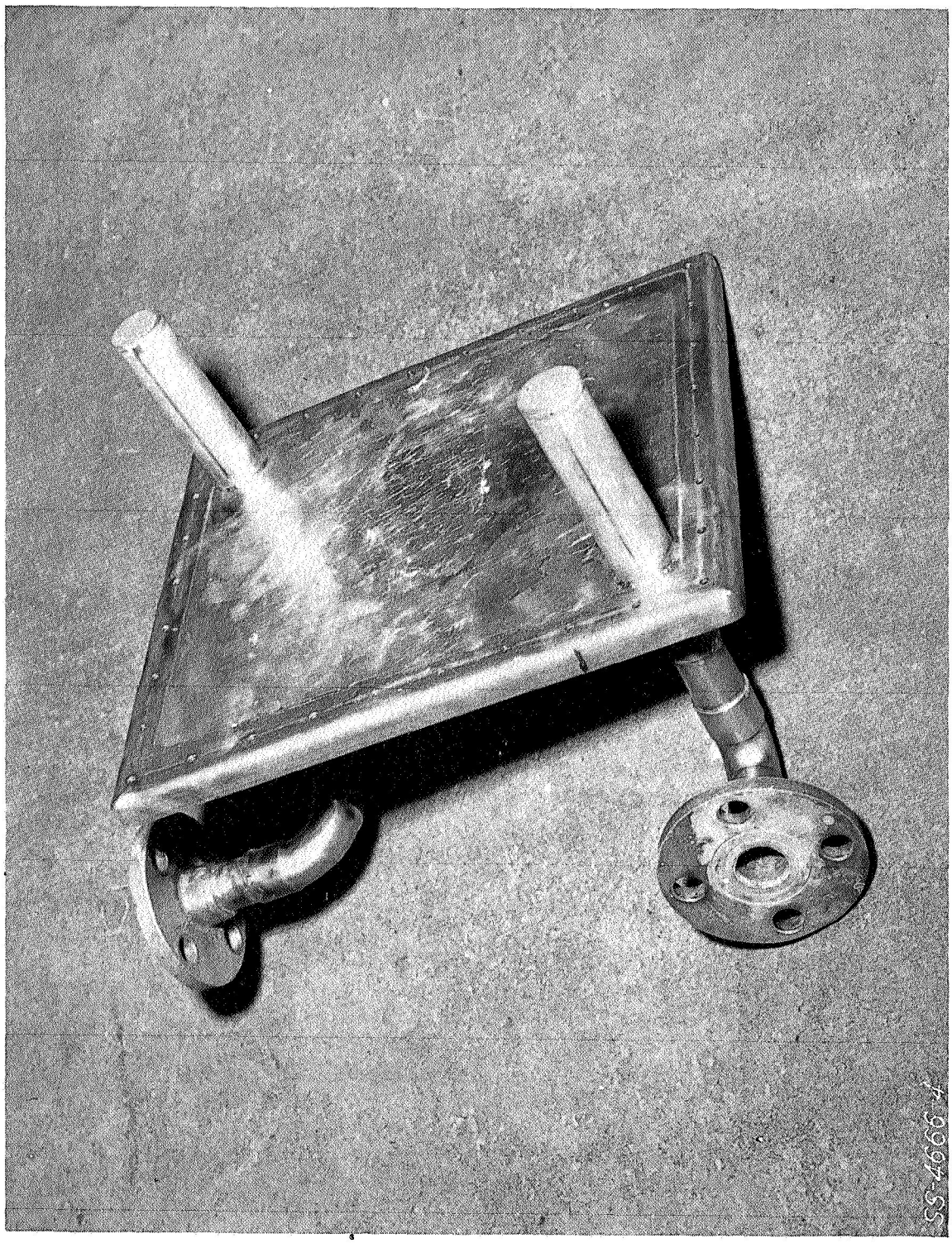

Figure 3-11. Typical Canister Lid

3.7 (Continued)

f. TBD - To be determined after more information is available

Chemical Form Evaluation

Test No.	Scale	No. of Tests	Test Description
MSC-1	1/3	1	Baseline conditions - low bulk density; Chemical - without catalyst - BT 550°F.
MSC-2	1/3	1	Repeat MSC-1, except high bulk density chemical.
MSC-3	1/3	1	Baseline conditions - low bulk density; Chemical - with catalyst BT 550°F
MSC-4	1/3	1	Repeat MSC-3, except high bulk density chemical.
MSC-5	1/3	1	Repeat MSC-1, except BT 350°F.
MSC-6	1/3	1	Repeat MSC-2, except BT 350°F.
MSC-7	1/3	1	Repeat MSC-3, except BT 350°F.
MSC-8	1/3	1	Repeat MSC-4, except BT 350°F.
MSC-9	Full	2	Baseline Conditions - Chemical form having best performance in previous scale model tests - BT for that performance.
MSC-10	Full	2	Same as MSC-9, except use second best chemical form.
		12	

The best chemical form has been established after series, and used for all subsequent testing.

Bed Temperature/Geometry Evaluation

Test No.	Scale	No. of Tests	Test Description
MSC-11	Full	1	Baseline Conditions - C1 - BT 250-300°F.
MSC-12	Full	1	Same as MSC-11, except BT 425-475°F.
MSC-13	Full		Same as MSC-11, except BT 550-600°F.
MSC-14	Full	1	Repeat MSC-11 with C3.
MSC-15	Full	1	Repeat MSC-12 with C3.
MSC-16	Full	1	Repeat MSC-13 with C3.
		6	

NOTE: If no significant difference in performance is observed between tests with canisters C1 and C3, the following three tests will not be performed.

3.7 (Continued)

Test No.	Scale	No. of Tests	Test Description
MSC-17	Full	1	Repeat MSC-11 with C2.
MSC-18	Full	1	Repeat MSC-12 with C2.
MSC-19	Full	1	Repeat MSC-13 with C2.
MSC-20	Full	2	Baseline Conditions - Repeat test having best performance.
MSC-21	Full	2	Baseline Conditions - Repeat test having second best performance.
		7	

The optimum bed temperature and canister cross-sectional area has been established and will be used for all subsequent testing.

Chemical Weight Evaluation

Test No.	Scale	No. of Tests	Test Description
MSC-22	Full	1	Variable profile - TBD lb. of chemical
MSC-23	Full	1	Variable profile - (TBD + 1) lb. of chemical
MSC-24	Full	1	Variable profile - (TBD + 2) lb. of chemical
MSC-25	Full	2	Variable profile - (TBD + x) lb. of chemical
MSC-26	Full	2	Variable profile - (TBD + y) lb. of chemical
		7	

The weight of chemical required to meet the program objectives has been established and will be used for the off-design test sequence.

Off-Design Evaluation

Test No.	Scale	No. of Tests	Test Description
MSC-27	Full	1	Baseline Conditions - no water vapor flow rate.
MSC-28	Full	1	Baseline Conditions - water vapor dew point 50°F.
MSC-29	Full	1	Baseline Conditions - water vapor dew point 85°F.
MSC-30	Full	1	Baseline Conditions - no CO_2 flow rate.
MSC-31	Full	1	Baseline Conditions, except CO_2 flow rate for 500 Btu/hr metabolic rate.
MSC-32	Full	1	Baseline Conditions, except CO_2 flow rate for 1000 Btu/hr metabolic rate.
MSC-33	Full	1	Baseline Conditions, except CO_2 flow rate for 3000 Btu/hr metabolic rate.

3.7 (Continued)

Test No.	Scale	No. of Tests	Test Description
MSC-34	Full	1	Variable profile, except total flow rate 5 cfm.
MSC-35	Full	1	Variable profile, except total flow rate 9 cfm.
		9	

3.8 Test Results

Data Reduction

Reduction of the test data was accomplished using the lithium peroxide data reduction computer program, H-137. This program, run on the UNIVAC 1108, performs the analytical reduction of the data. The performance results are provided in both tabular and graphical form as a function of time. The performance curves include the following for each test:

1. Li_2O_2 Canister Outlet CO_2 Partial Pressure vs. Time
2. Li_2O_2 Canister O_2 Generator Rate vs. Time
3. Li_2O_2 H_2O Removal Rate vs. Time
4. Total CO_2 Removed vs. Time
5. Total O_2 Generated vs. Time
6. CO_2 Utilization Efficiency vs. Time
7. O_2 Utilization Efficiency vs. Time
8. CO_2 Removal Efficiency vs. Time
9. CO_2 Removal Rate vs. Time
10. Li_2O_2 Canister Inlet Temperature vs. Time
11. Li_2O_2 Canister Outlet Temperature vs. Time
12. Li_2O_2 Canister Inlet Pressure vs. Time
13. Li_2O_2 Canister Inlet Flow Rate vs. Time
14. Li_2O_2 Canister Inlet H_2O Vapor Flow Rate vs. Time
15. Li_2O_2 Canister Inlet CO_2 Flow Rate vs. Time
16. Li_2O_2 Canister Inlet CO_2 Partial Pressure vs. Time
17. Li_2O_2 Canister Heat Removal Rate vs. Time
18. Average Li_2O_2 Bed Temperature vs. Time

Gas Sample Analysis

Periodic gas samples were taken from the test rig loop and stored for chemical analysis after the test was completed. These were analyzed for N_2, O_2, CO_2, CO, H_2O, and trace constituents using gas chromatography.

3.8 (Continued)

Li_2O_2 Chemical Analysis

Samples of the test beds were collected before and after testing and analyzed for chemical composition. The results of these chemical analyses were correlated with the measured test results to assure the validity of the performance results.

Section 4.0 presents the test data that was generated during the program.

4.0 TEST DATA PRESENTATION

This section presents the data for the 54 tests which were completed during this program. The data for carbon dioxide removal and oxygen generation performance are shown in Figures 4-1 through 4-54 for all of the tests. Figures 4-55 through 4-64 present the average bed temperature data for the full scale tests.

4.1 PERFORMANCE DATA

Table 4-1 is a tabulation of the major parameters for each test and the columns of this tabulation are defined as follows:

1. Test number
2. Canister number
3. Time in the test that the canister outlet partial pressure of carbon dioxide reached 0.5, 1.0, and 4.0 mmHg. (minutes)
4. Chemical weight (lb)
5. Average useable oxygen generation rate (lb/hr). This excludes all oxygen that was vented overboard during peak generation rates.
6. Test duration that the oxygen supply requirement (0.36 lb/hr) was exceeded (minutes)
7. Total quantity of useable oxygen produced during 4 hours, or at test termination if earlier (lb)
8. Total quantity of oxygen generated during 4 hours, or at test termination if earlier (lb)
9. Oxygen utilization efficiency at 4 hours, or at test termination if earlier (Percent of theoretical capacity - 0.35 lb. of O_2 per lb. of Li_2O_2)
10. Total quantity of carbon dioxide removed during 4 hours, or at test termination if earlier (lb)
11. Carbon dioxide utilization efficiency at 4 hours, or at test termination if earlier (Percent of theoretical capacity - 0.96 lb. of CO_2 per lb. of Li_2O_2)
12. Chemical type
13. Maximum bed temperature ($^\circ$F)

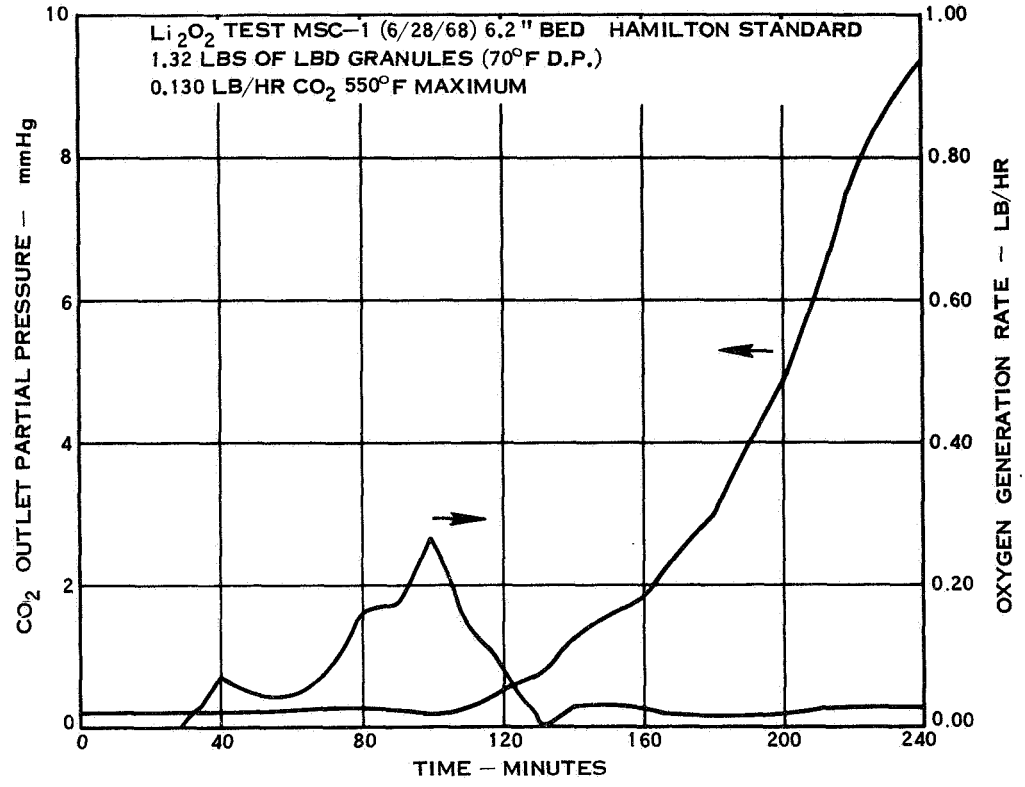

Figure 4-1. Lithium Peroxide Performance Data

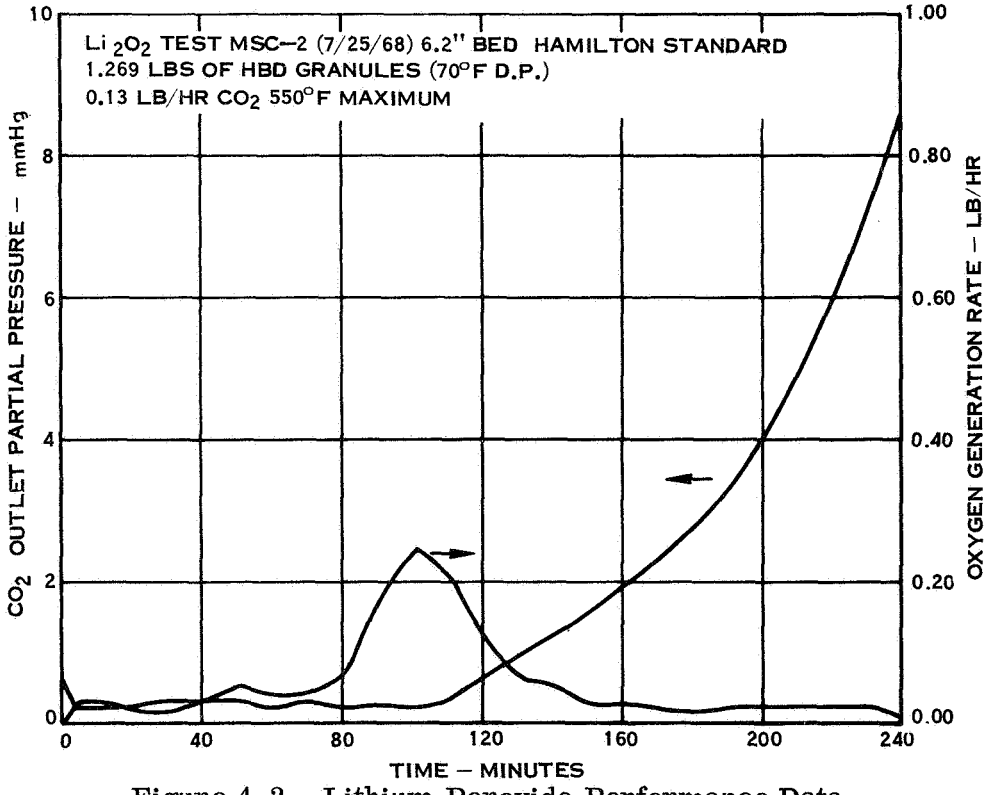

Figure 4-2. Lithium Peroxide Performance Data

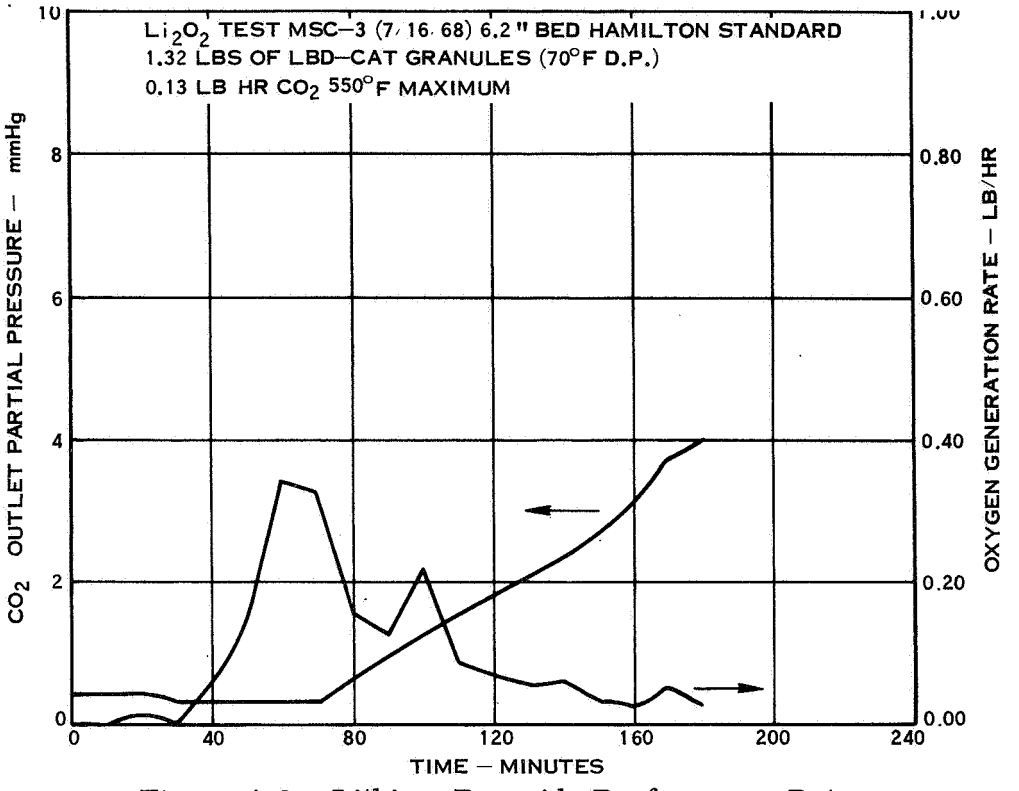

Figure 4-3. Lithium Peroxide Performance Data

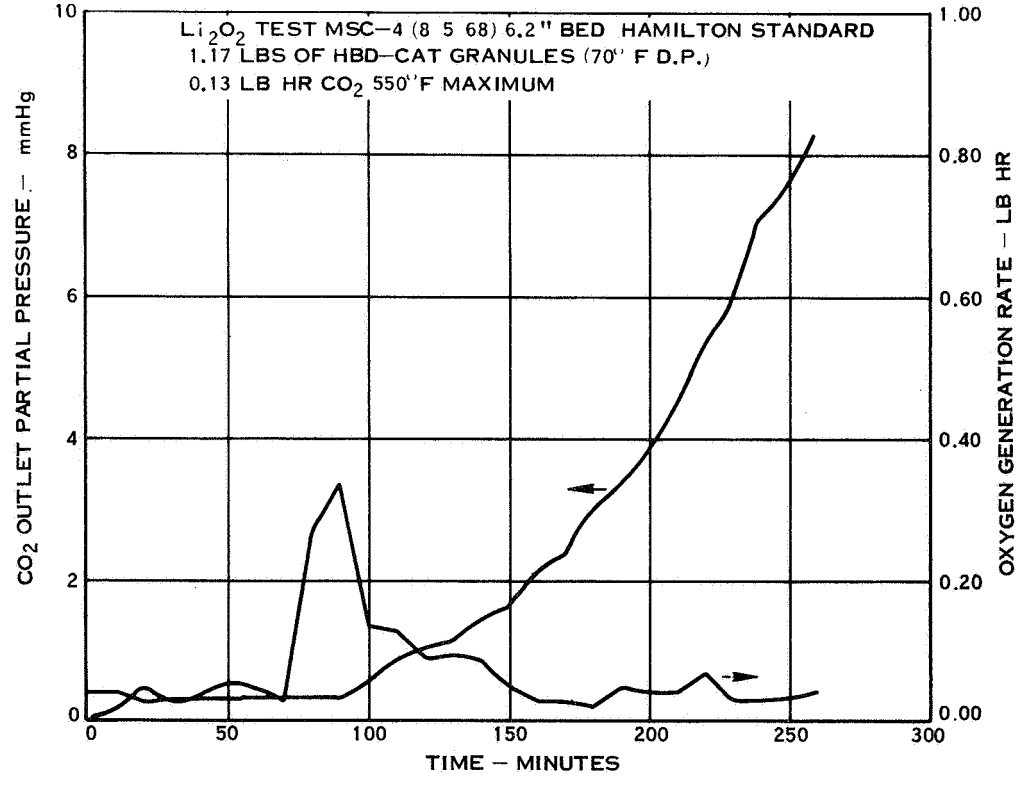

Figure 4-4. Lithium Peroxide Performance Data

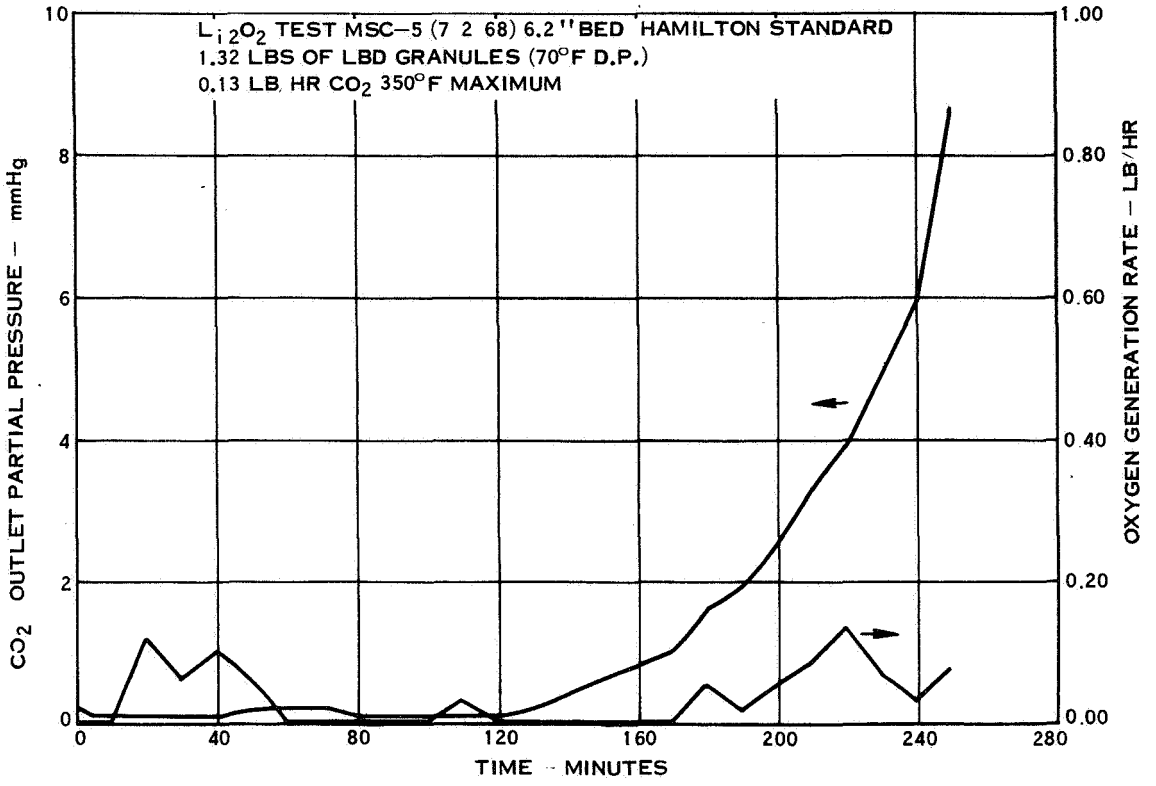

Figure 4-5. Lithium Peroxide Performance Data

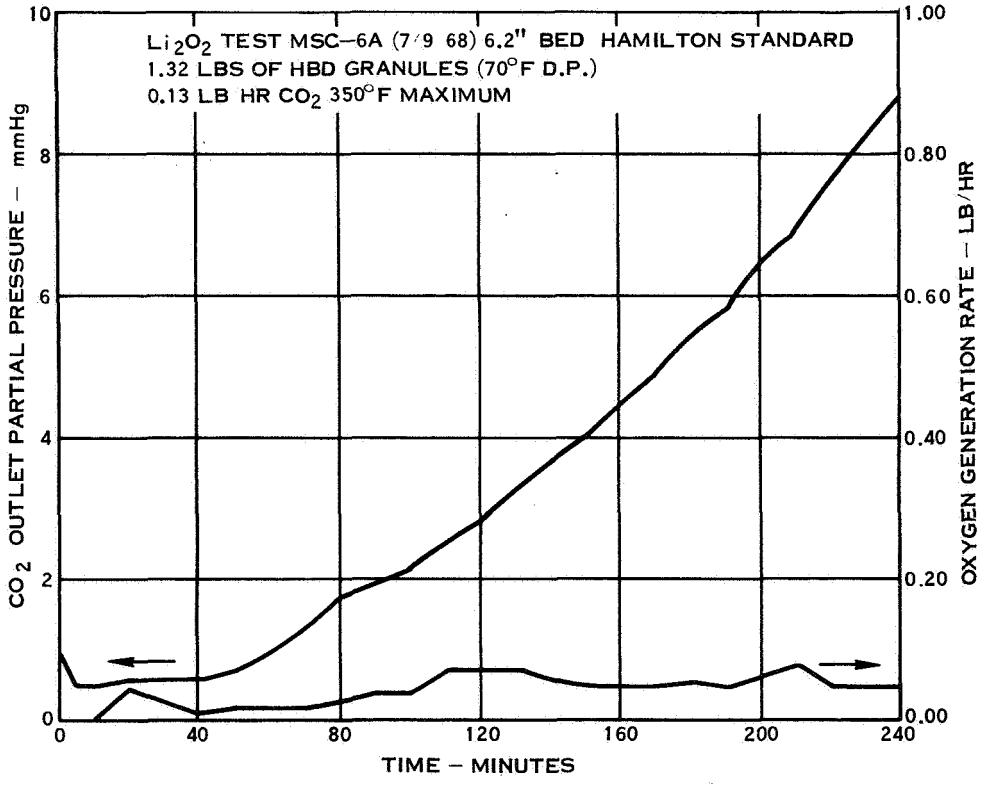

Figure 4-6. Lithium Peroxide Performance Data

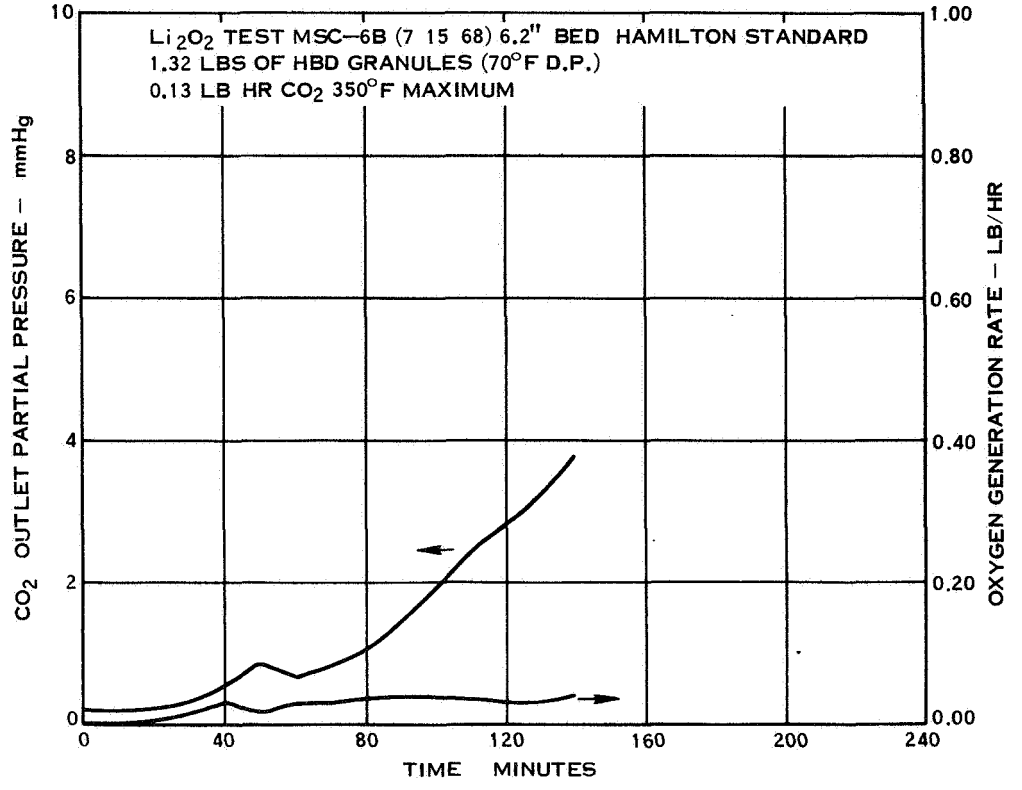

Figure 4-7. Lithium Peroxide Performance Data

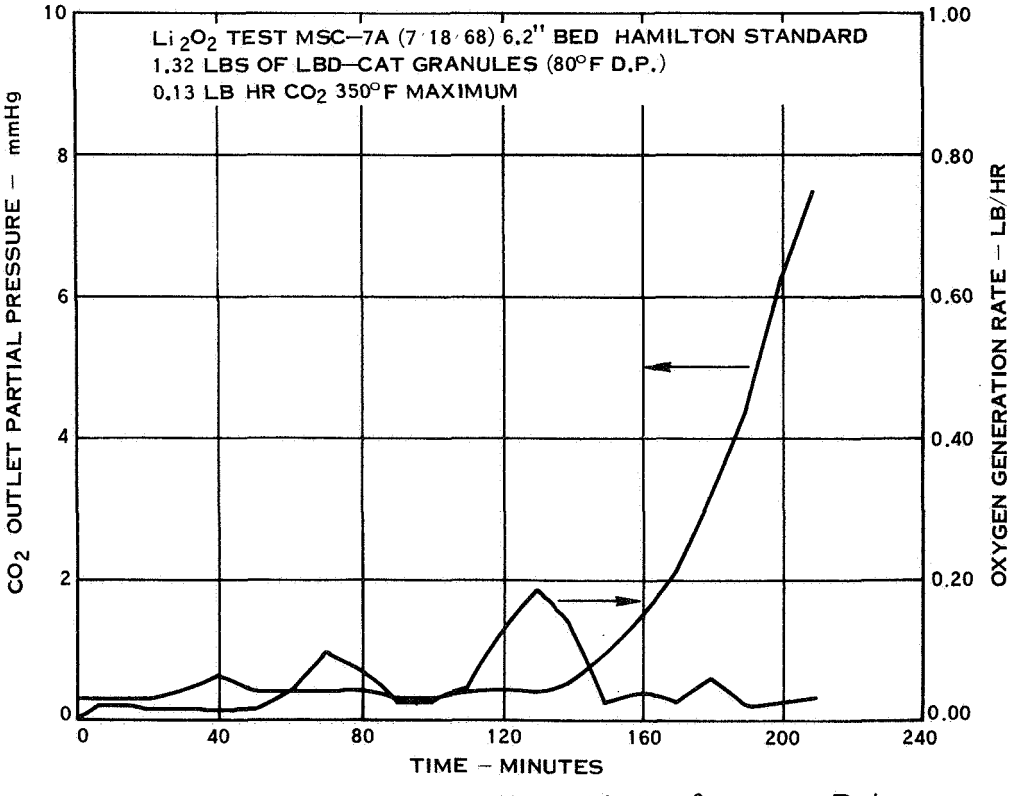

Figure 4-8. Lithium Peroxide Performance Data

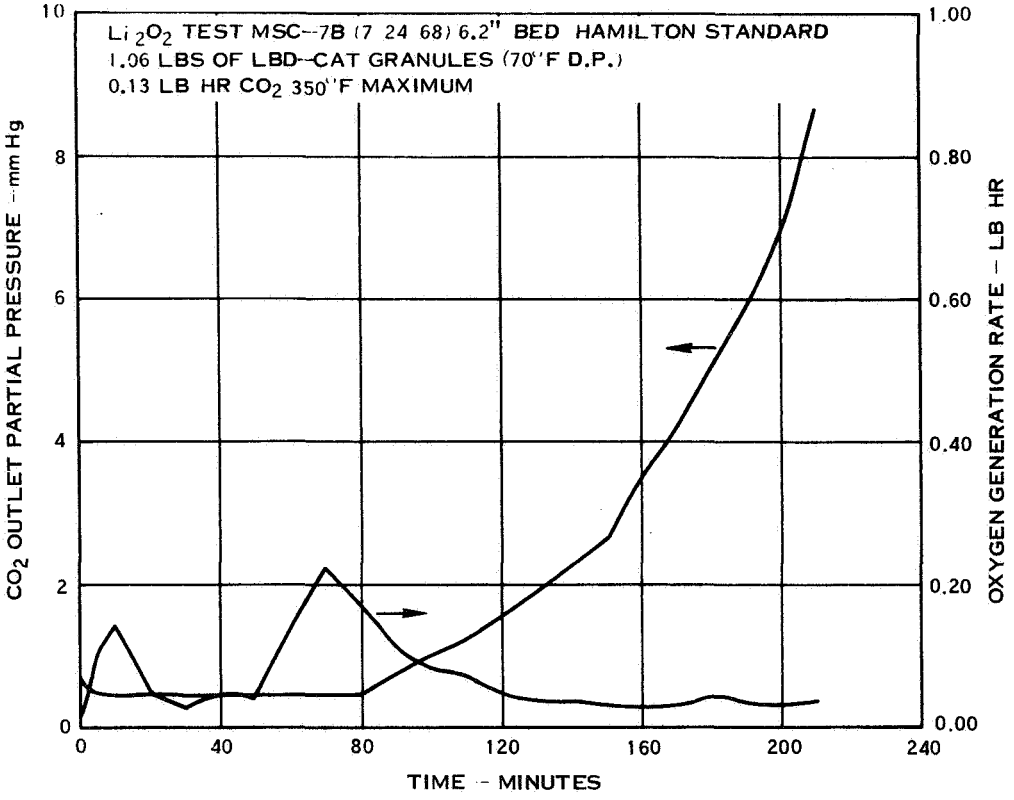

Figure 4-9. Lithium Peroxide Performance Data

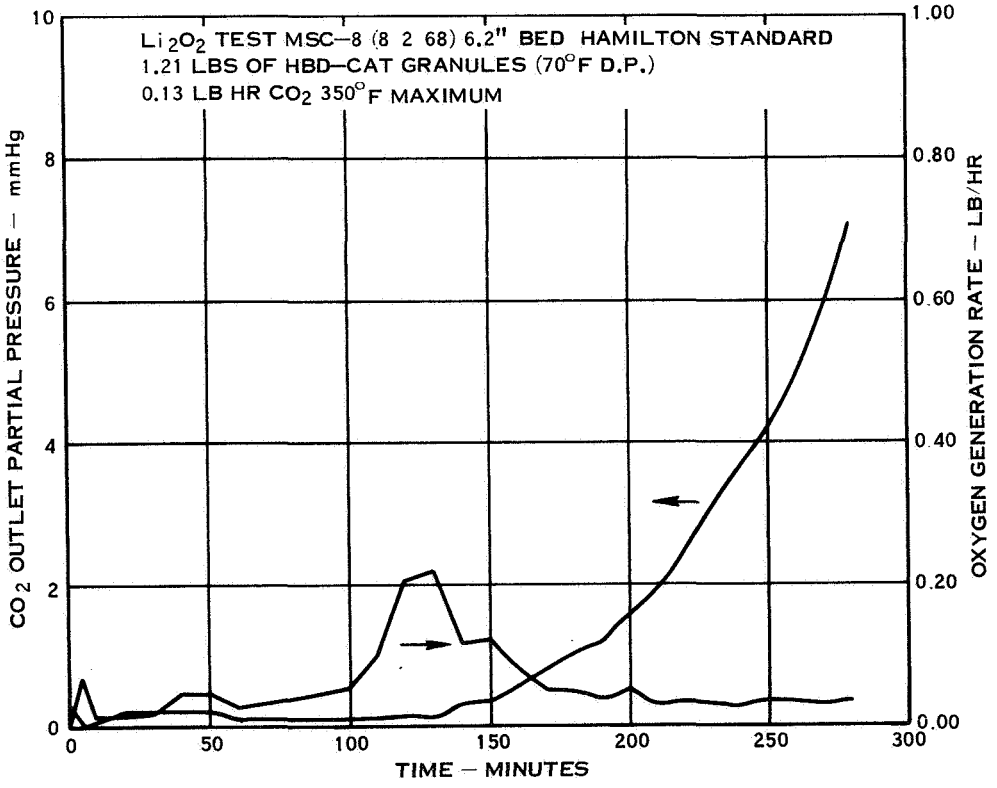

Figure 4-10. Lithium Peroxide Performance Data

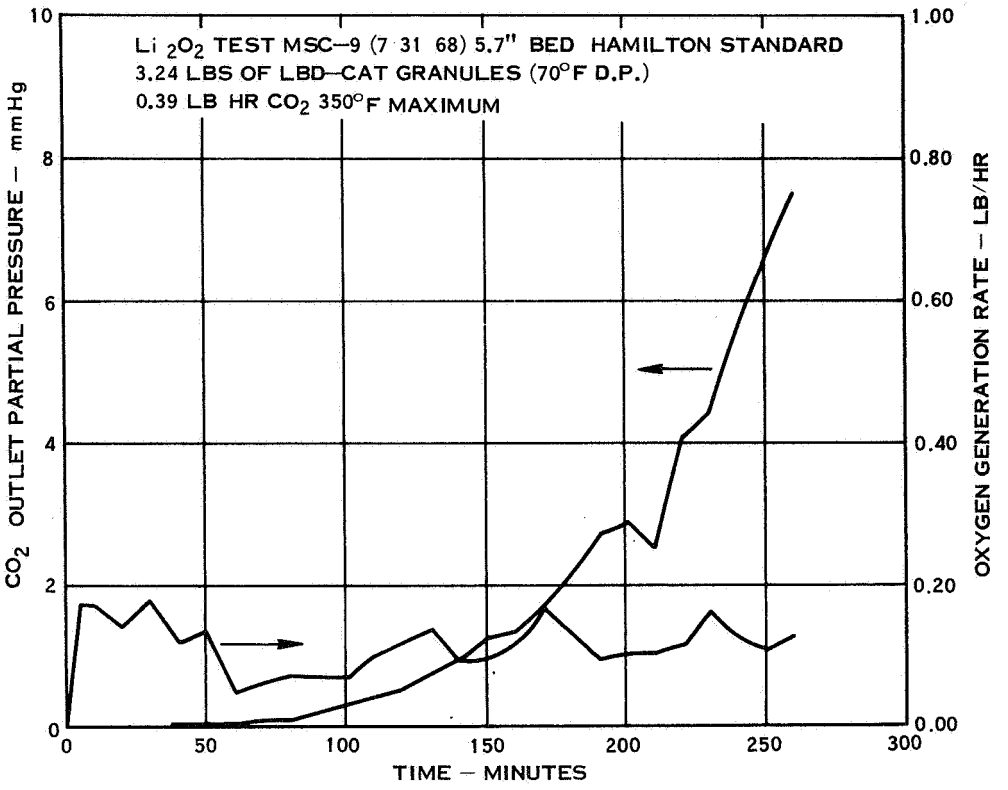

Figure 4-11. Lithium Peroxide Performance Data

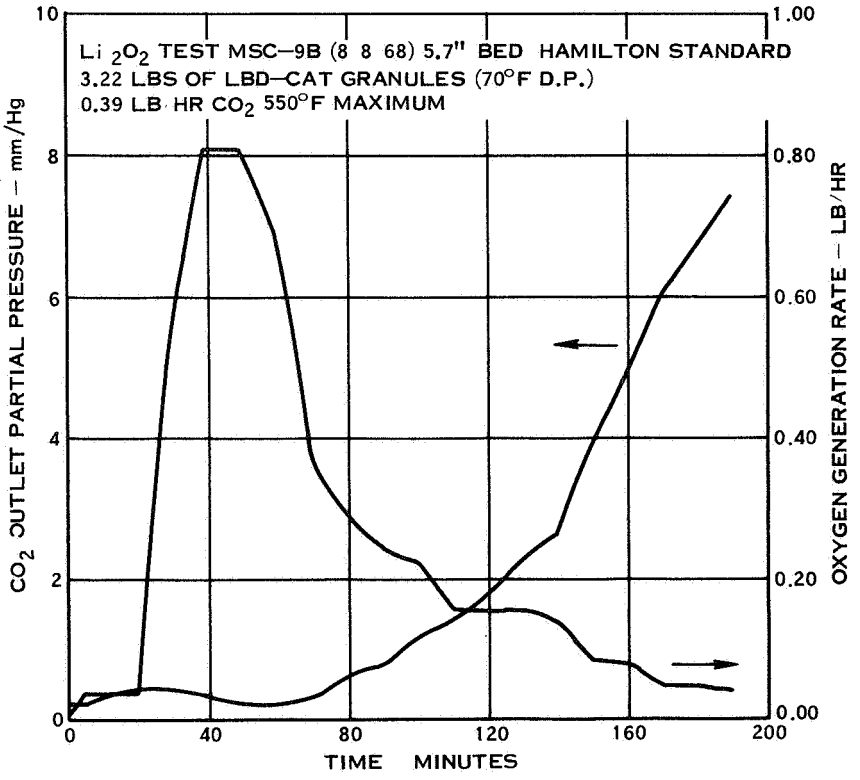

Figure 4-12. Lithium Peroxide Performance Data

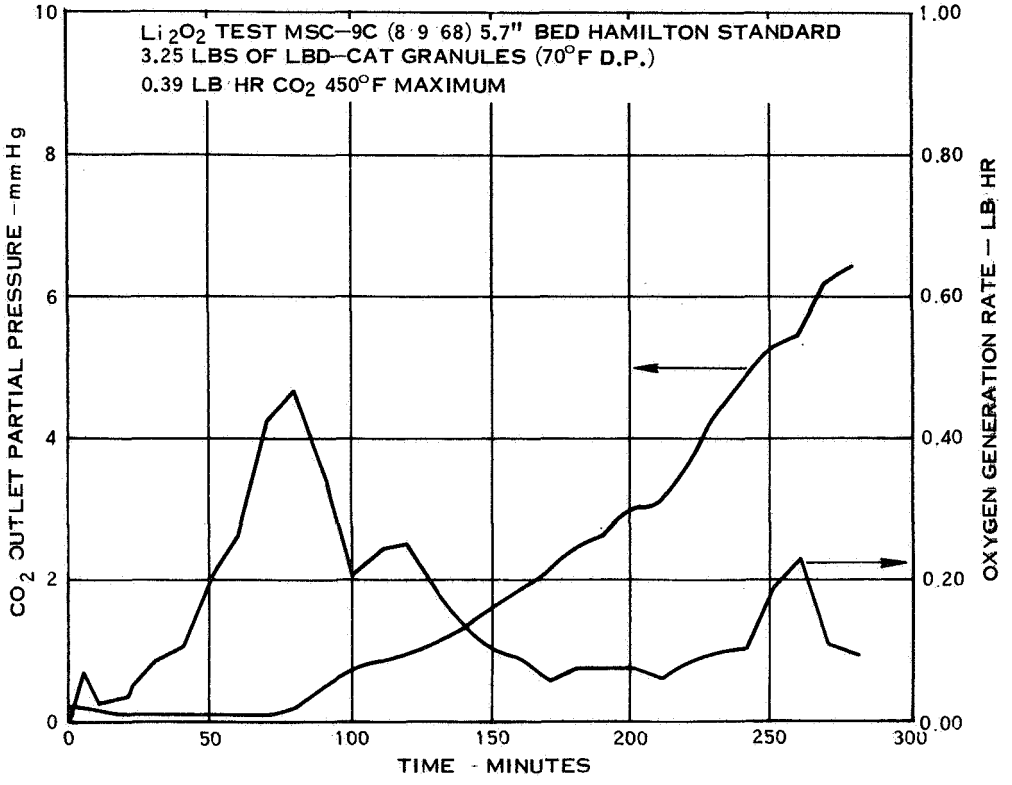

Figure 4-13. Lithium Peroxide Performance Data

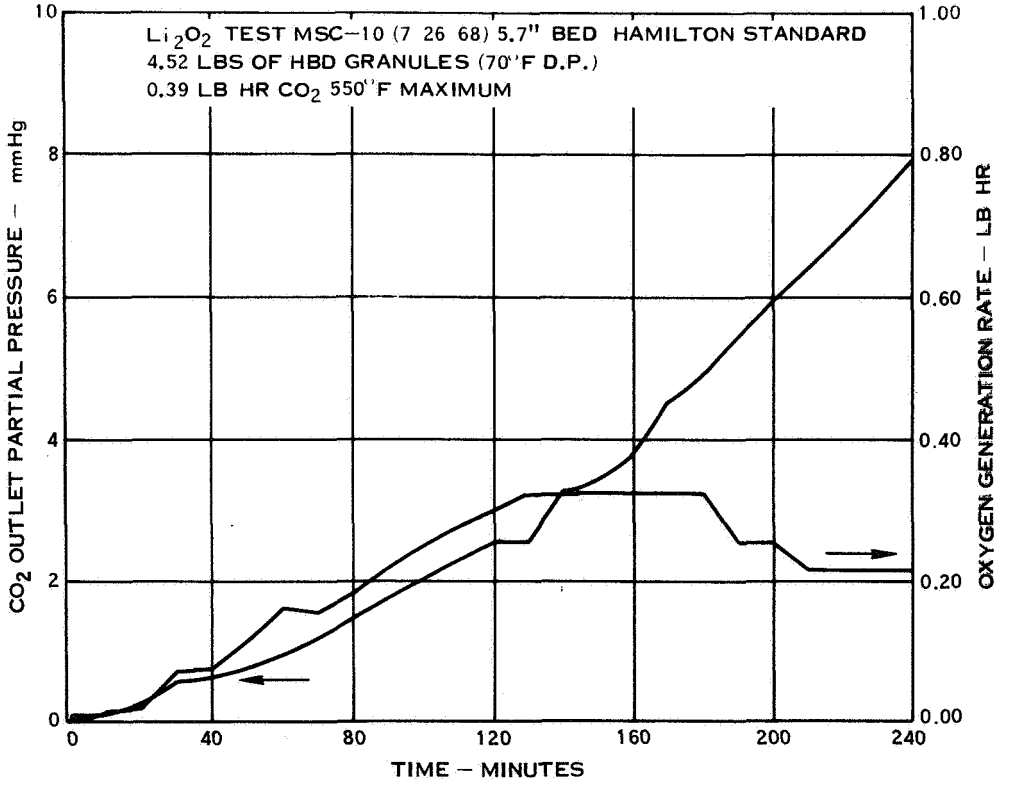

Figure 4-14. Lithium Peroxide Performance Data

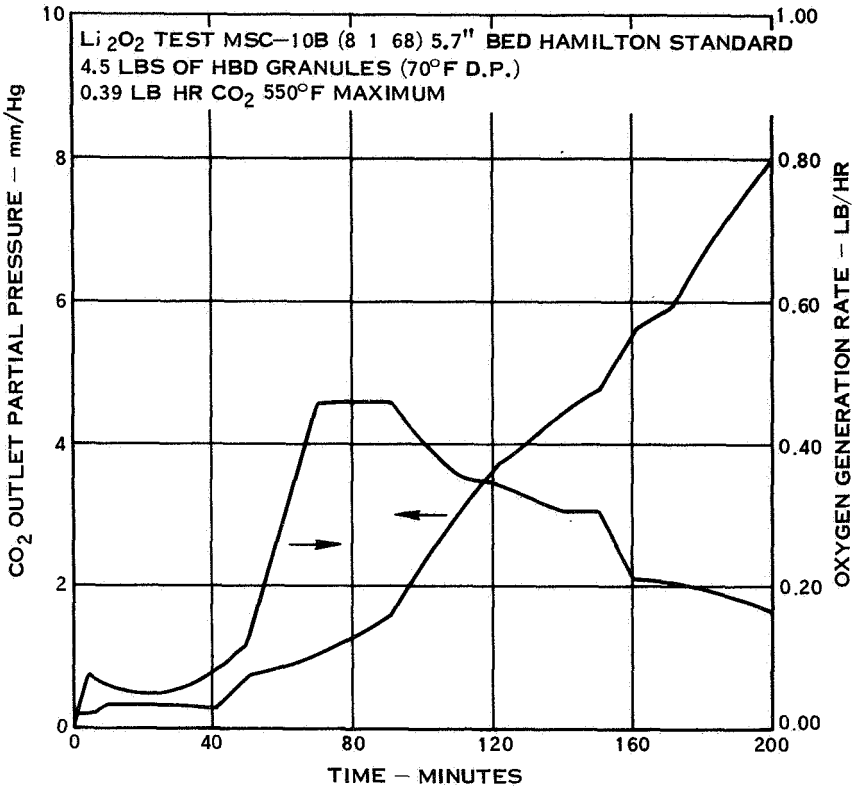

Figure 4-15. Lithium Peroxide Performance Data

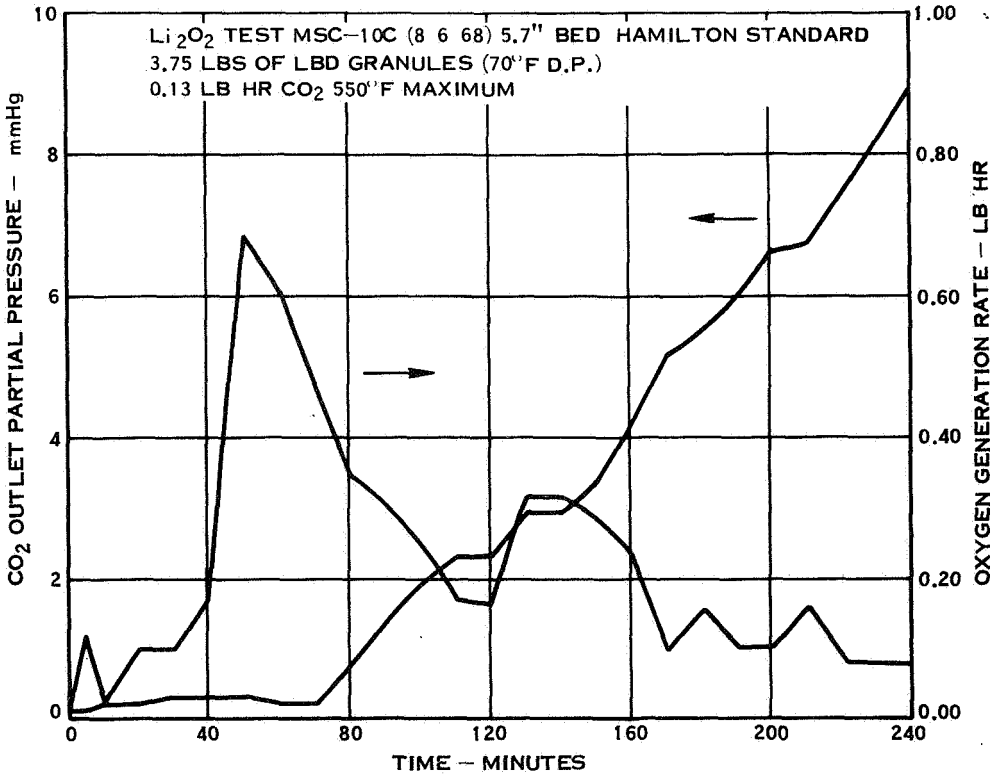

Figure 4-16. Lithium Peroxide Performance Data

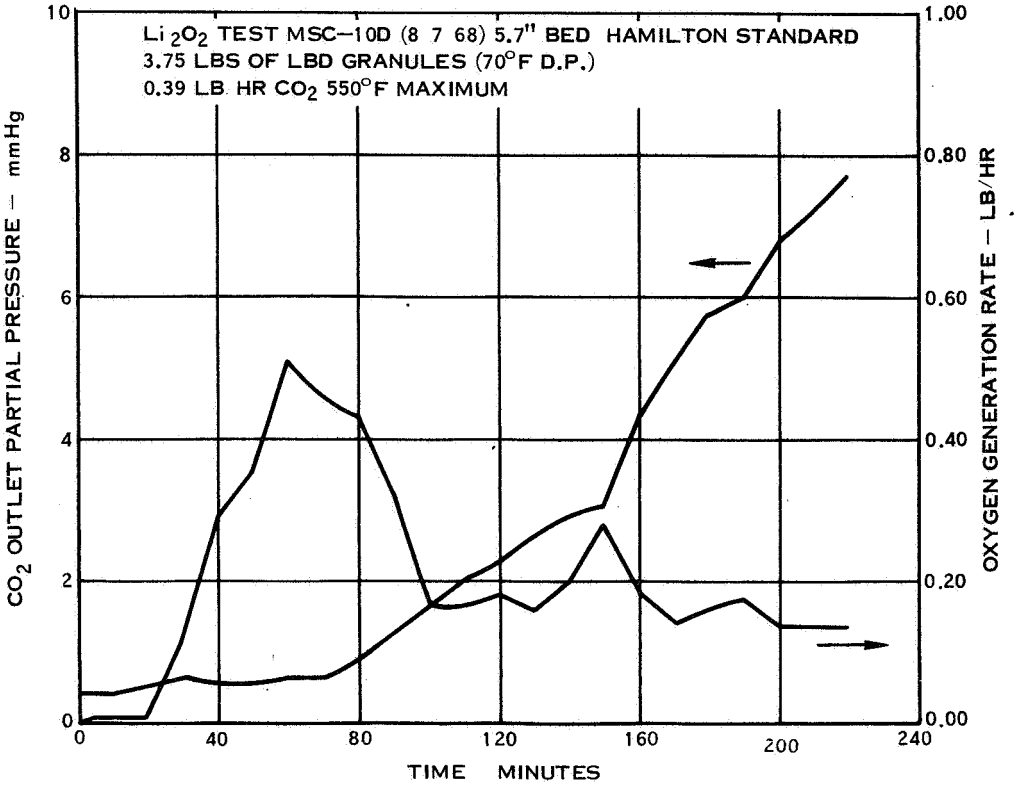

Figure 4-17. Lithium Peroxide Performance Data

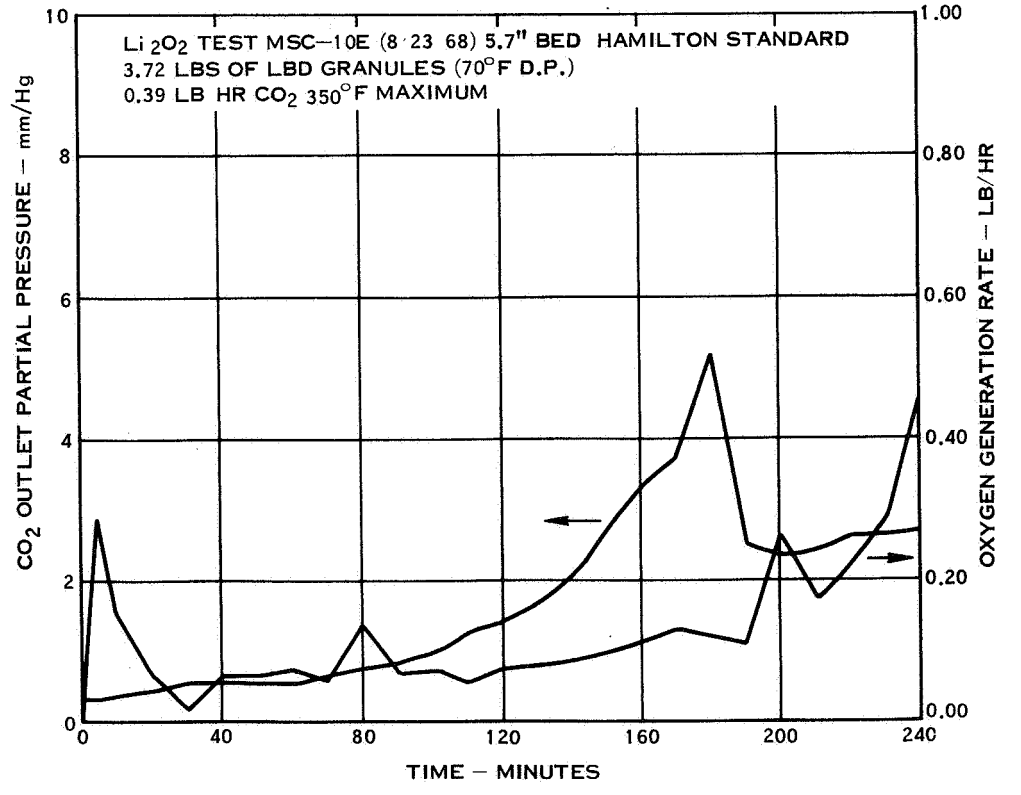

Figure 4-18. Lithium Peroxide Performance Data

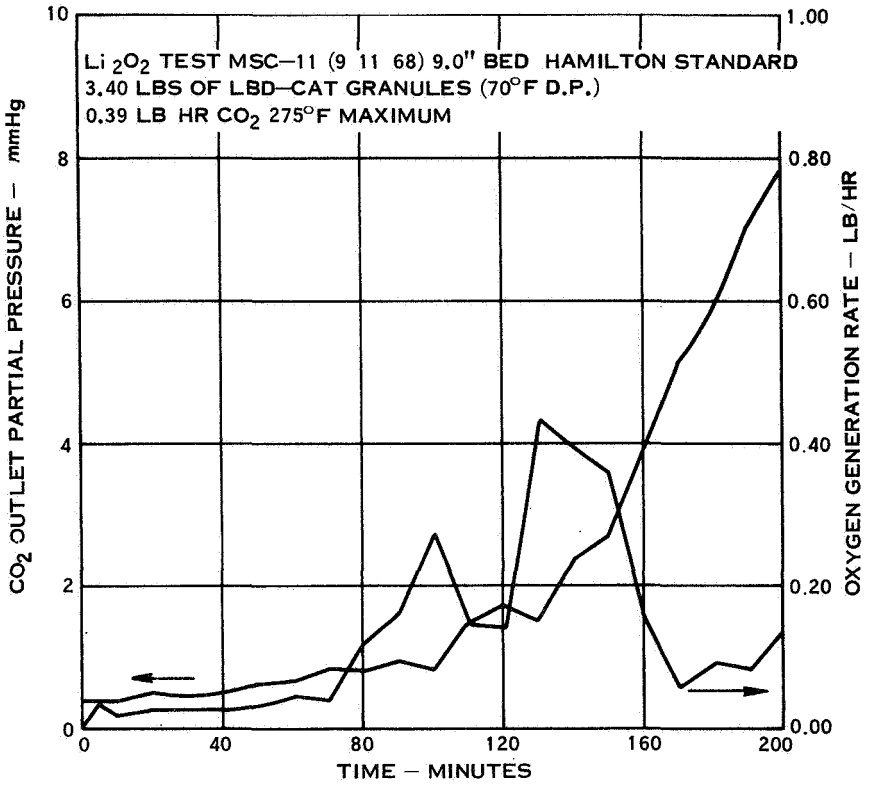

Figure 4-19. Lithium Peroxide Performance Data

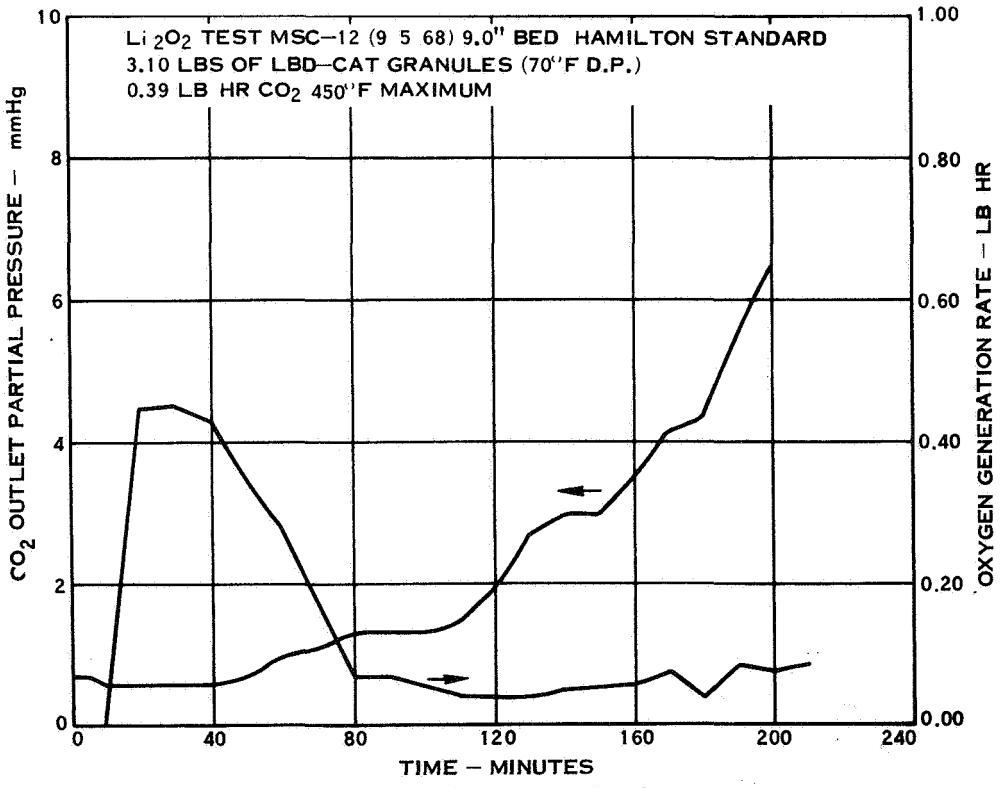

Figure 4-20. Lithium Peroxide Performance Data

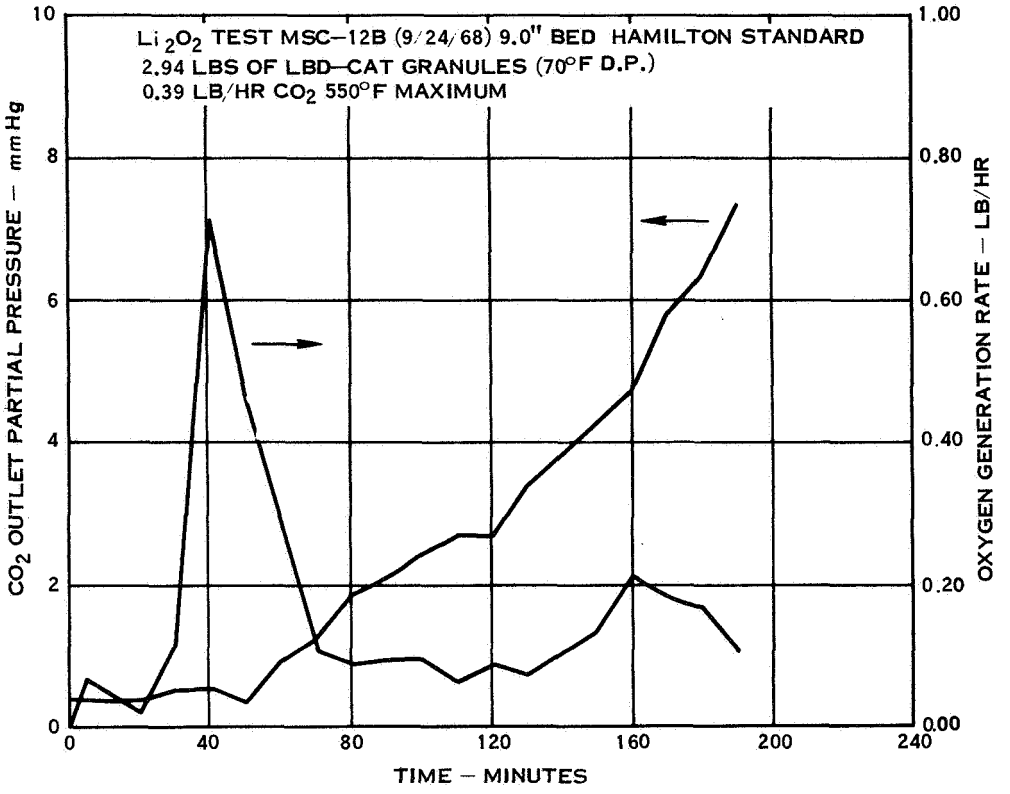

Figure 4-21. Lithium Peroxide Performance Data

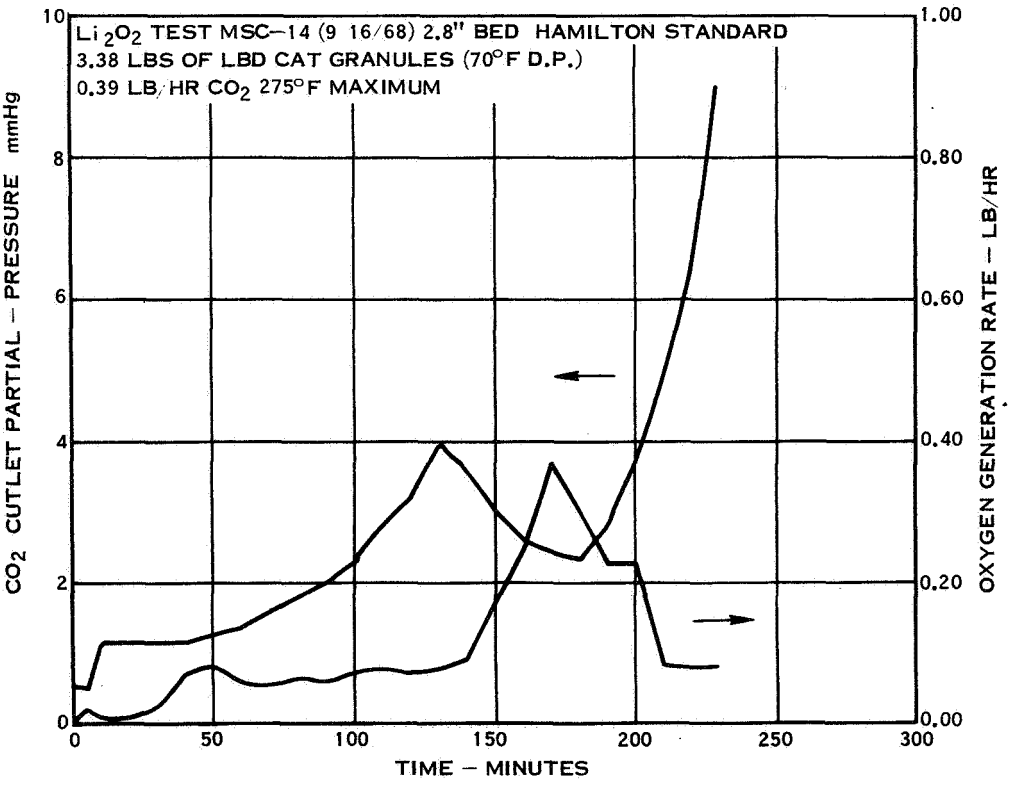

Figure 4-22. Lithium Peroxide Performance Data

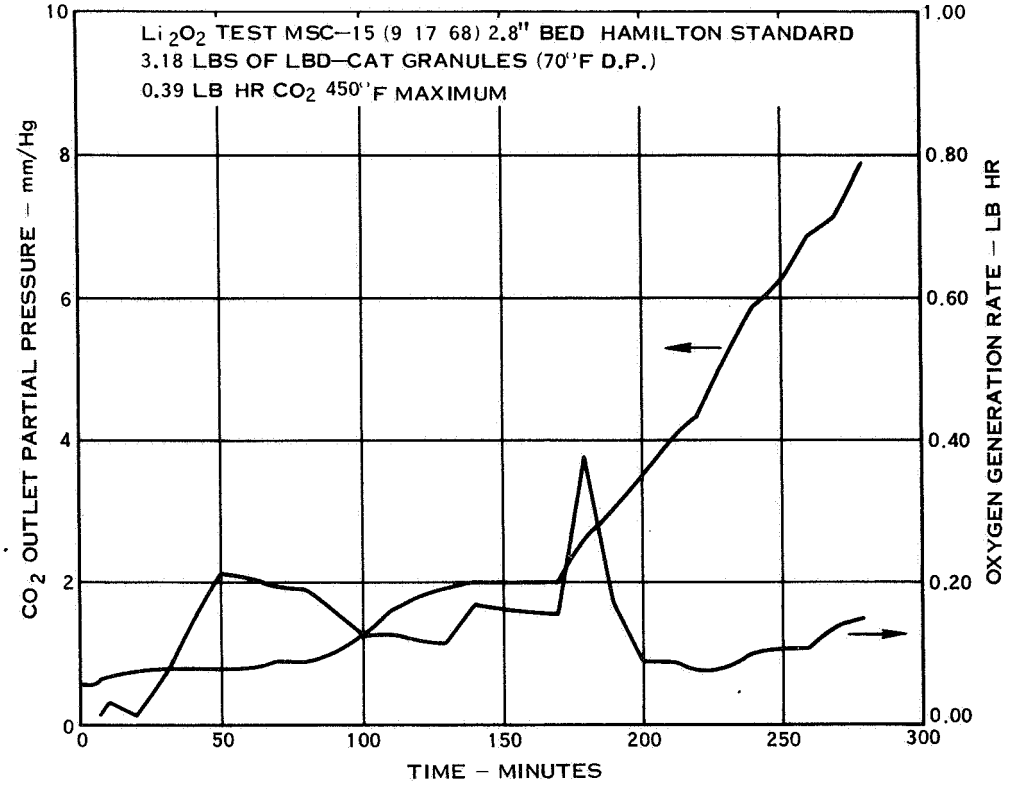

Figure 4-23. Lithium Peroxide Performance Data

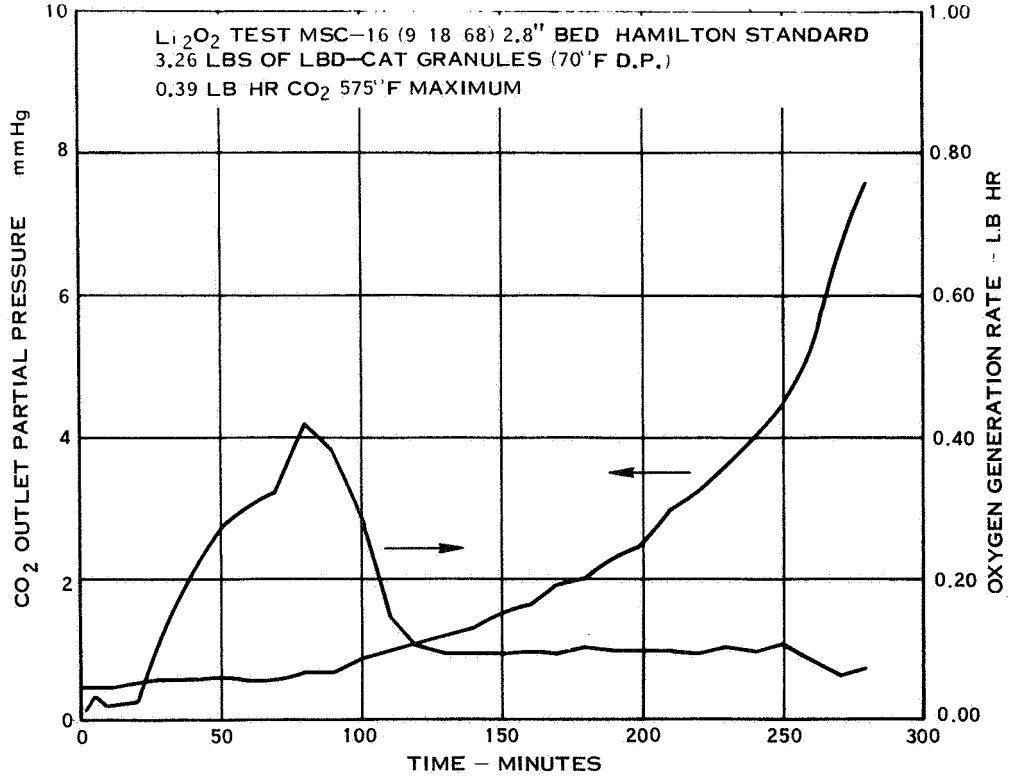

Figure 4-24. Lithium Peroxide Performance Data

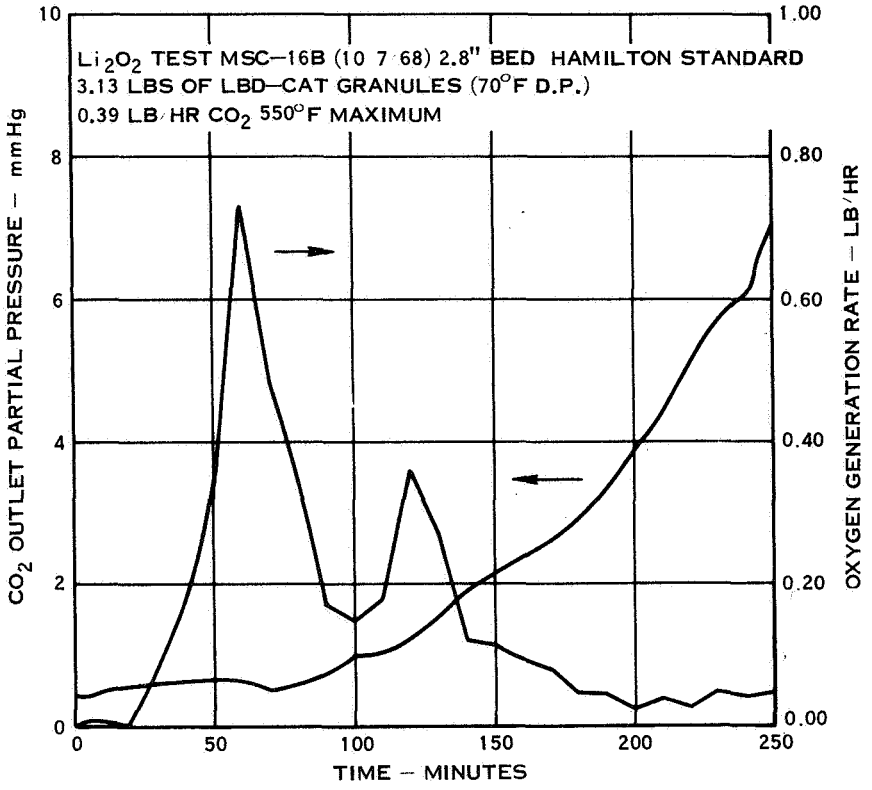

Figure 4-25. Lithium Peroxide Performance Data

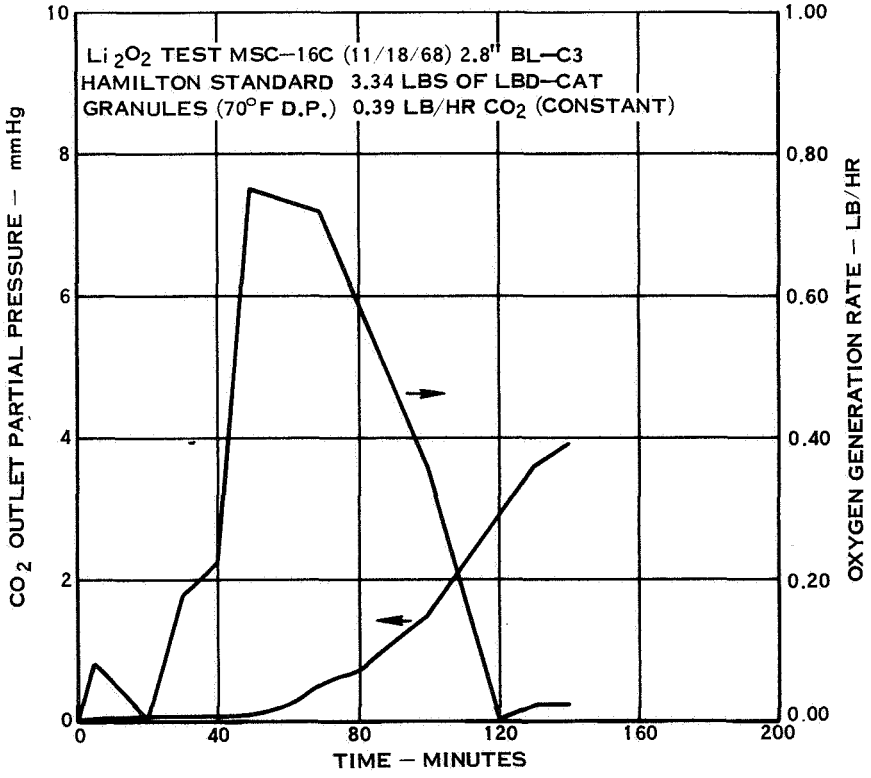

Figure 4-26. Lithium Peroxide Performance Data

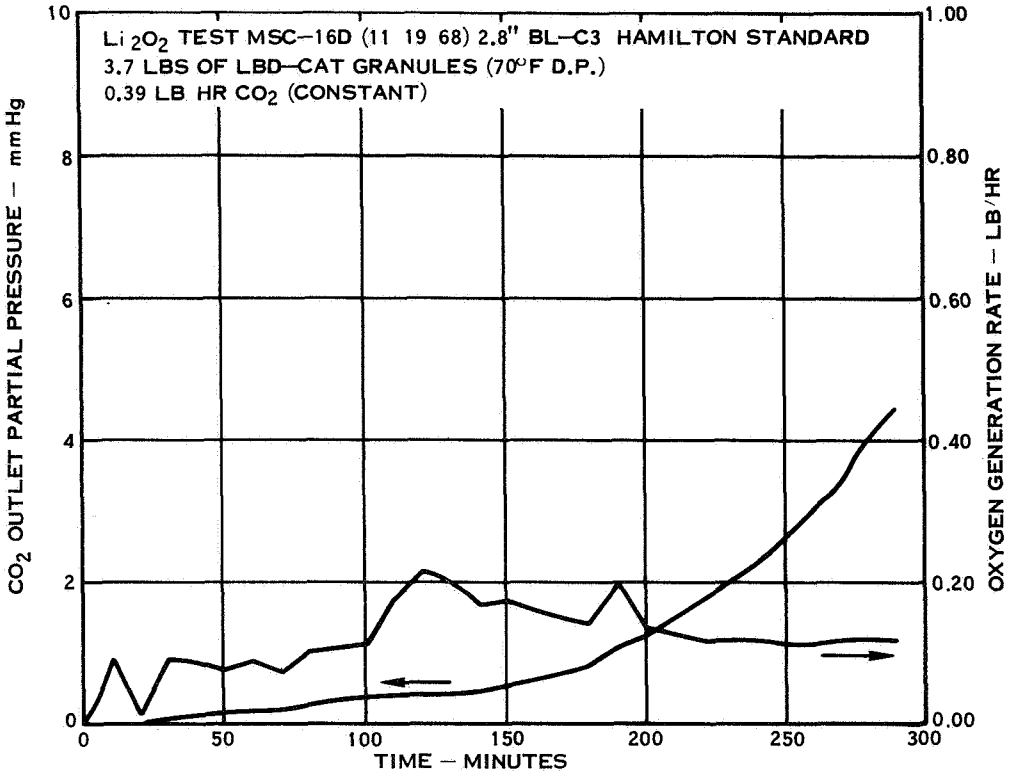

Figure 4-27. Lithium Peroxide Performance Data

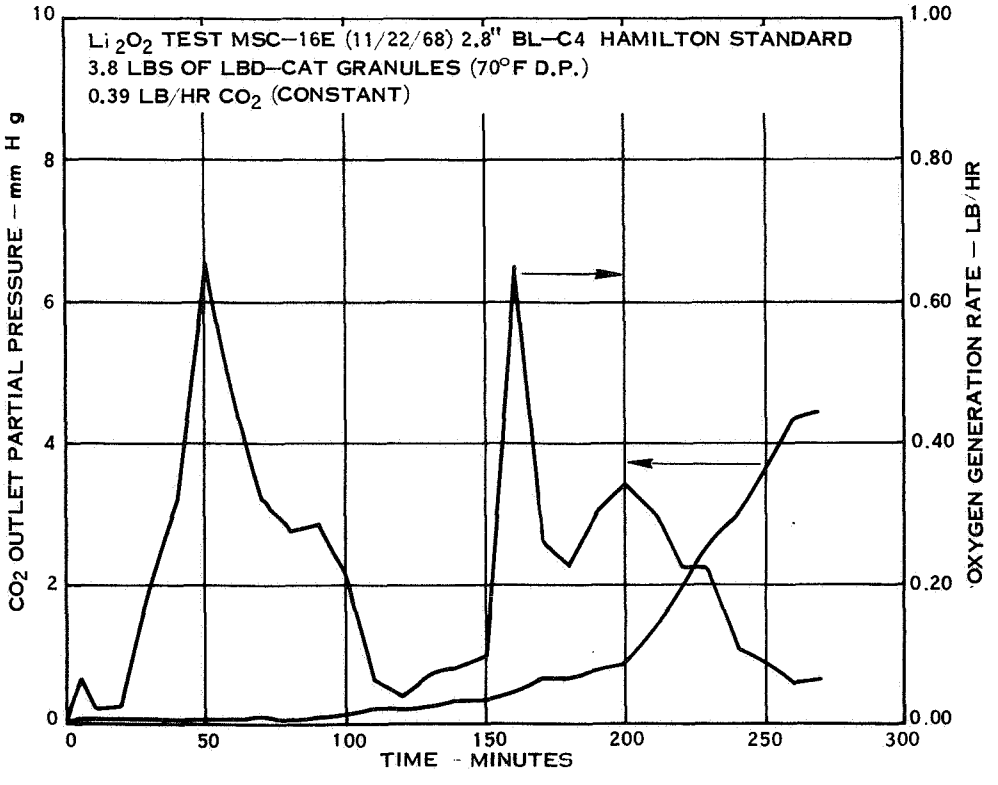

Figure 4-28. Lithium Peroxide Performance Data

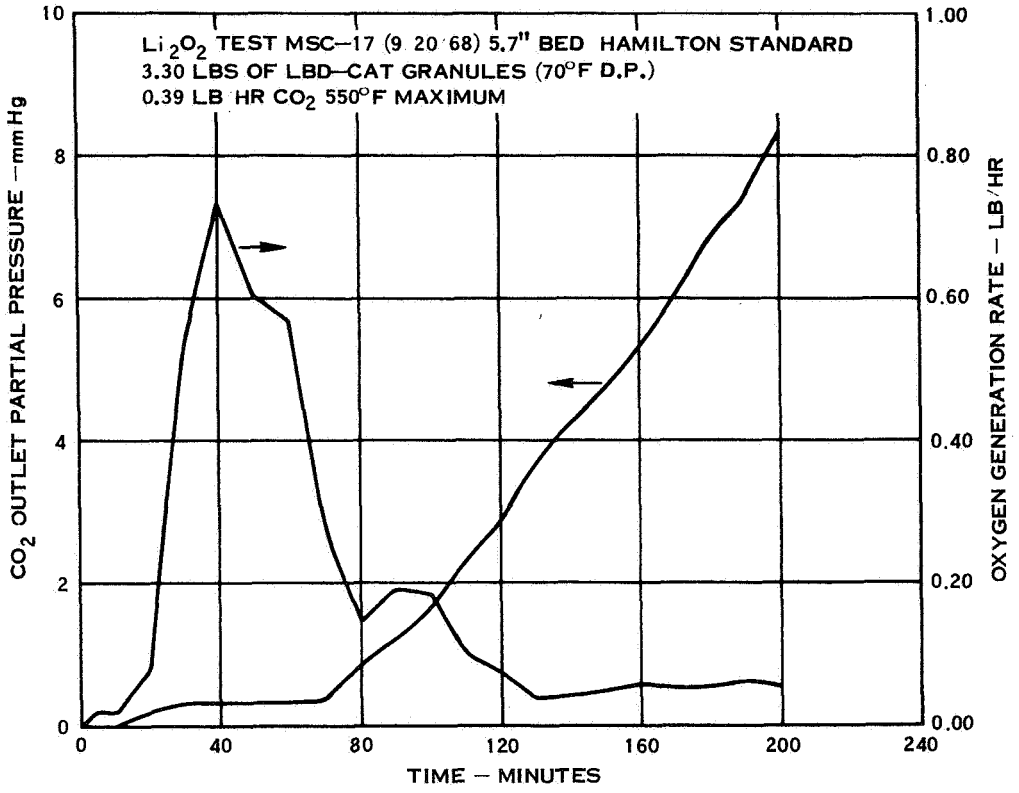

Figure 4-29. Lithium Peroxide Performance Data

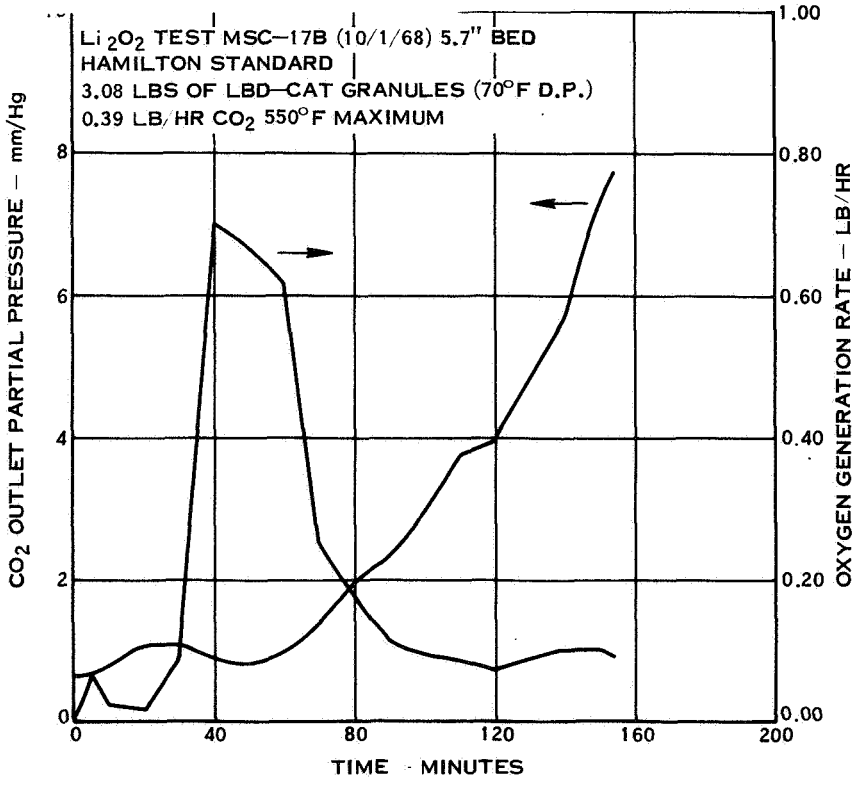

Figure 4-30. Lithium Peroxide Performance Data

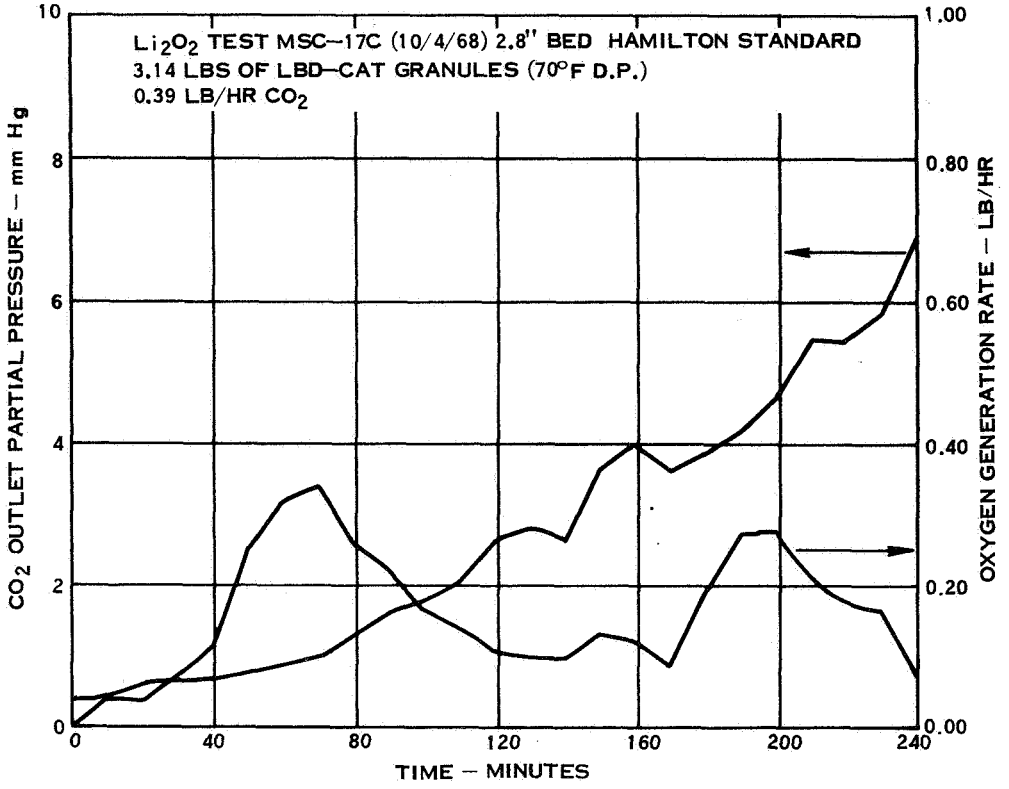

Figure 4-31. Lithium Peroxide Performance Data

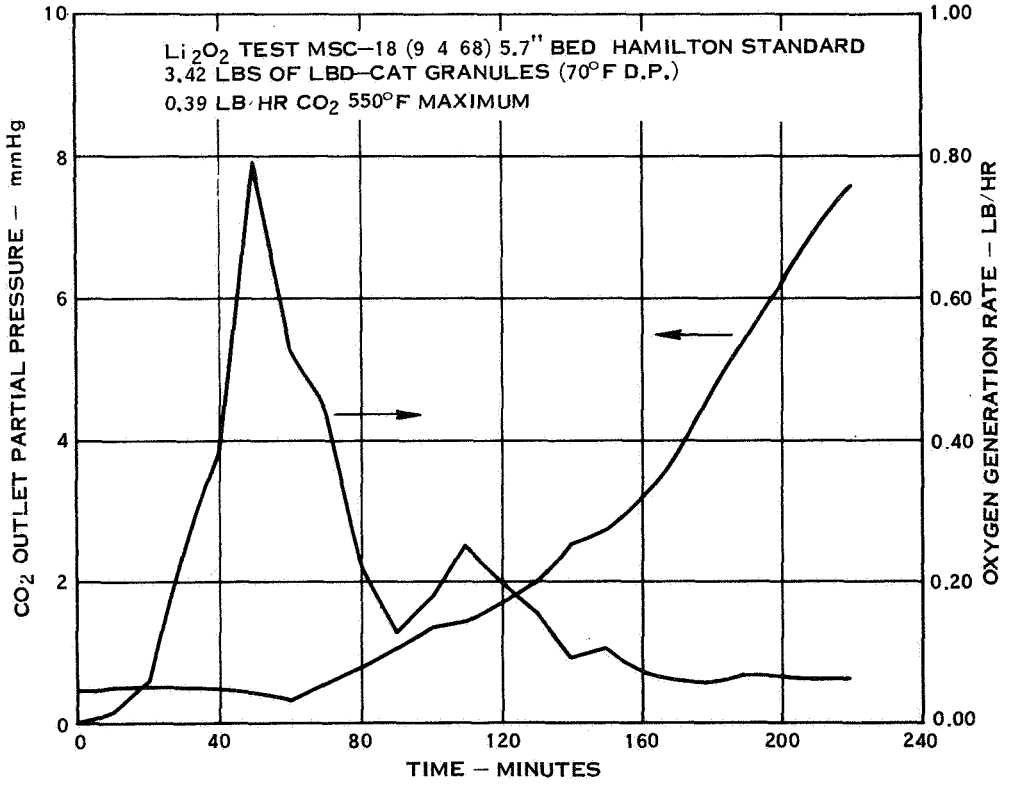

Figure 4-32. Lithium Peroxide Performance Data

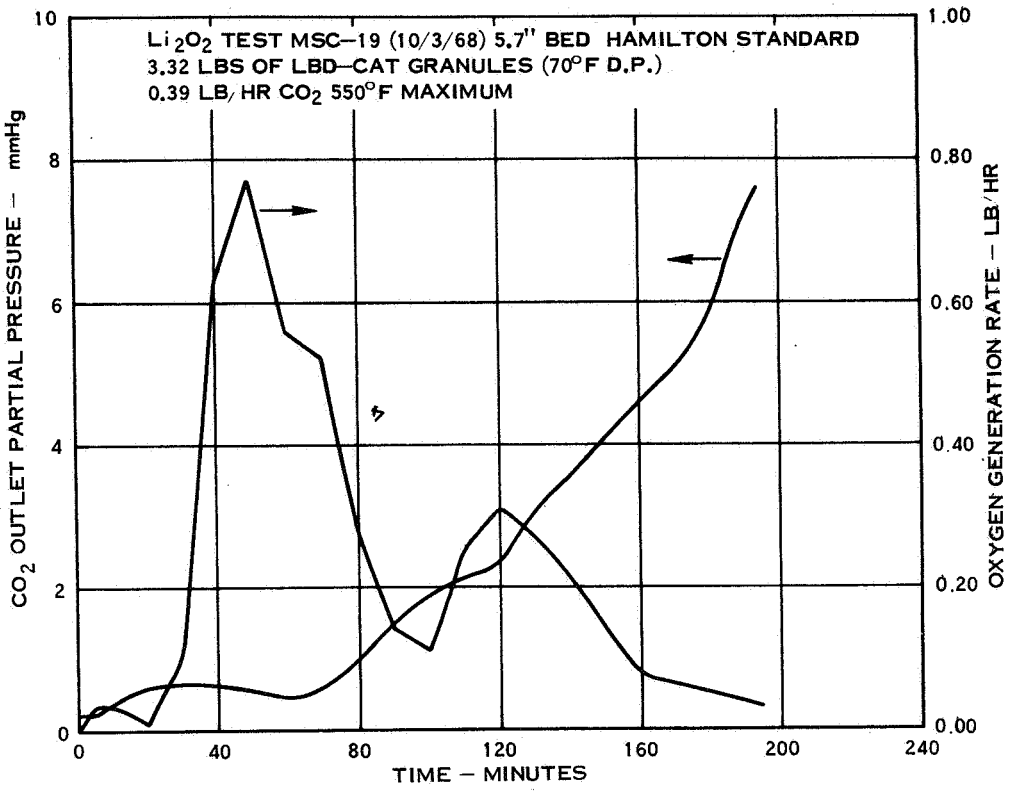

Figure 4-33. Lithium Peroxide Performance Data

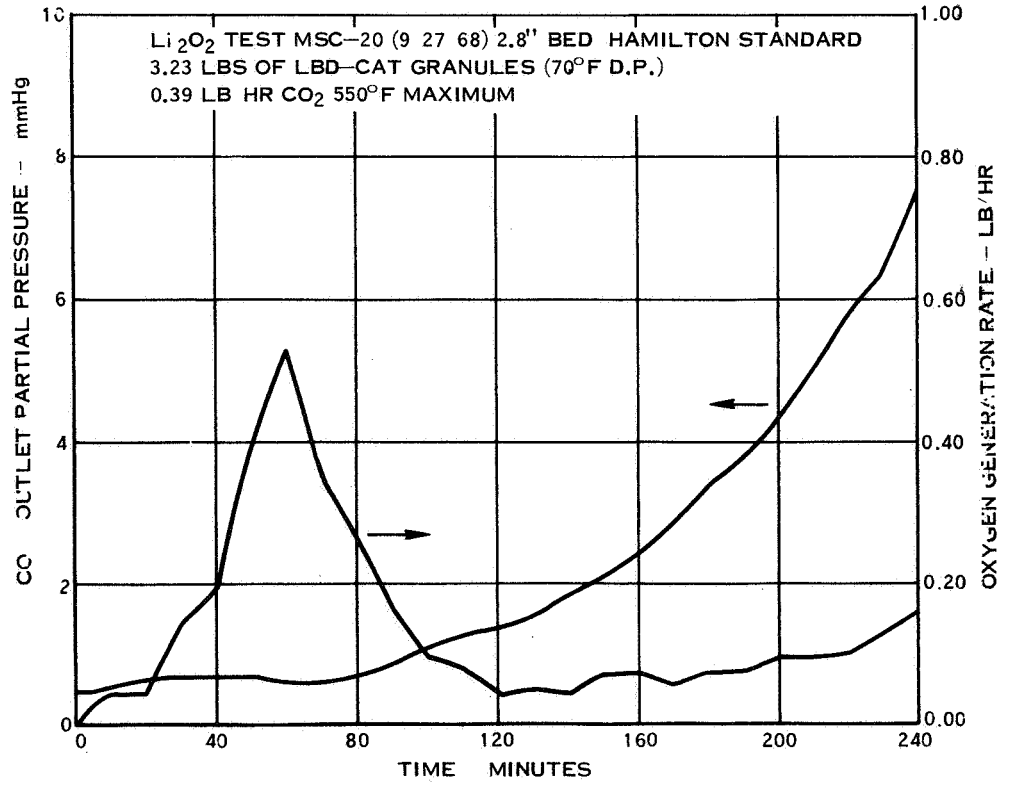

Figure 4-34. Lithium Peroxide Performance Data

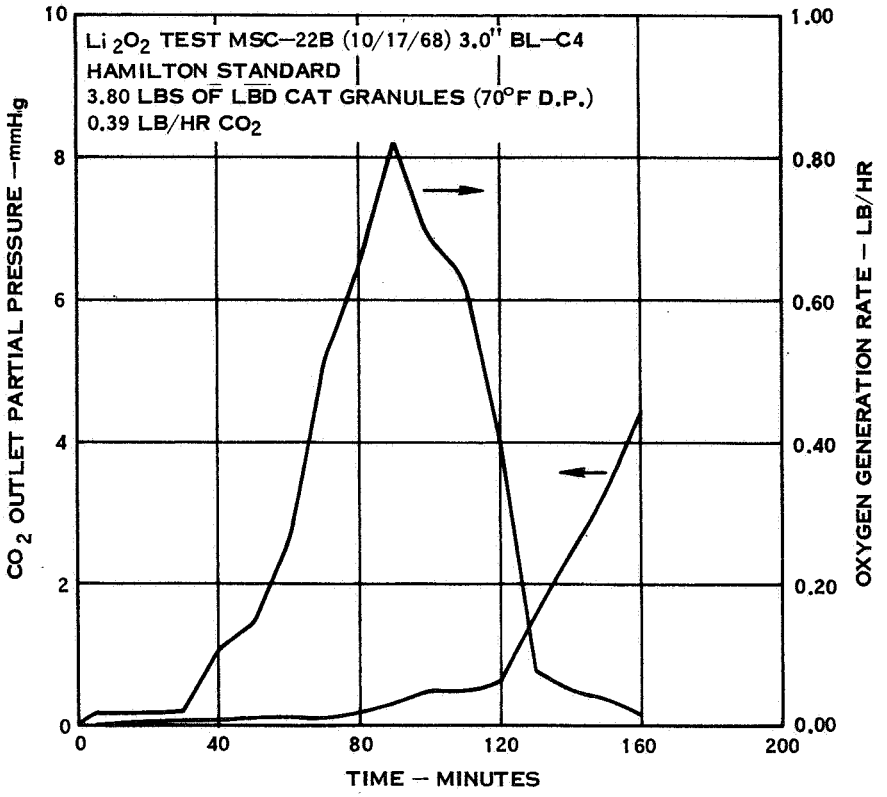

Figure 4-35. Lithium Peroxide Performance Data

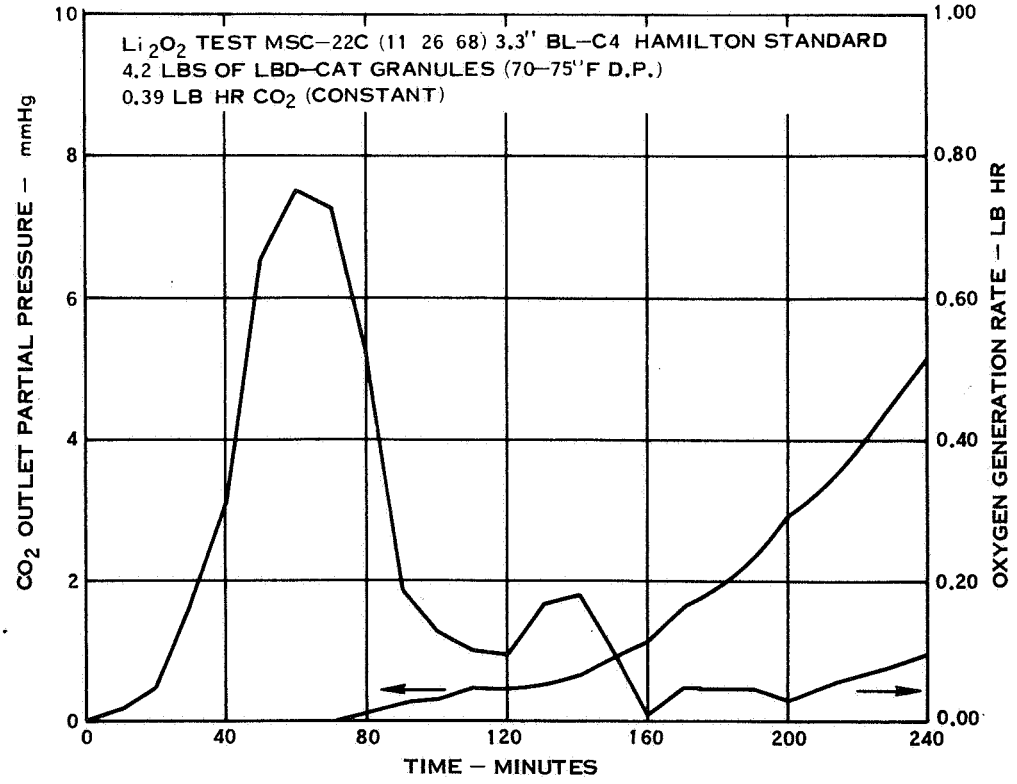

Figure 4-36. Lithium Peroxide Performance Data

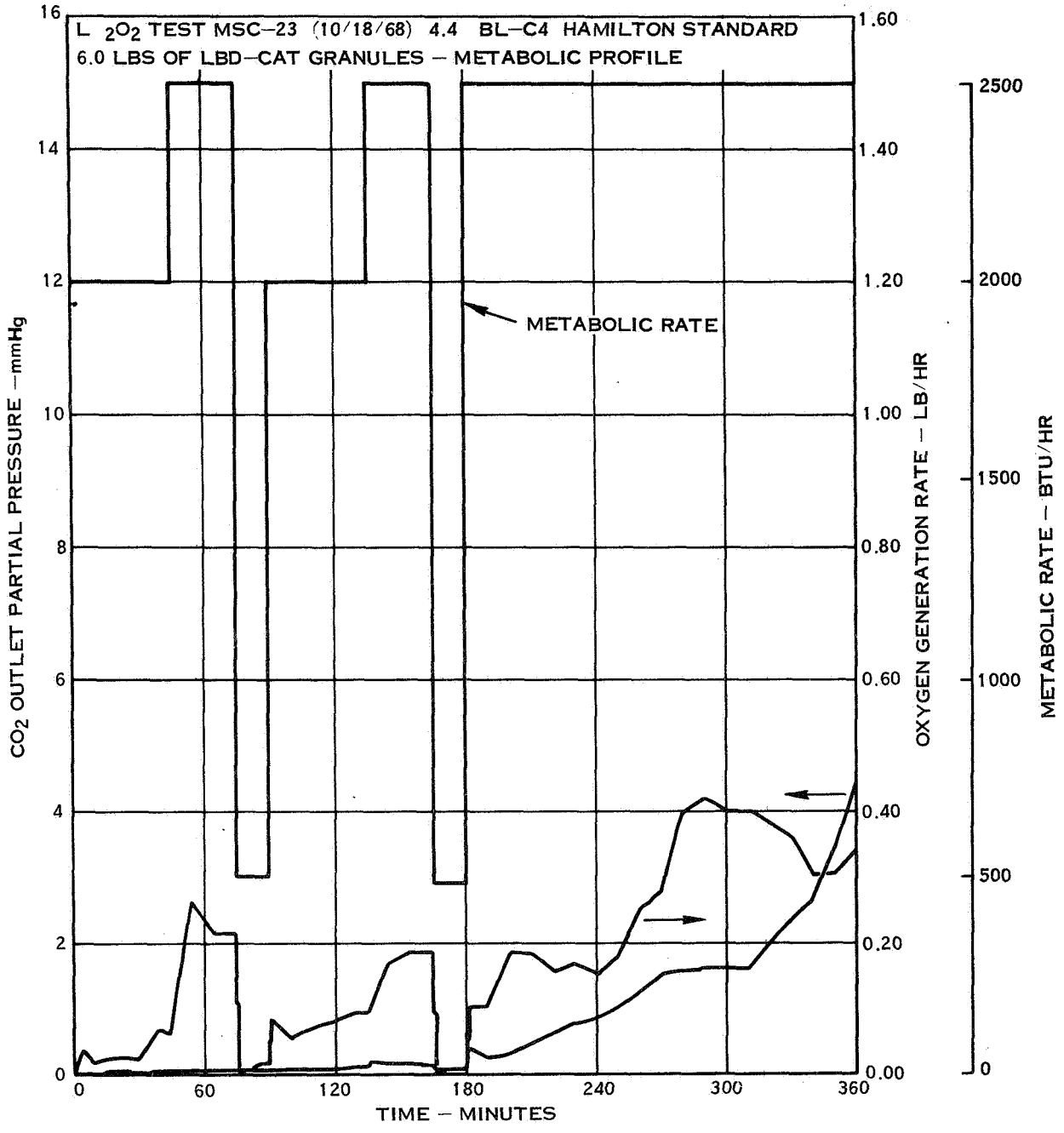

Figure 4-37. Lithium Peroxide Performance Data

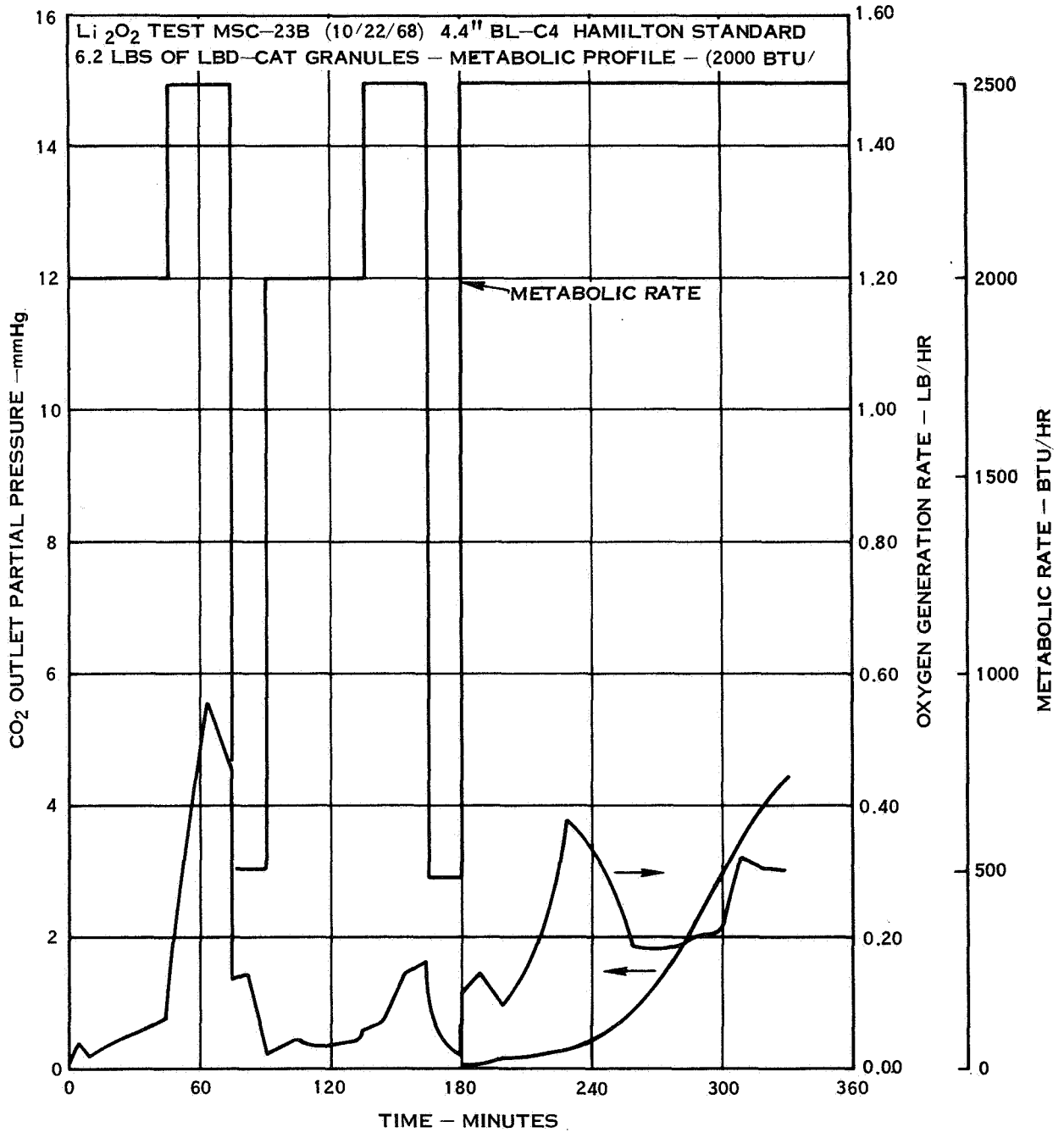

Figure 4-38. Lithium Peroxide Performance Data

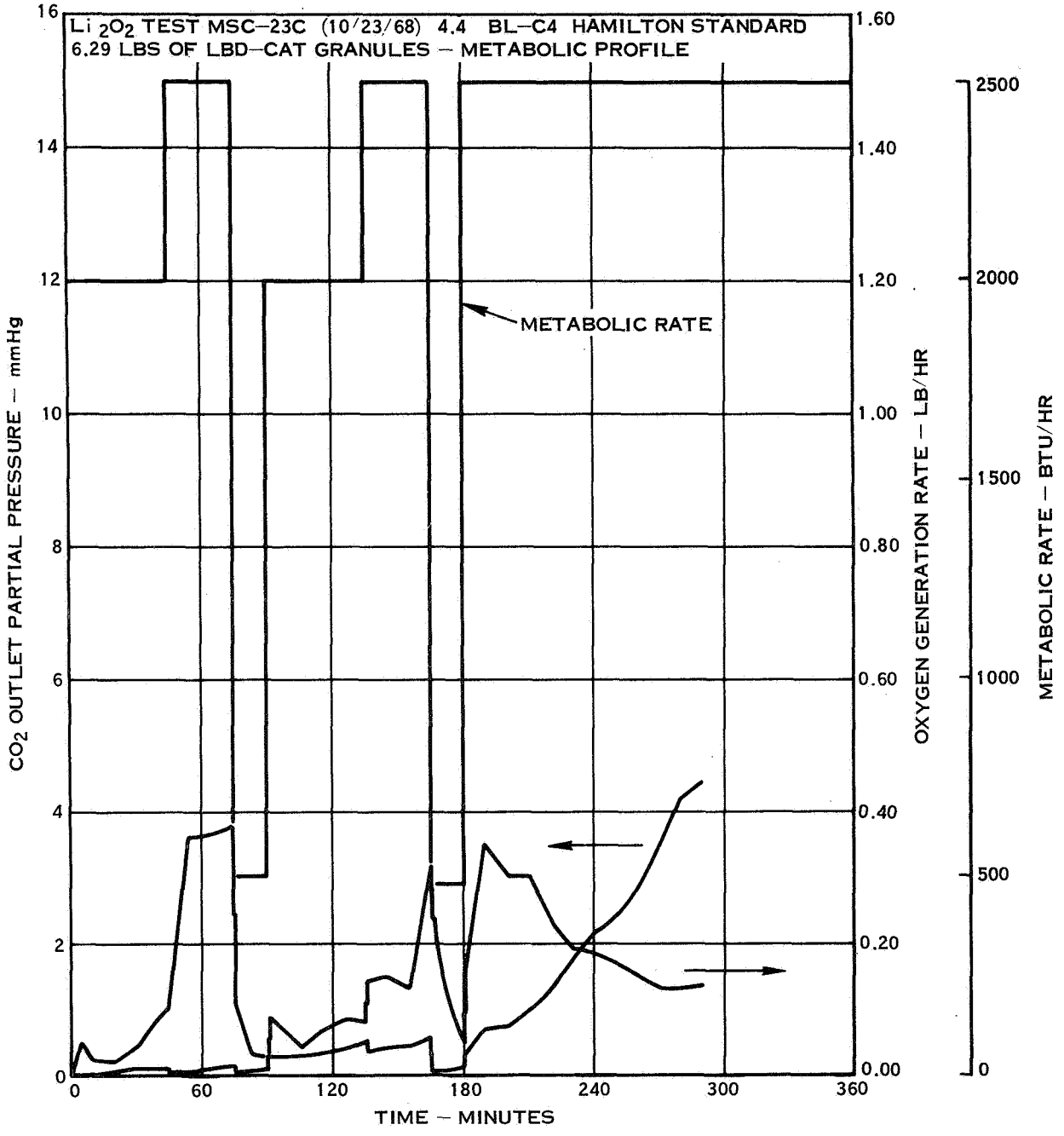

Figure 4-39. Lithium Peroxide Performance Data

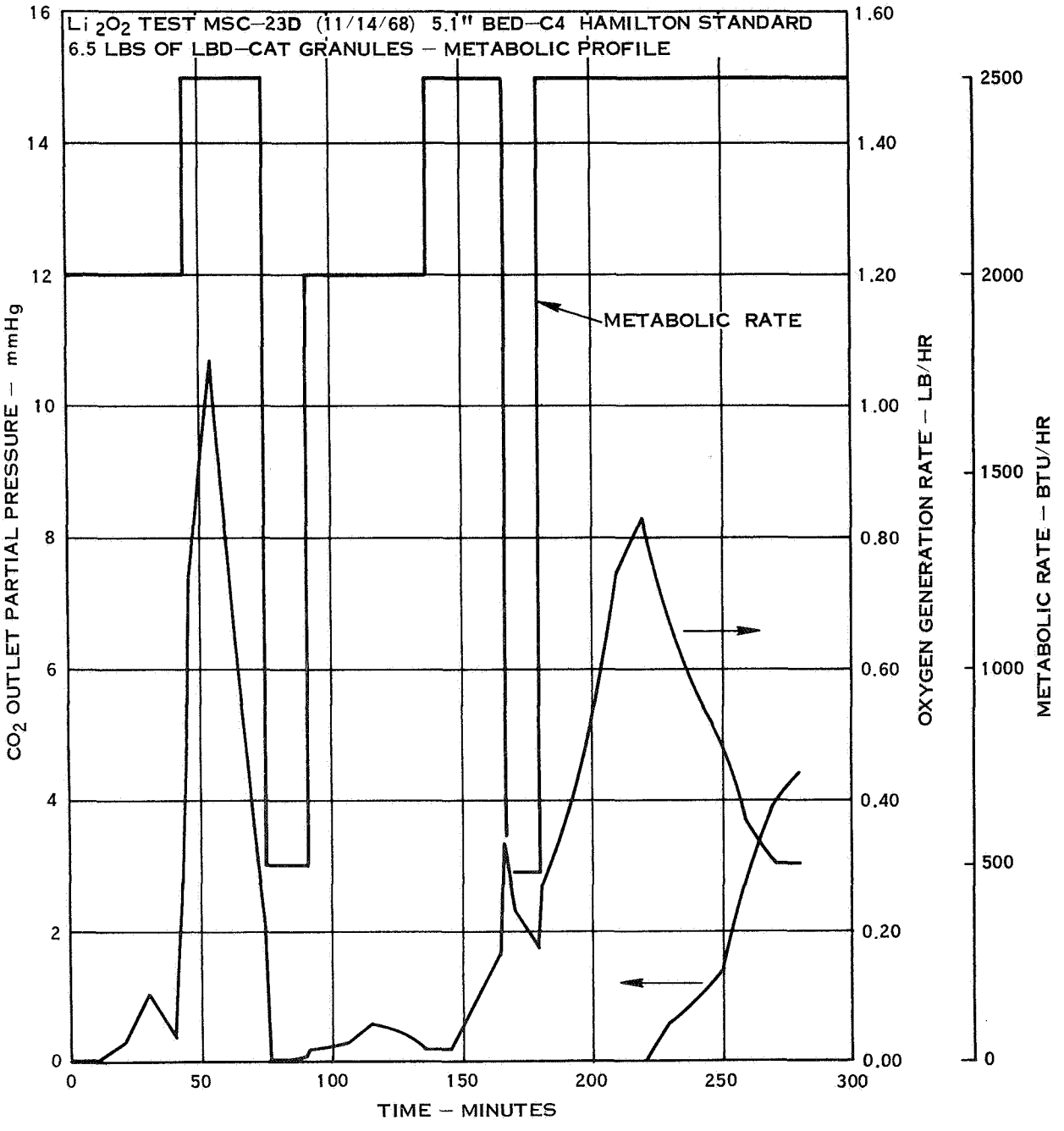

Figure 4-40. Lithium Peroxide Performance Data

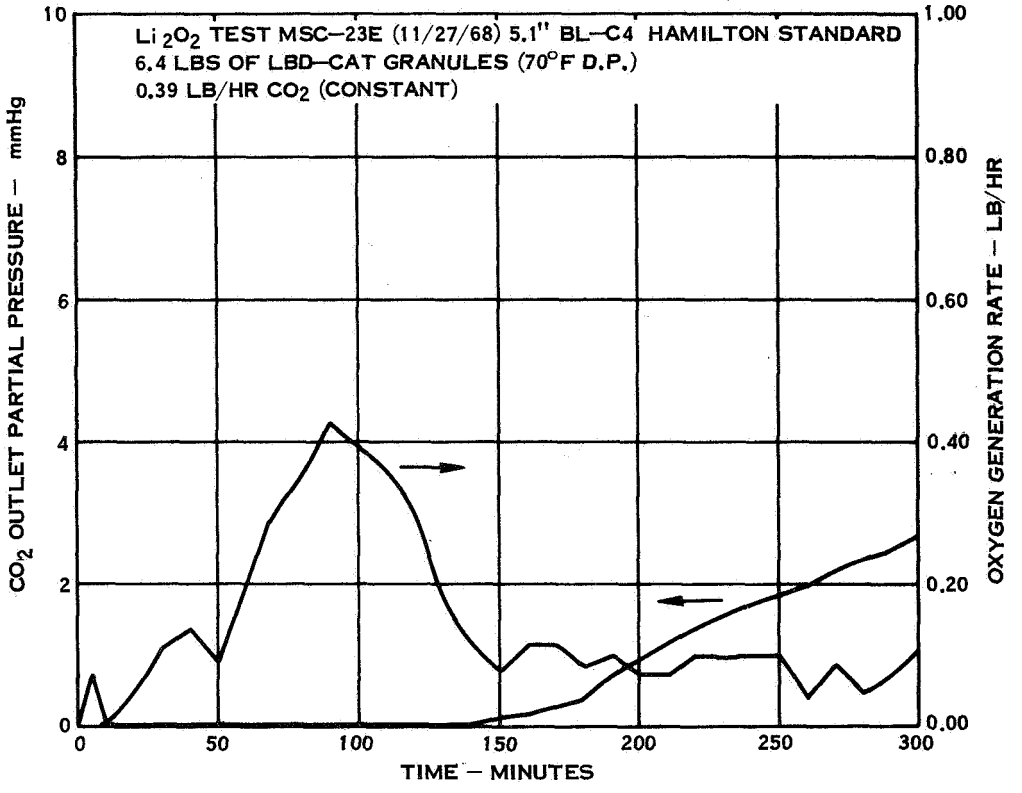

Figure 4-41. Lithium Peroxide Performance Data

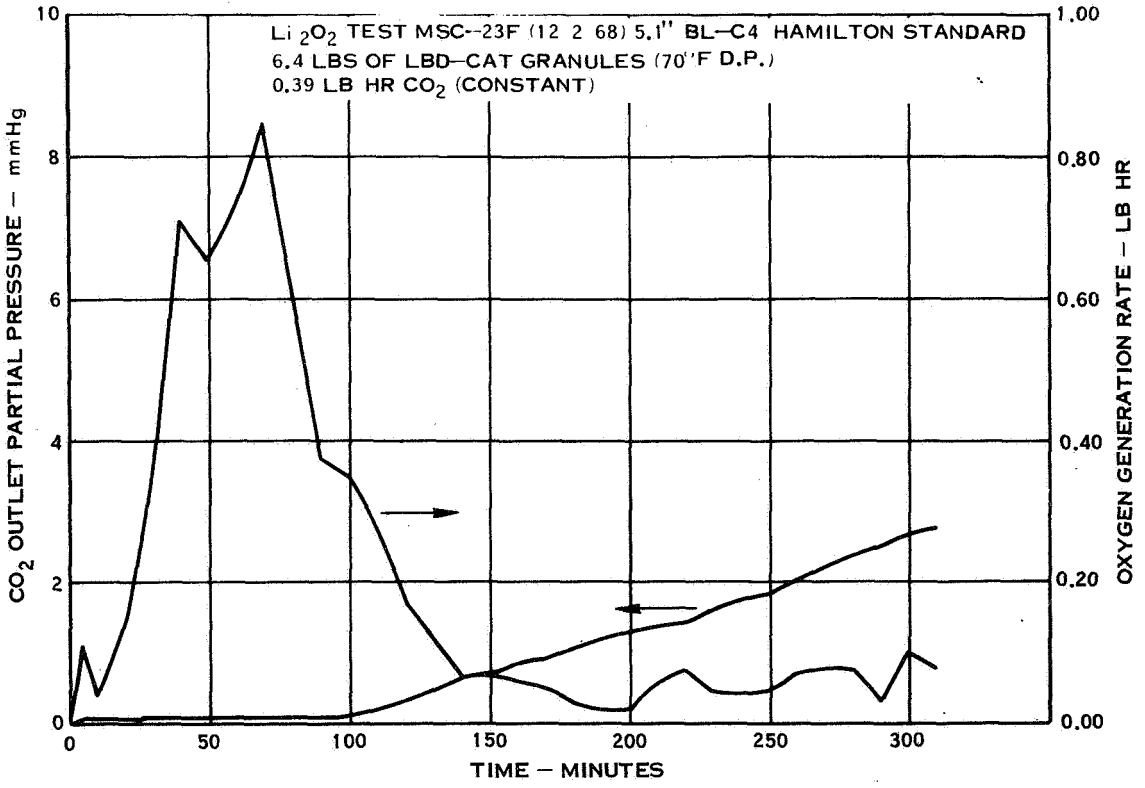

Figure 4-42. Lithium Peroxide Performance Data

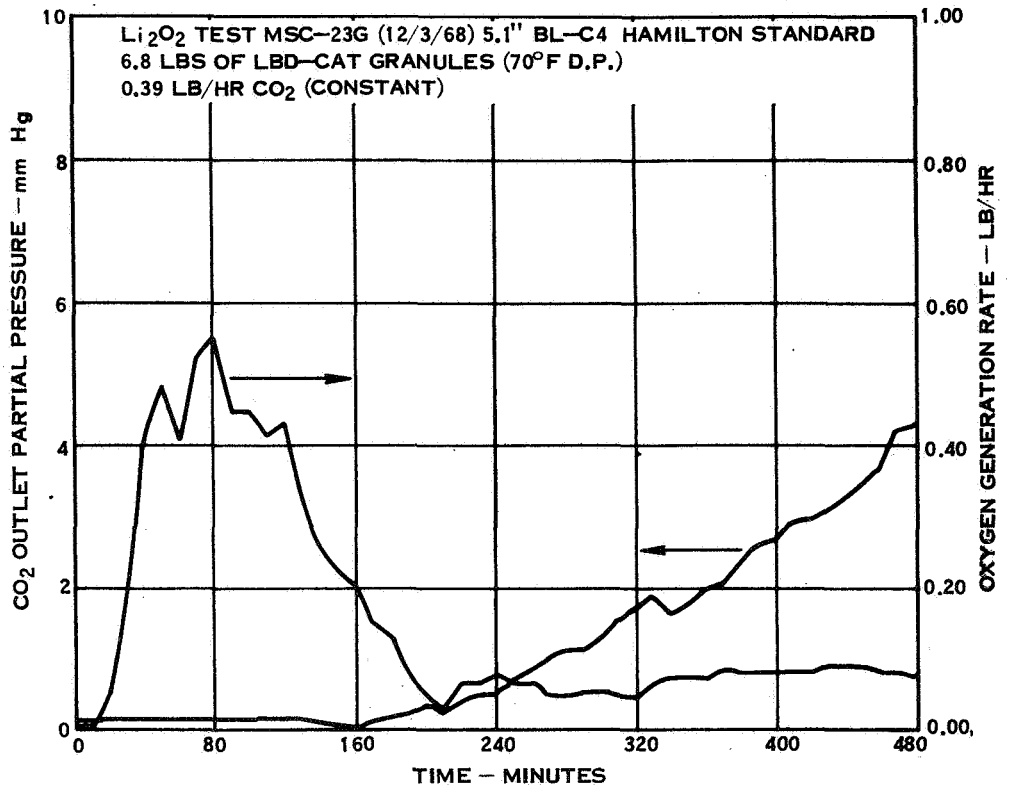

Figure 4-43. Lithium Peroxide Performance Data

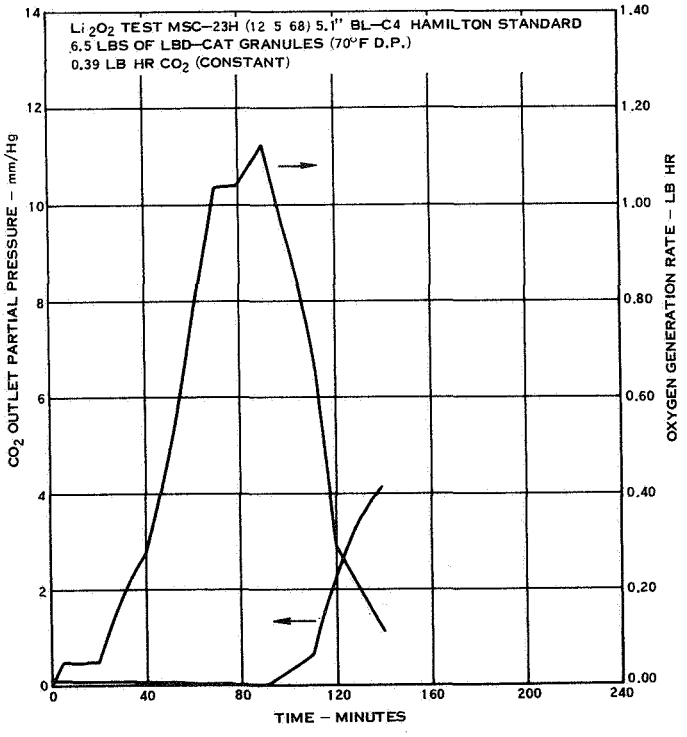

Figure 4-44. Lithium Peroxide Performance Plan

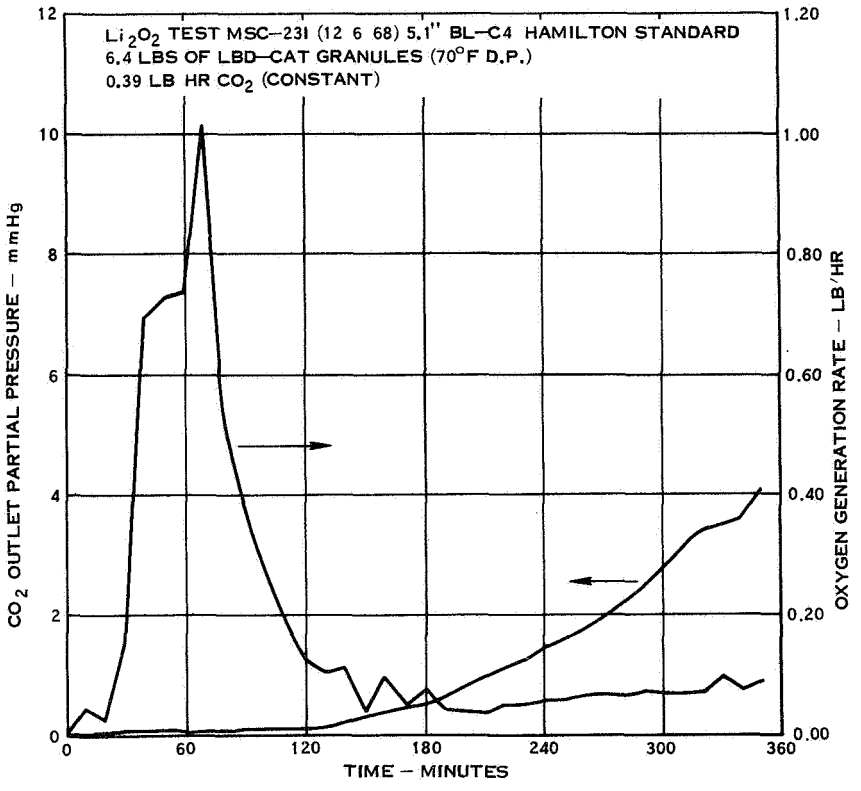

Figure 4-45. Lithium Peroxide Performance Data

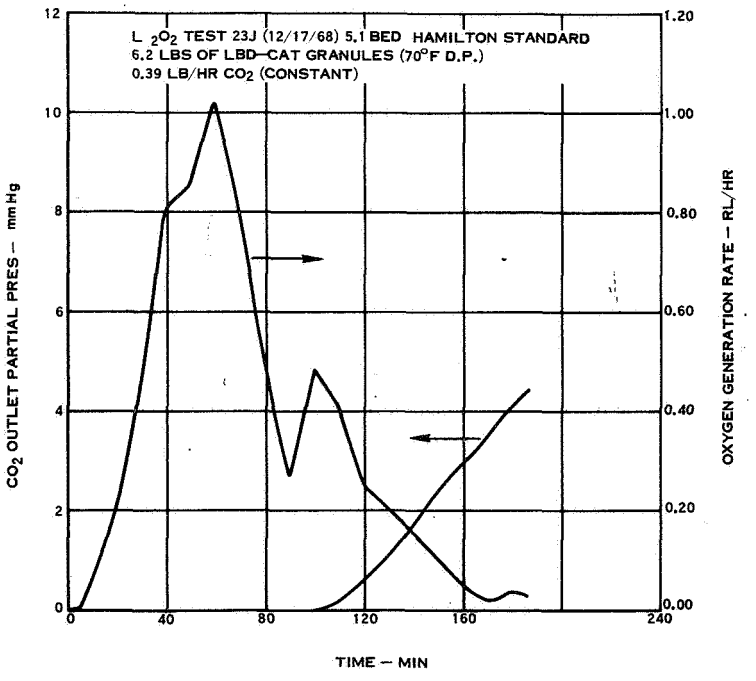

Figure 4-46. Lithium Peroxide Performance Data

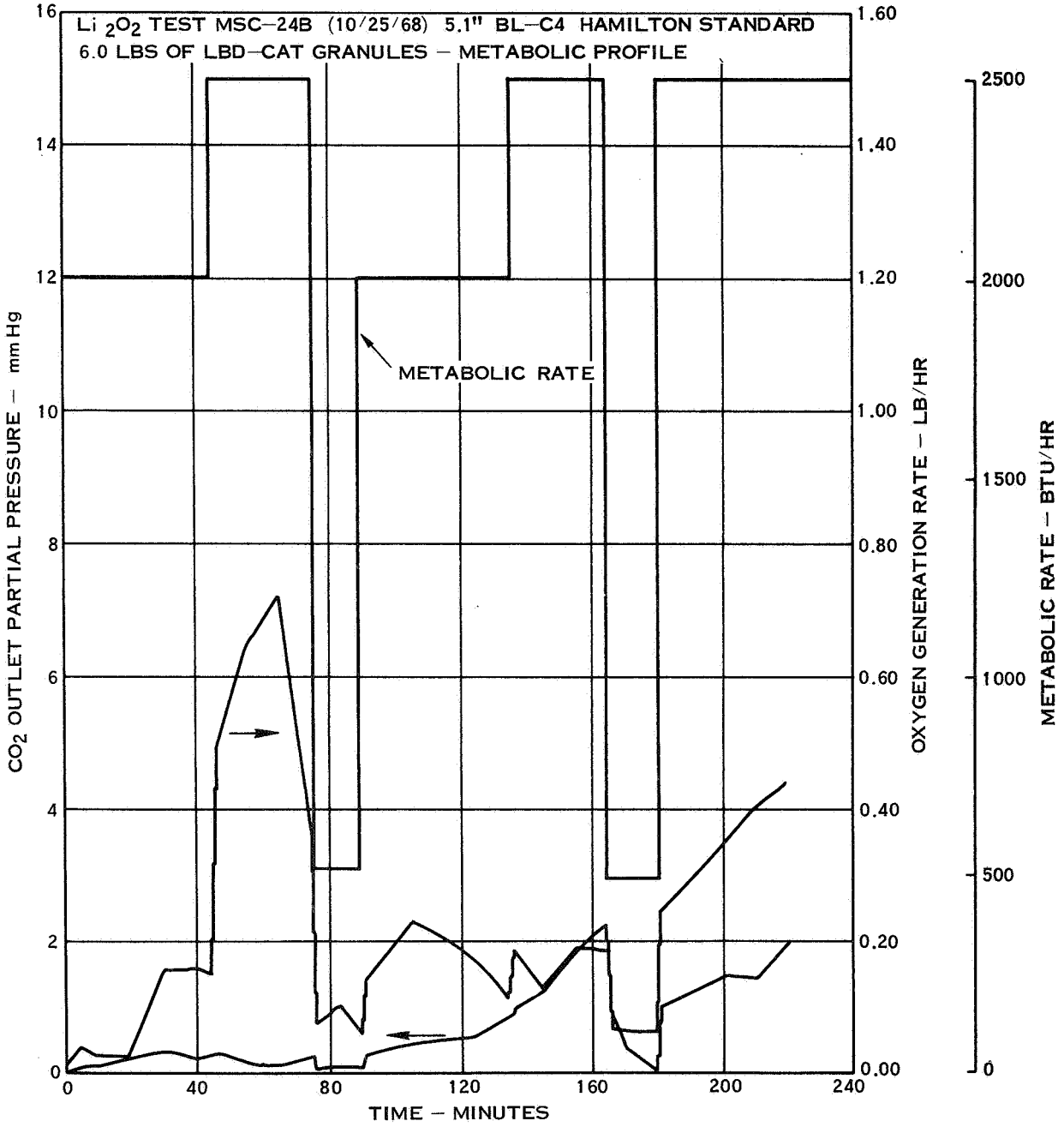

Figure 4-47. Lithium Peroxide Performance Plan

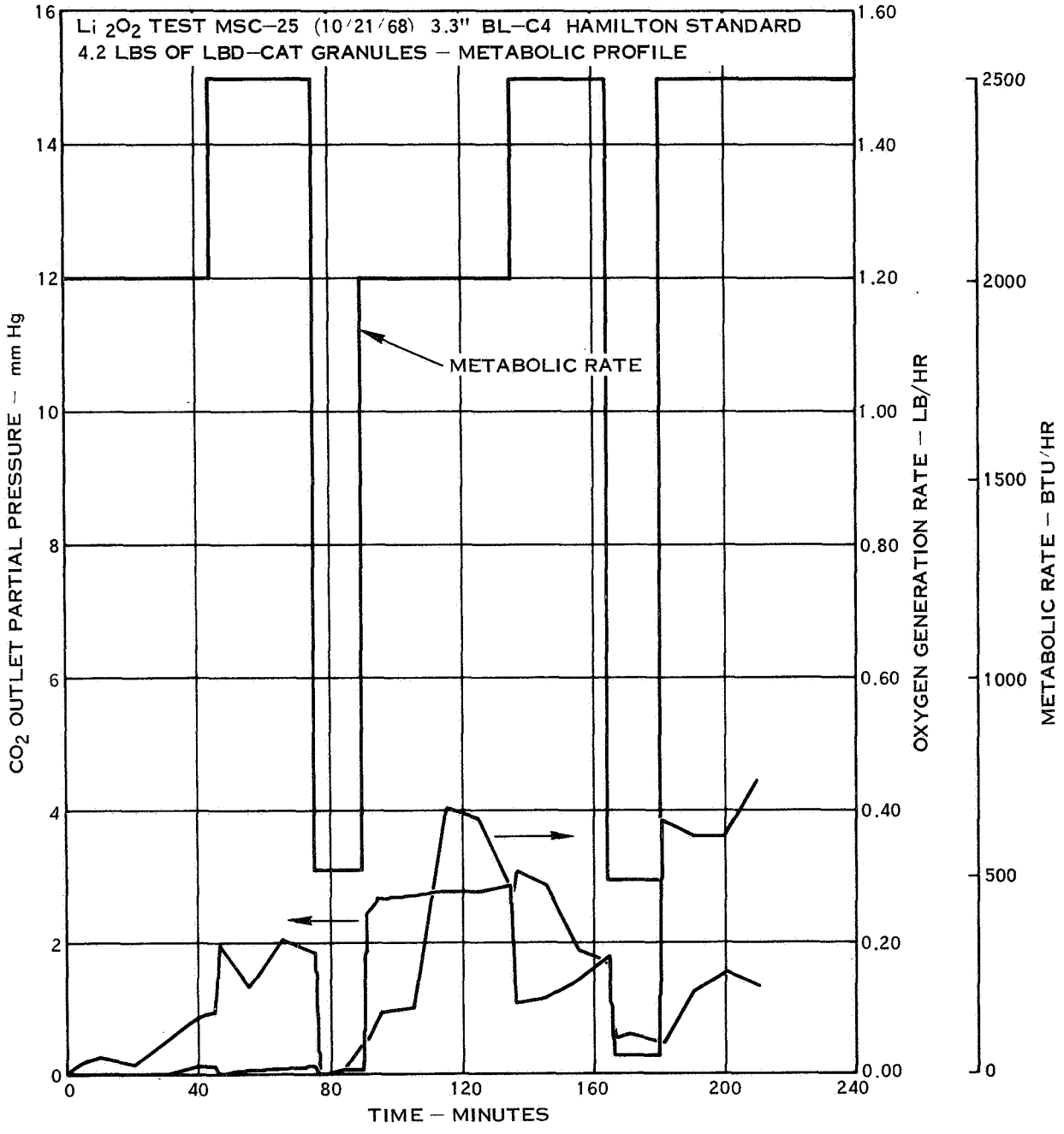

Figure 4-48. Lithium Peroxide Performance Plan

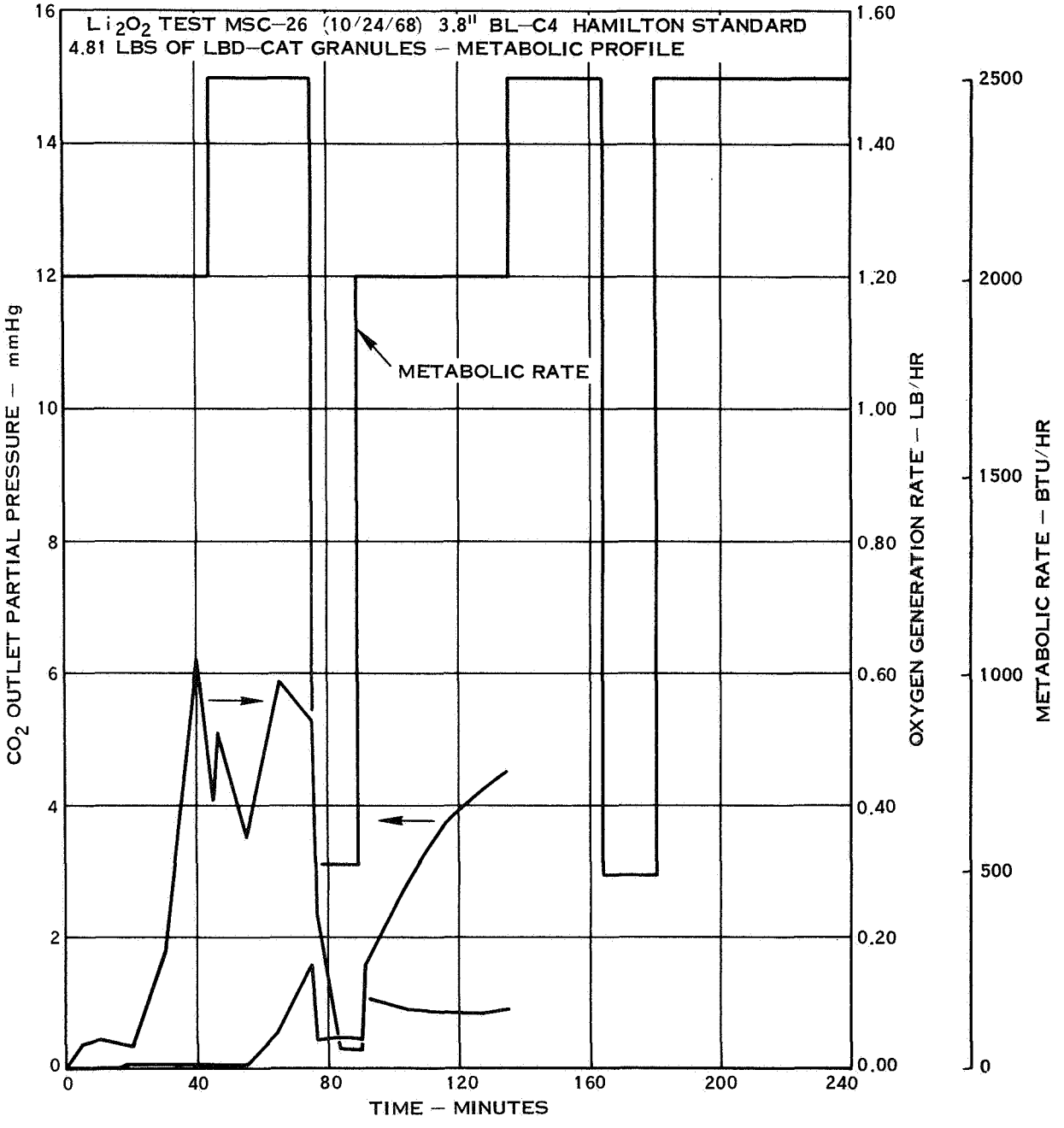

Figure 4-49. Lithium Peroxide Performance Plan

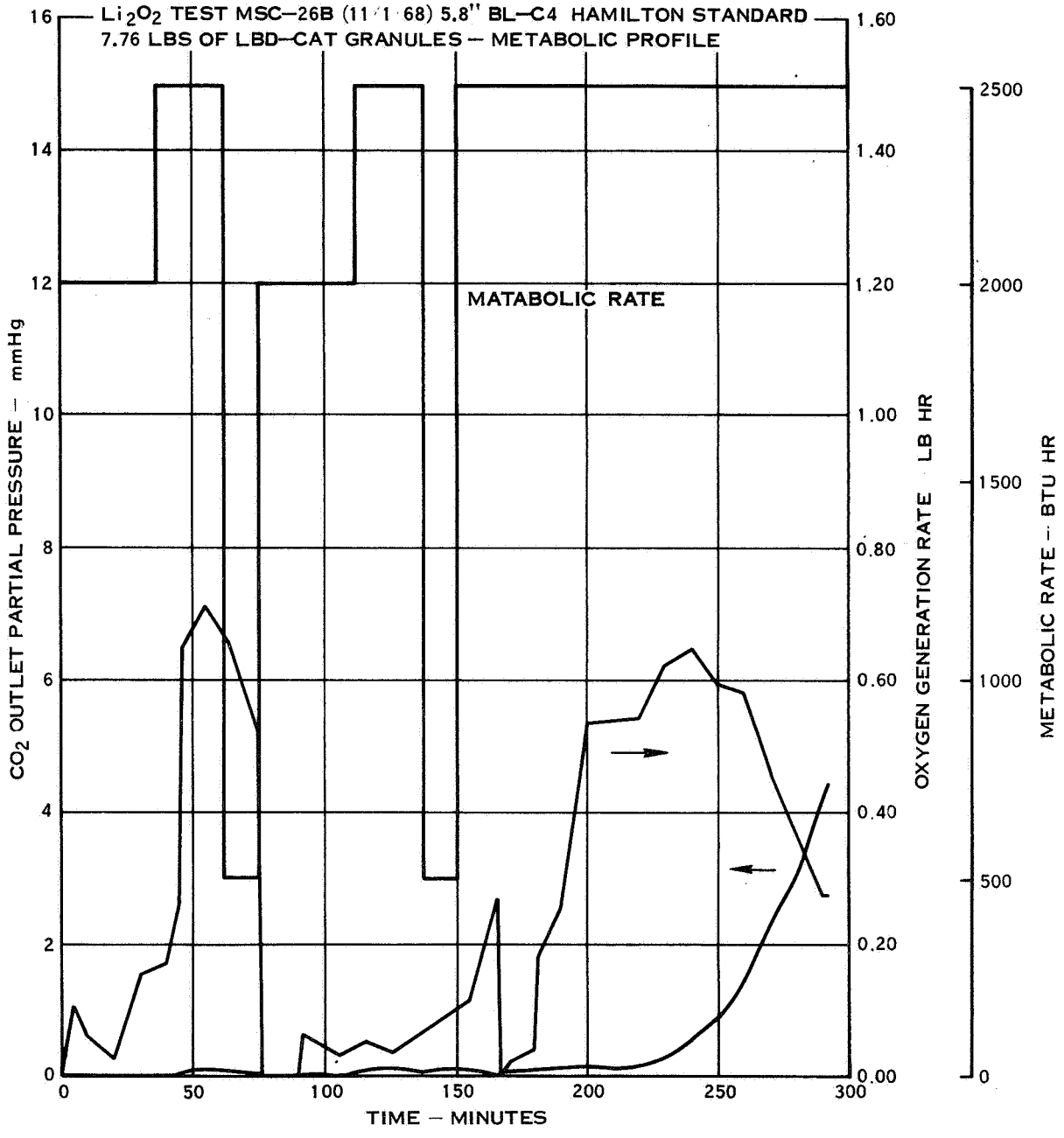

Figure 4-50. Lithium Peroxide Performance Data

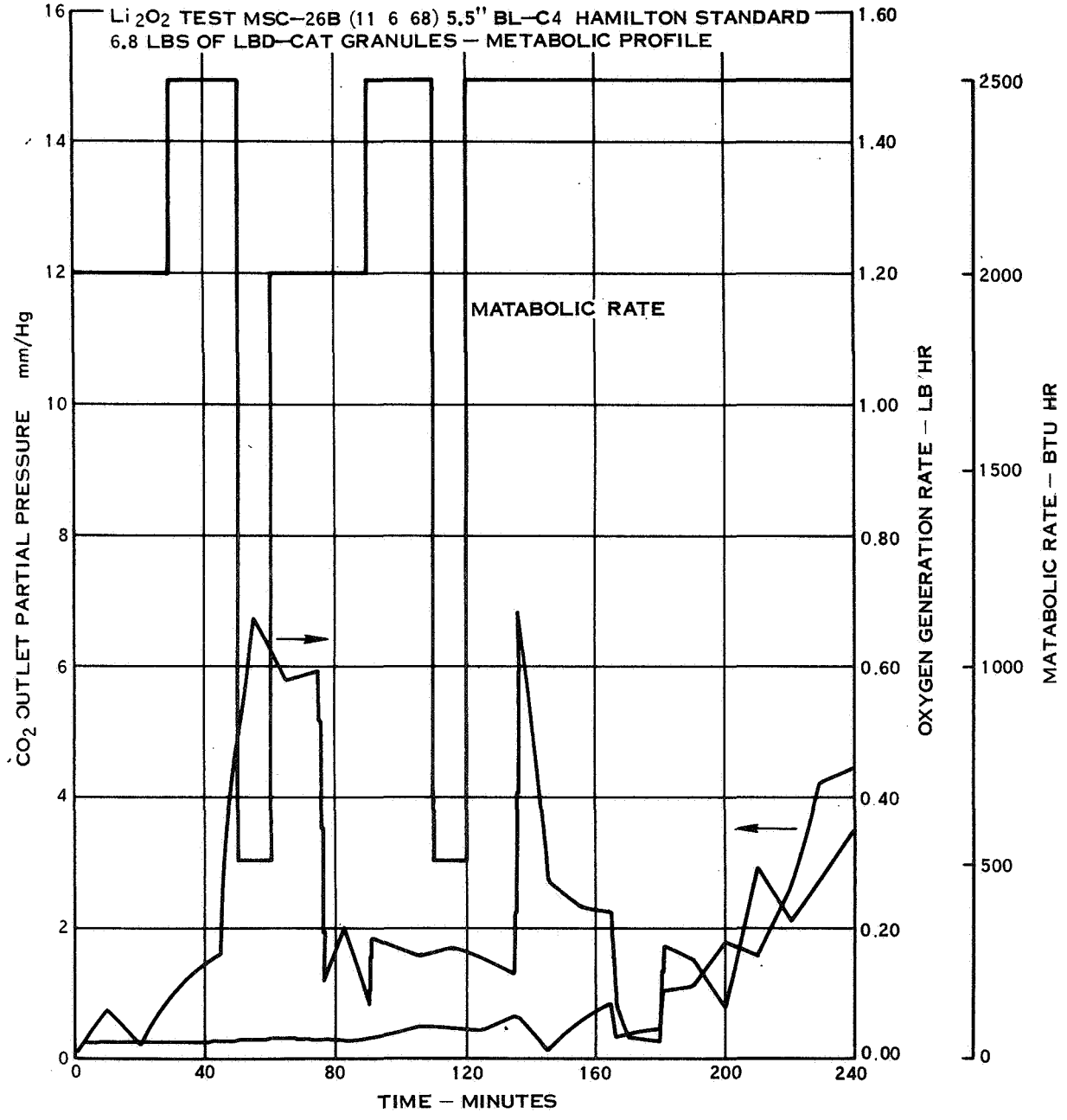

Figure 4-51. Lithium Peroxide Performance Data

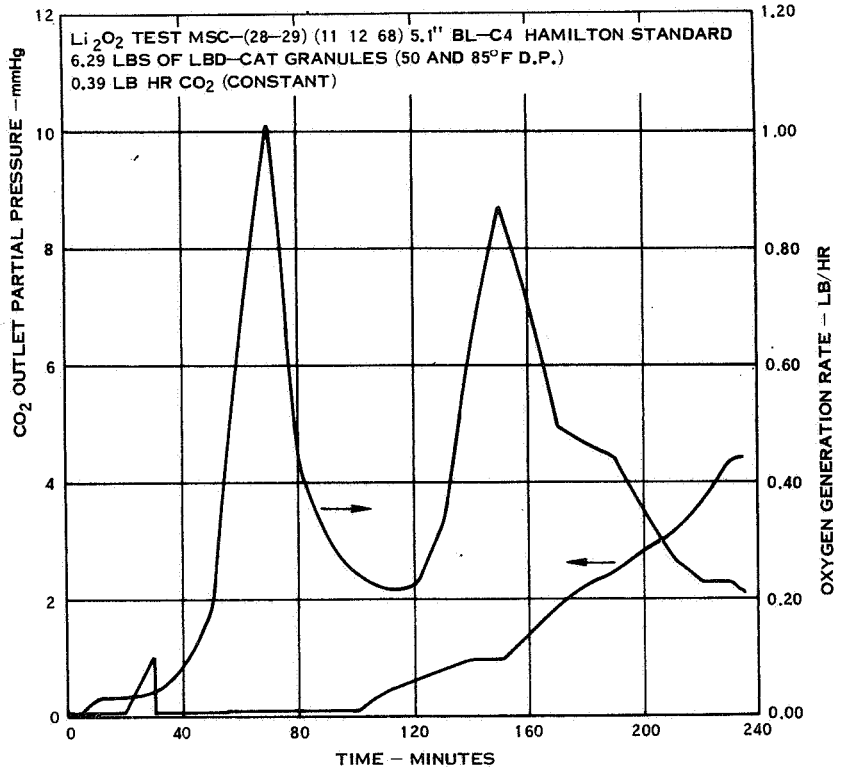

Figure 4-52. Lithium Peroxide Performance Plan

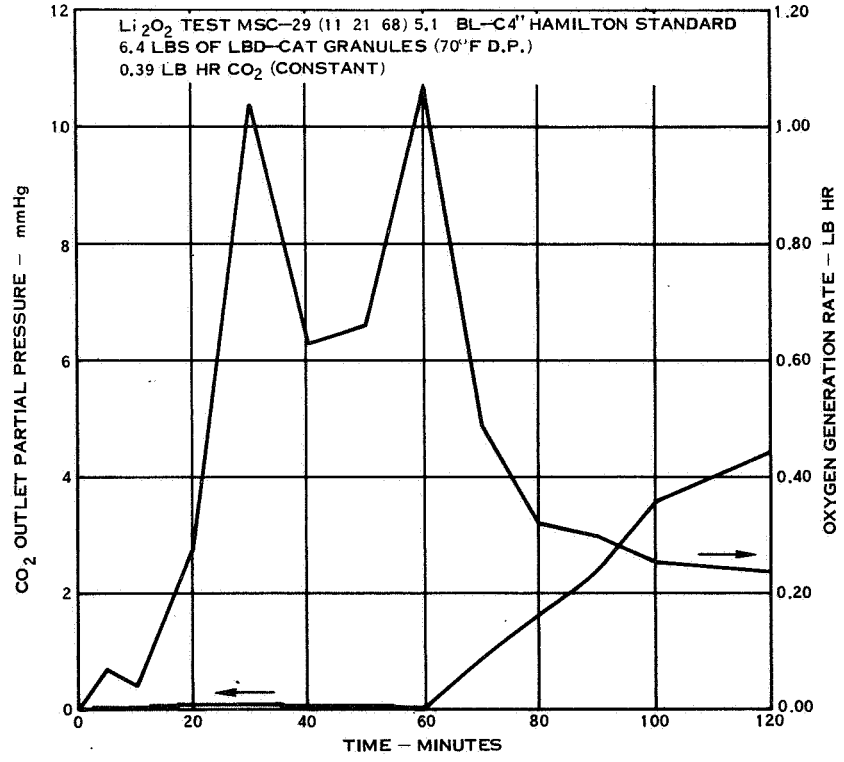

Figure 4-53. Lithium Peroxide Performance Plan

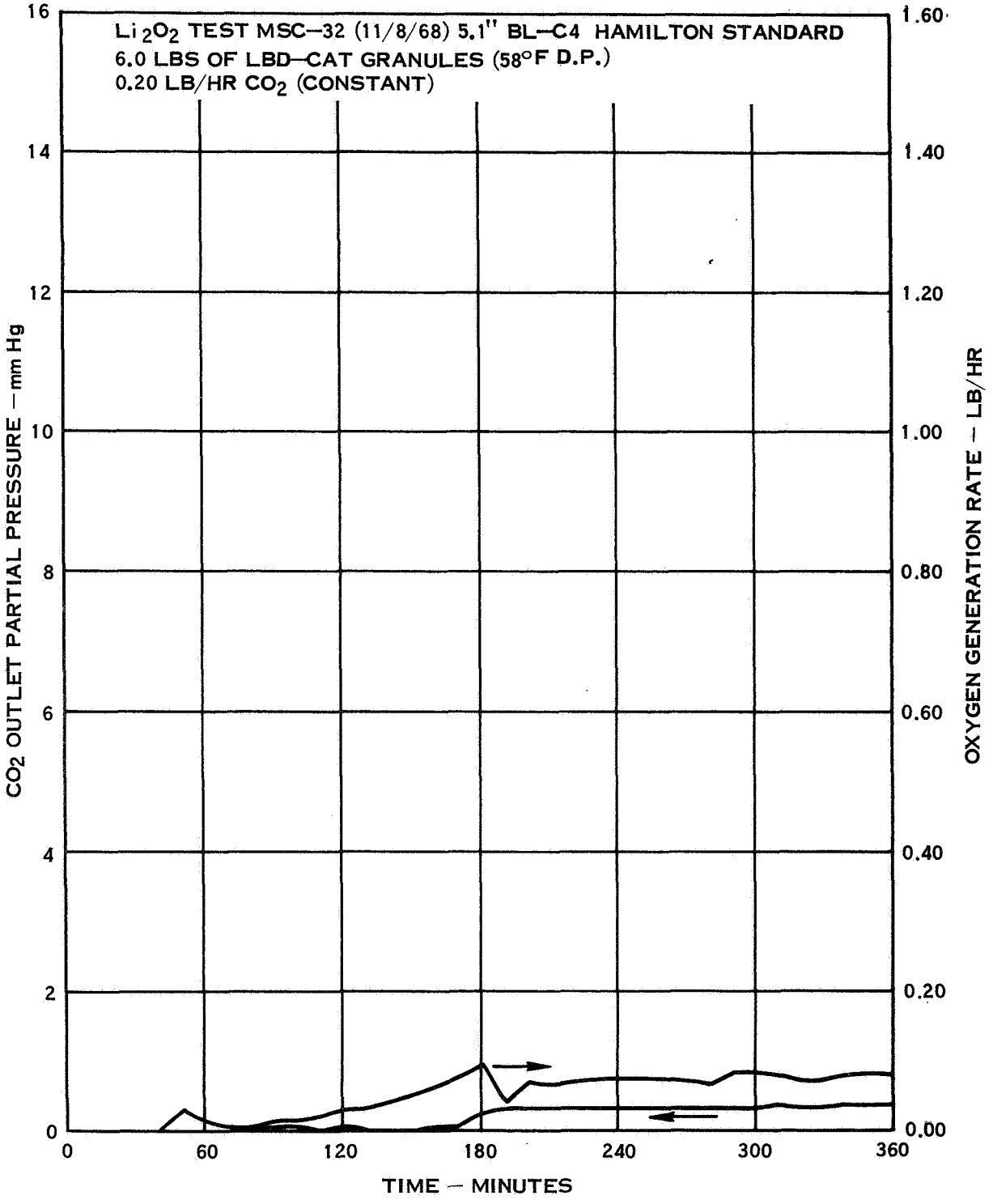

Figure 4-54. Lithium Peroxide Performance Plan

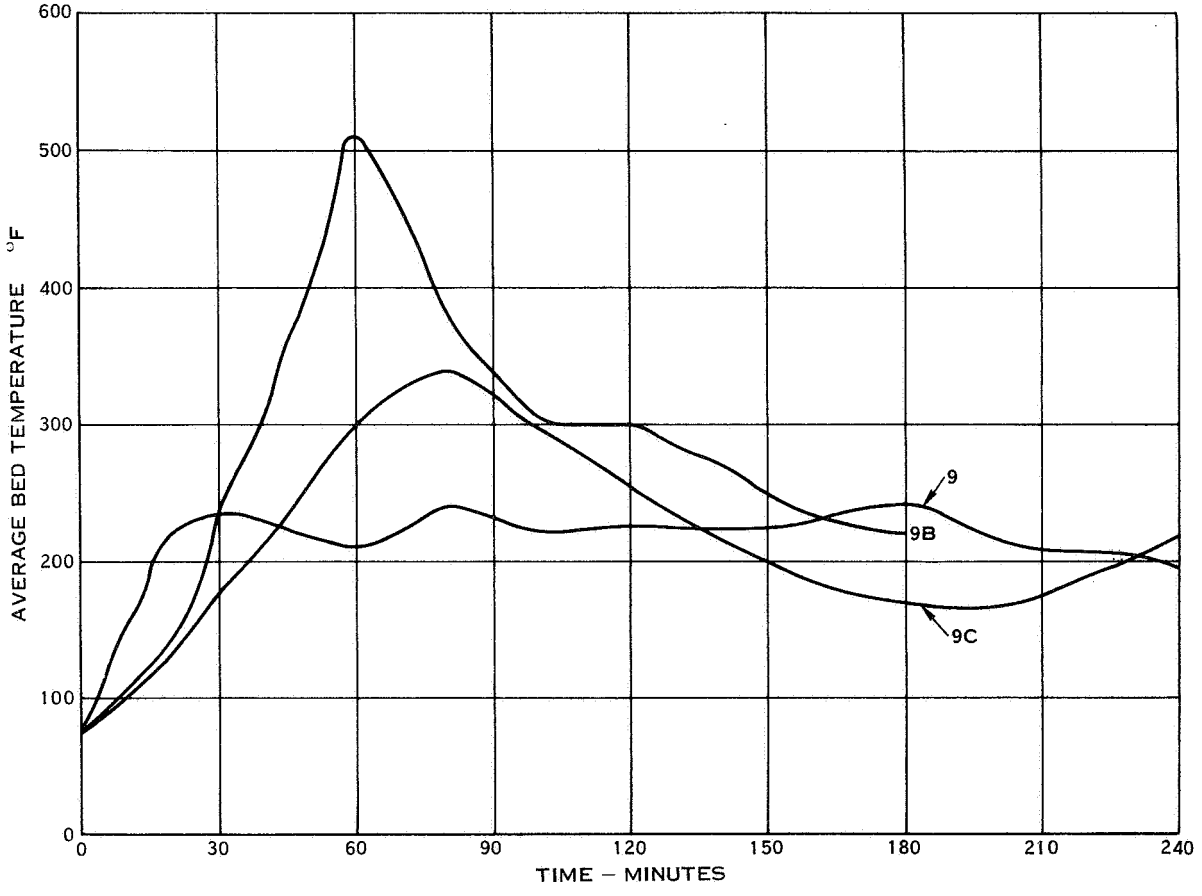

Figure 4-55. Average Bed Temperature Data

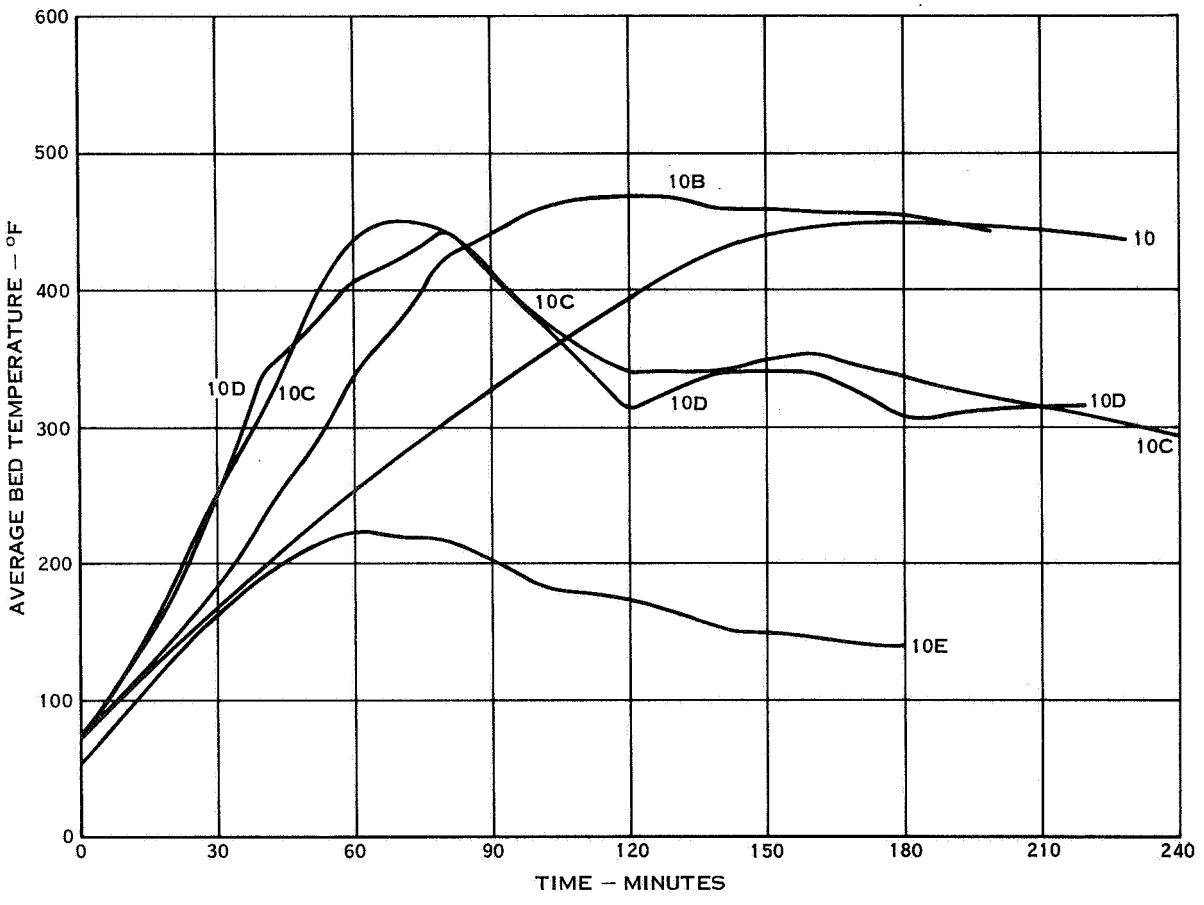

Figure 4-56. Average Bed Temperature Data

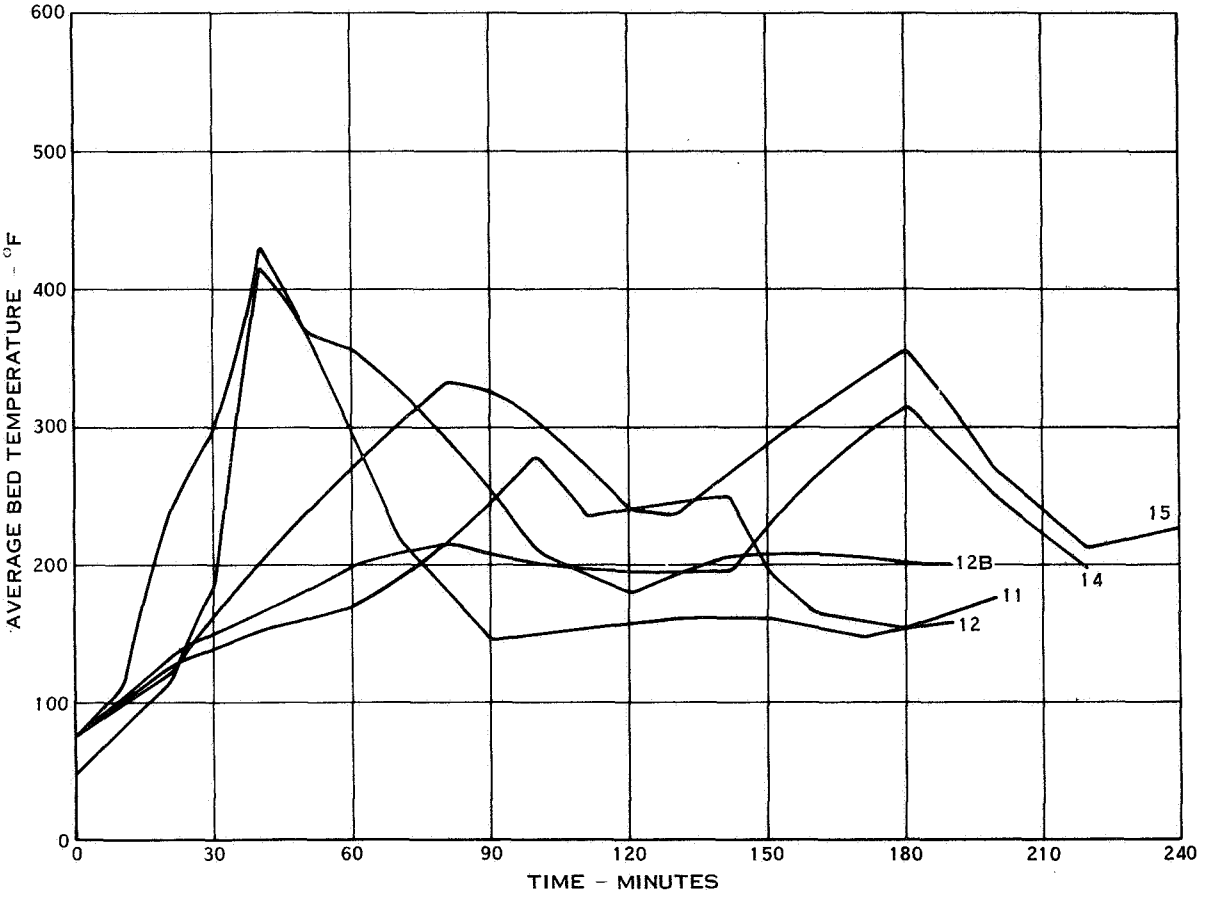

Figure 4-57. Average Bed Temperature Data

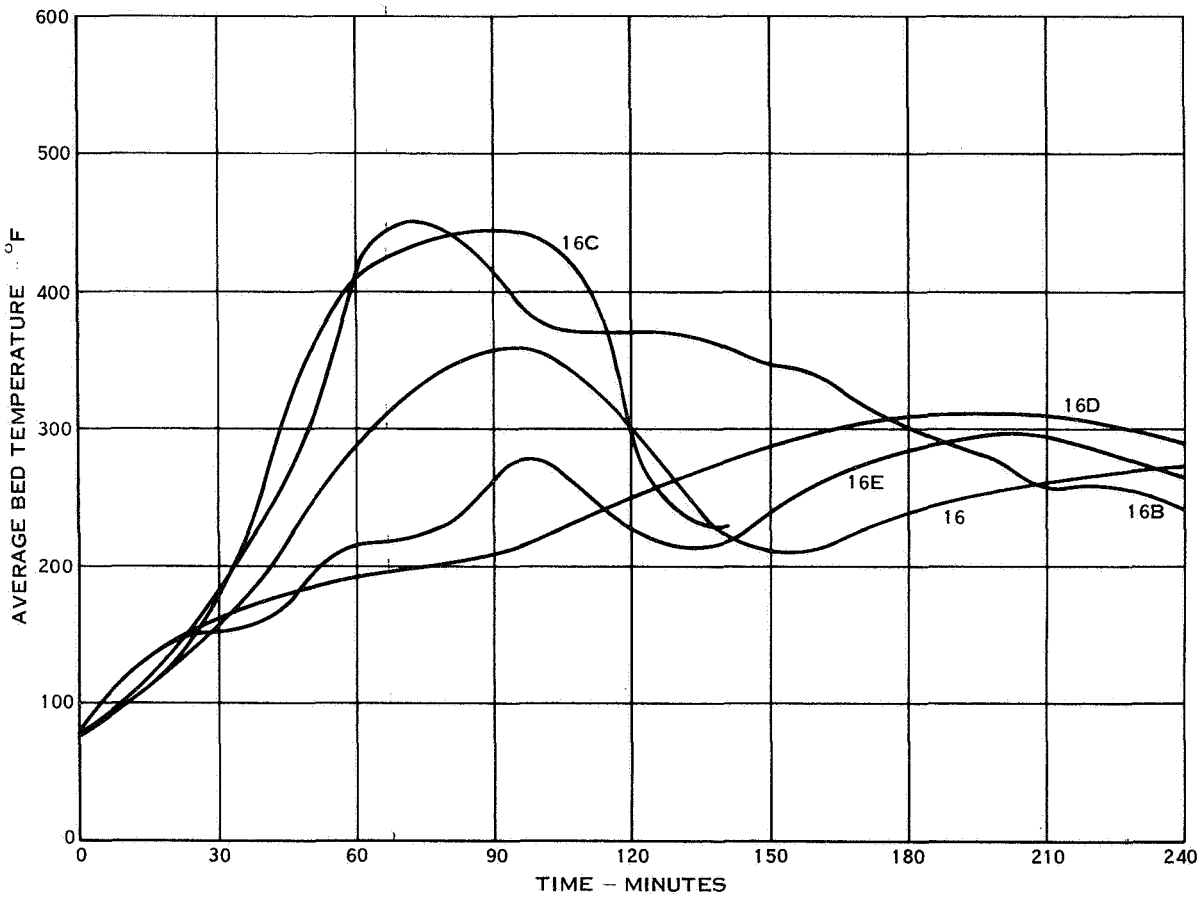

Figure 4-58. Average Bed Temperature Data

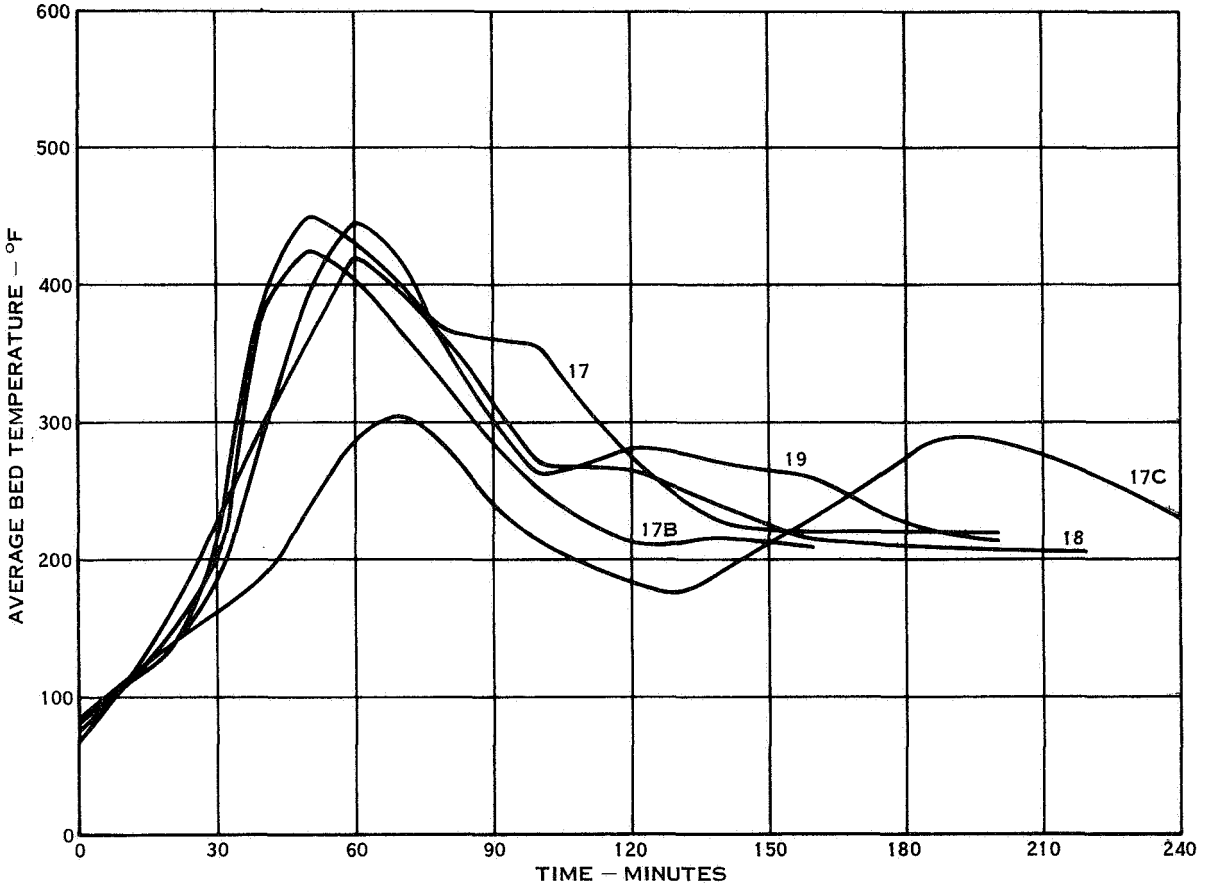

Figure 4-59. Average Bed Temperature Data

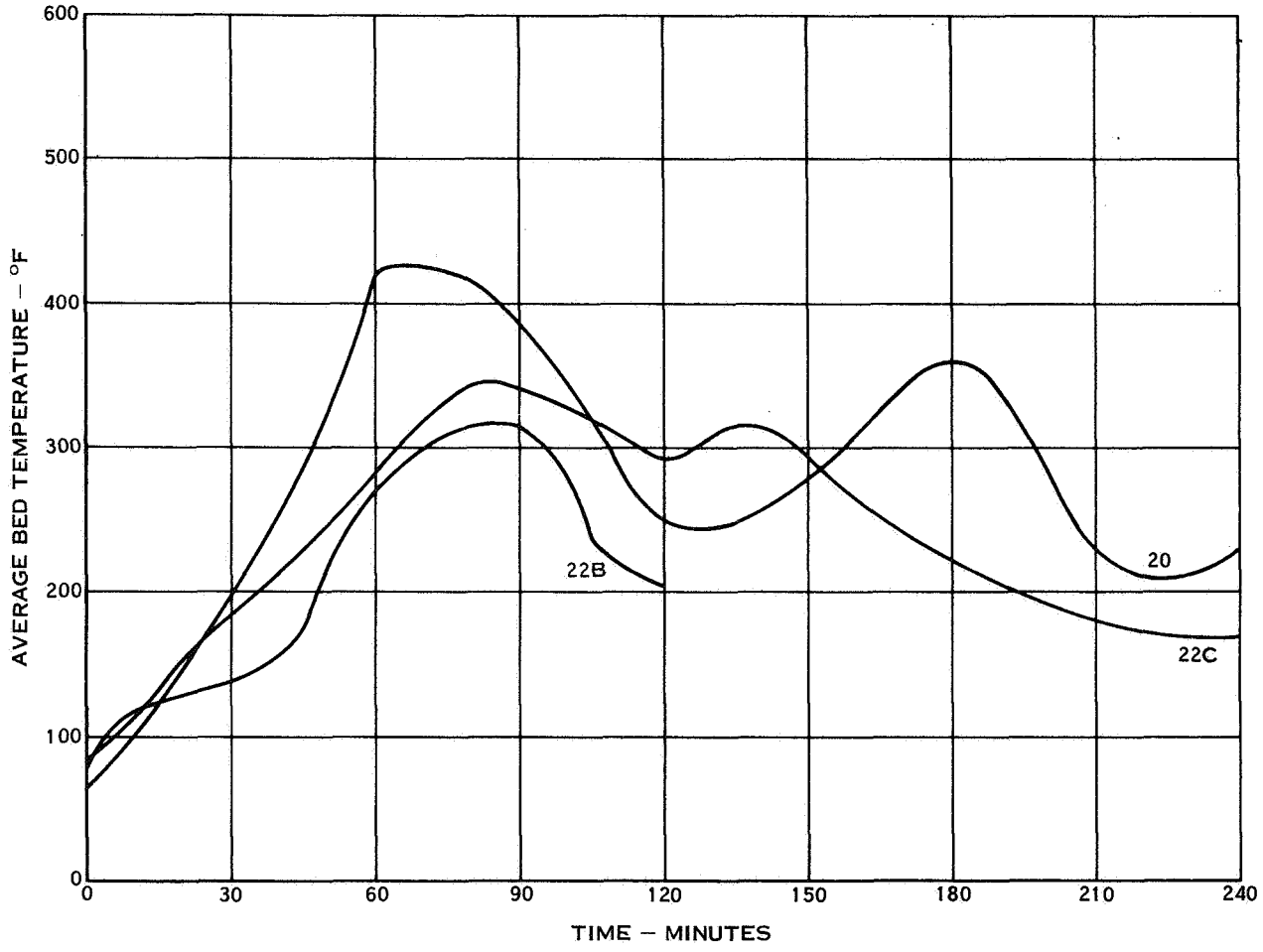

Figure 4-60. Average Bed Temperature Data

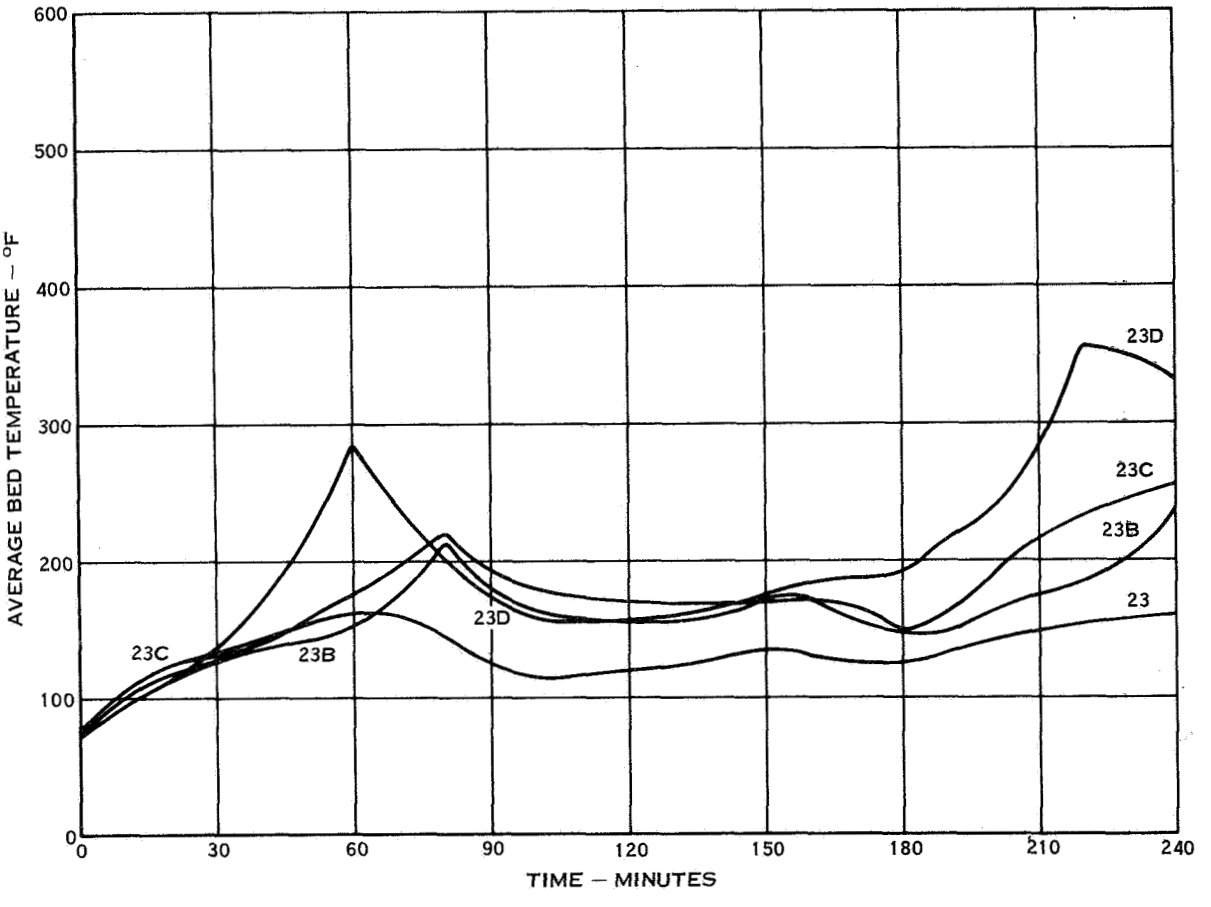

Figure 4-61. Average Bed Temperature Data

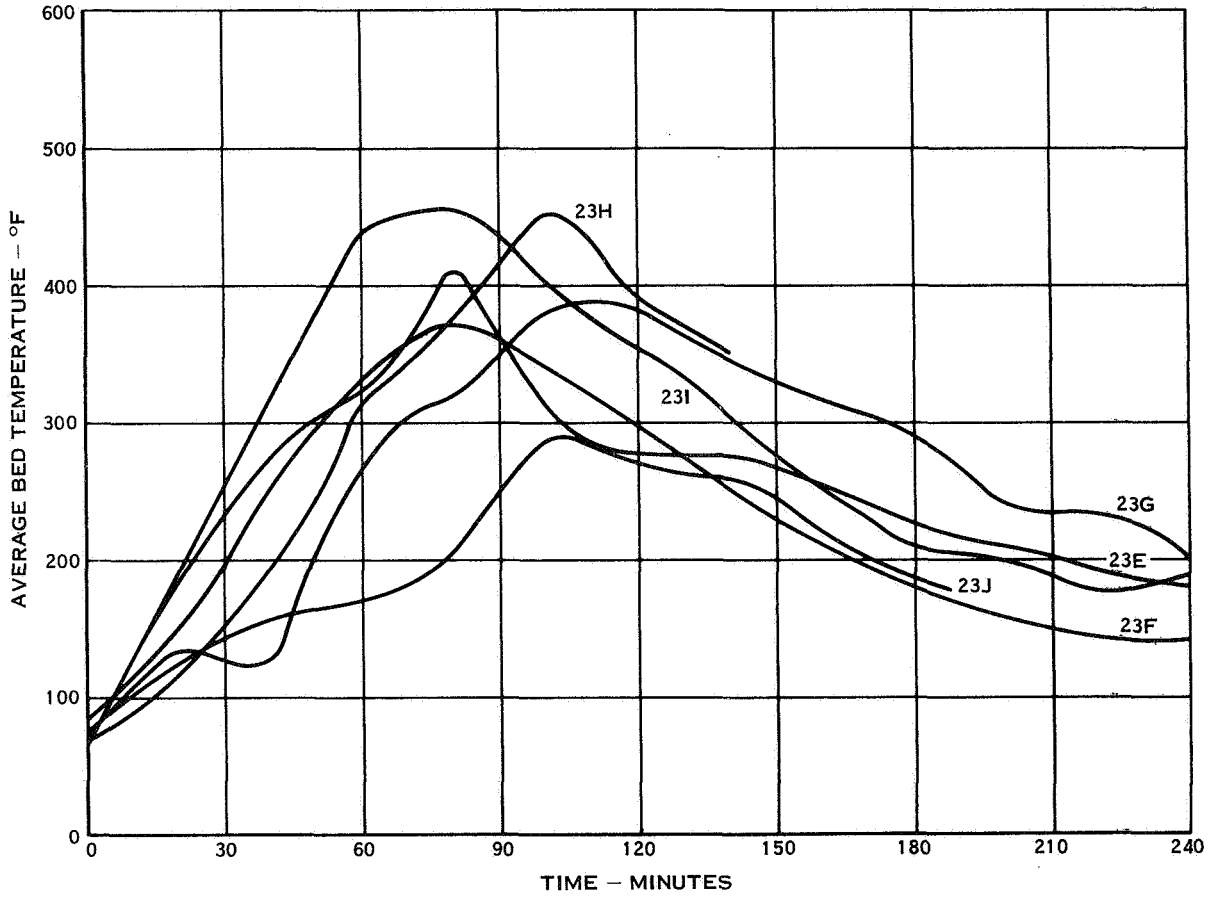

Figure 4-62. Average Bed Temperature Data

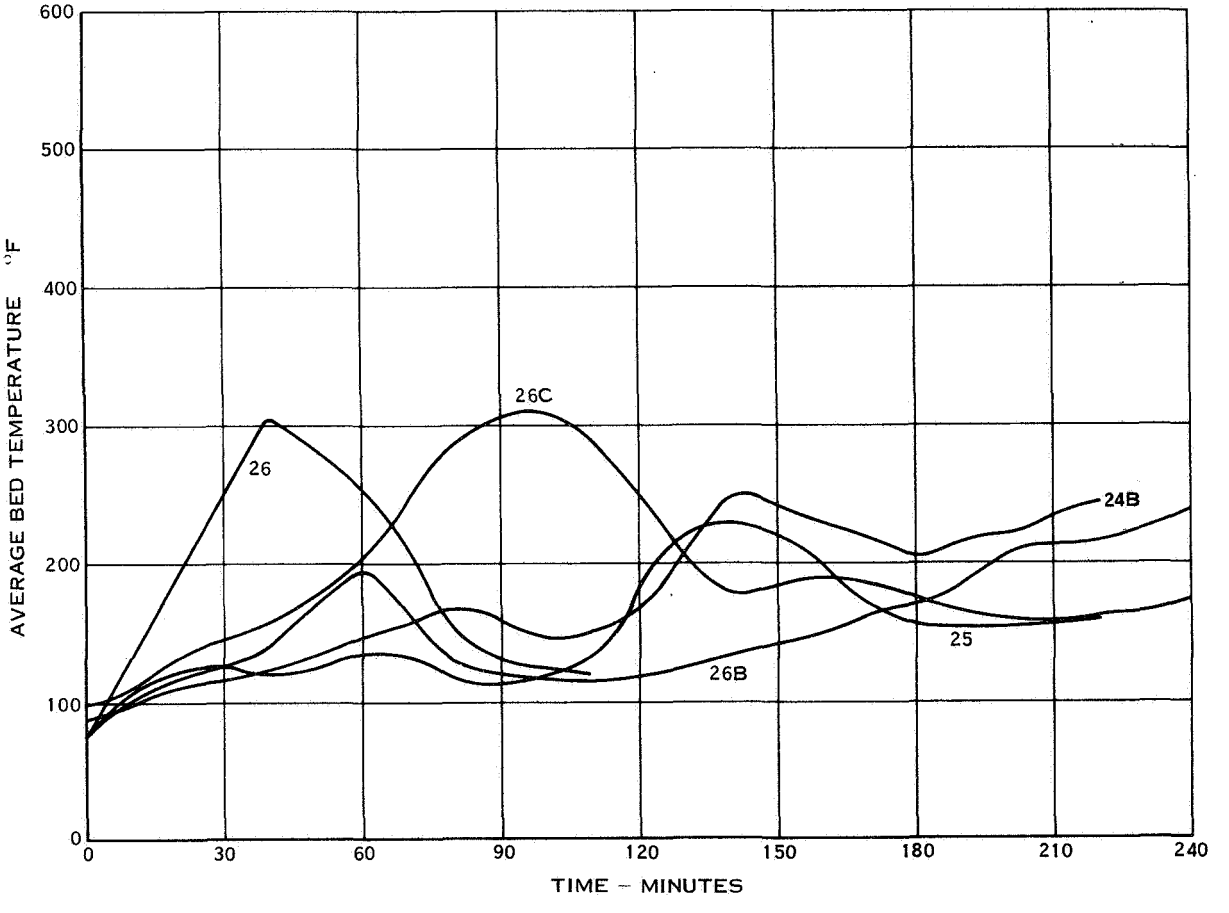

Figure 4-63. Average Bed Temperature Data

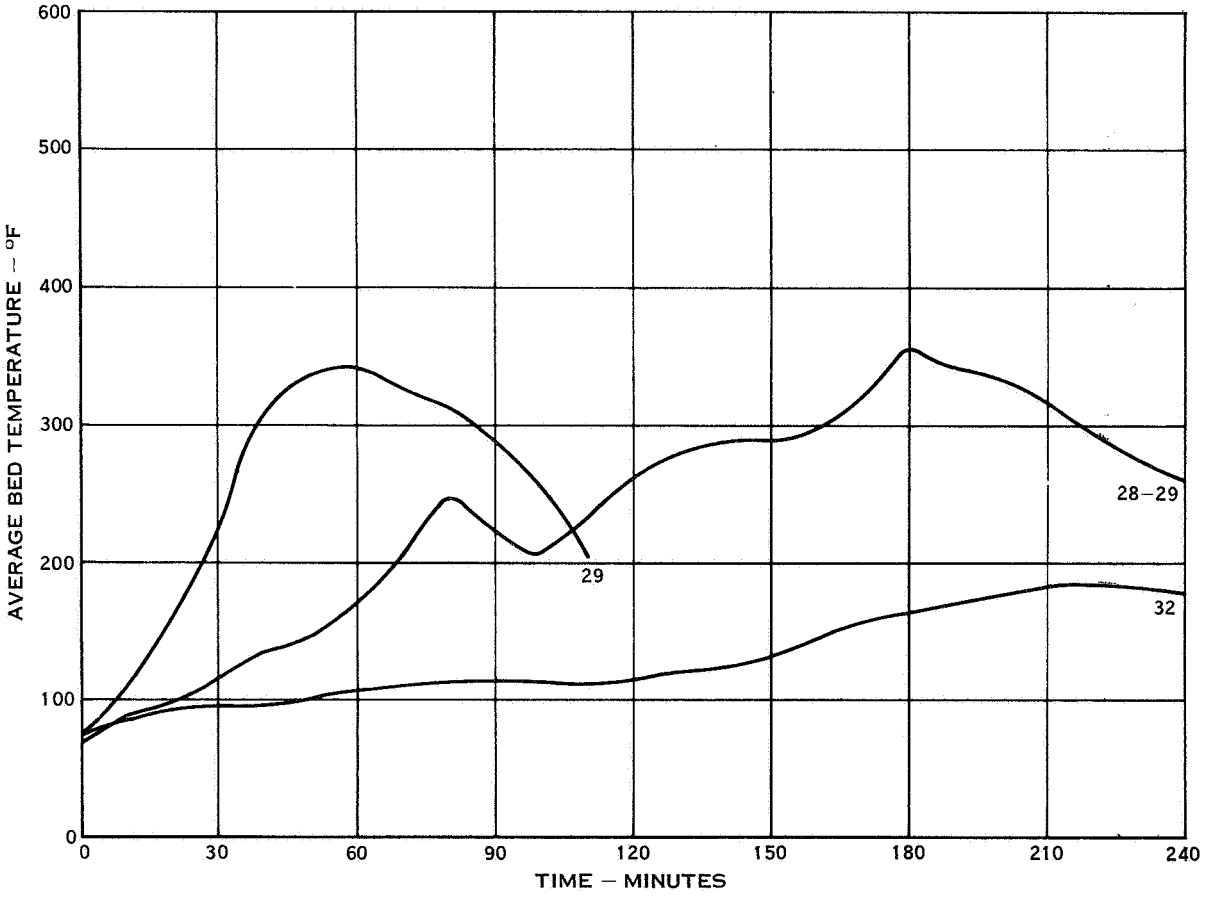

Figure 4-64. Average Bed Temperature Data

TABLE 4-1
TEST DATA SUMMARY

Test No.	Canister	Time (min.) to 0.5-1.0-4.0 mmHg	Weight (lb)	Avg. $\dot{m}_{O_2}$ (lb/hr)	Time $\dot{m}_{O_2}$> Spec. (min)	Useable O_2 (lb)	Total O_2 (lb)	O_2 Util. (%)	Total CO_2 (lb)	CO_2 Util. (%)	Chemical Type	Max. T. (°F)	Thermal Decomposition	Test Duration (min.)	Comments
MSC-1	Sm	120-135-190	1.32	0.14	42.	0.56	0.66	51.	0.55	46.	LBD	485.	No	240.	Scale Model Test
MSC-2	Sm	115-130-198	1.27	0.15	38.	0.60	0.72	57.	0.51	44.	HBD	541.	No	240.	
MSC-3	Sm	75-90-180	1.32	0.21	60.	0.63	0.90	68.	0.37	31.	LBD-CAT	526.	No	180.	
MSC-4	Sm	96-115-205	1.21	0.18	25.	0.72	0.84	74.	0.51	48.	LBD-CAT	486.	No	260.	
MSC-5	Sm	145-170-220	1.32	0.11	12.	0.44	0.44	33.	0.51	43.	LBD	346.	No	250.	
MSC-6a	Sm	40-62-150	1.32	0.13	0.	0.52	0.52	39.	0.51	42.	HBD	385.	No	240.	
MSC-6b	Sm	38-80-145	1.32	0.09	0.	0.20	0.20	15.	0.30	25.	HBD	281.	No	140.	
MSC-7a	Sm	140-150-186	1.32	0.13	14.	0.45	0.51	48.	0.45	42.	LBD-CAT	500.	No	210.	
MSC-7b	Sm	80-100-166	1.06	0.18	34.	0.63	0.72	70.	0.45	47.	LBD-CAT	442.	No	210.	
MSC-8	Sm	160-180-250	1.21	0.16	0.	0.64	0.75	63.	0.51	47.	LBD-CAT	338.	No	280.	Scale Model Test
MSC-9	2	125-142-225	3.24	0.12	0.	0.48	0.48	42.	1.55	54.	LBD-CAT	428.	No	260.	
MSC-9b	2	76-95-150	3.22	0.20	45.	0.63	0.82	77.	1.24	42.	LBD-CAT	622.	Yes	190.	
MSC-9c	2	90-125-225	3.25	0.16	25.	0.63	0.64	59.	1.57	53.	LBD-CAT	488.	No	280.	
MSC-10	2	28-60-162	4.52	0.21	52.	0.85	0.85	66.	1.55	38.	HBD	569.	No	240.	
MSC-10b	2	44-65-128	4.50	0.24	45.	0.80	0.83	56.	1.28	32.	HBD	608.	Yes	200.	
MSC-10c	2	75-85-160	3.75	0.20	35.	0.80	0.90	72.	1.56	46.	LBD	642.	Yes	240.	
MSC-10d	2	50-83-158	3.75	0.20	36.	0.73	0.79	63.	1.43	42.	LBD	631.	Yes	220.	
MSC-10e	2	60-100-174	3.72	0.13	0.	0.50	0.50	40.	1.56	47.	LBD	478.	No	240.	Cooling off at 180 min. P_{CO_2} dropped to 2.5 mmHg
MSC-11	1	40-104-160	3.40	0.13	22.	0.43	0.45	41.	1.30	42.	LBD-CAT	401.	No	200.	
MSC-12	1	0-60-168	3.10	0.14	20.	0.48	0.49	48.	1.37	49.		654.	Yes	210.	
MSC-12b	1	55-62-145	2.94	0.15	20.	0.47	0.52	54.	1.24	46.		594.	Yes	190.	
MSC-14	3	0-8-202	3.38	0.11	0.	0.43	0.43	38.	1.47	48.		309.	No	230.	
MSC-15	3	0-90-210	3.18	0.14	0.	0.53	0.53	52.	1.56	54.		542.	Slight	280.	
MSC-16	3	25-110-240	3.26	0.14	20.	0.58	0.62	58.	1.57	53.		560.	Slight	280.	
MSC-16b	3	20-100-205	3.13	0.15	30.	0.60	0.66	64.	1.57	55.		552.	Slight	255.	
MSC-16c	3	67-86-140	3.30	0.25	60.	0.58	0.72	65.	0.92	30.		592.	Yes	140.	
MSC-16d	3	145-185-280	3.70	0.12	0.	0.49	0.49	40.	1.56	47.		360.	No	290.	
MSC-16e	4	162-204-255	3.80	0.22	40.	0.88	0.94	31.	1.56	27.		412.	No	270.	Run in canister 4
MSC-17	2	70-85-135	3.30	0.15	40.	0.50	0.63	60.	1.30	43.		563.	Slight	200.	
MSC-17b	2	40-60-120	3.08	0.17	30.	0.44	0.53	52.	1.01	36.		618.	Yes	155.	
MSC-17c	2	40-70-185	3.14	0.17	40.	0.66	0.66	64.	1.52	55.		577.	Yes	245.	
MSC-18	2	65-90-172	3.42	0.16	38.	0.59	0.70	63.	1.44	46.		703.	Yes	220.	
MSC-19	2	60-80-148	3.32	0.18	42.	0.59	0.76	70.	1.27	42.		610.	Yes	195.	
MSC-20	3	70-95-195	3.23	0.13	22.	0.52	0.54	51.	1.56	53.		563.		240.	
MSC-22b	4	112-124-156	3.80	0.22	58.	0.59	0.75	60.	1.05	30.		644.	Yes	160.	
MSC-22c	4	110-155-222	4.20	0.14	45.	0.56	0.76	22.	1.56	30.		606.	Yes	240.	
MSC-23	4	210-248-356	6.00	0.11	0.	0.44	0.44	22.	1.60	30.		286.	No	360.	
MSC-23b	4	240-260-320	6.20	0.13	25.	0.52	0.56	28.	1.60	29.		449.	No	330.	
MSC-23c	4	180-210-277	6.29	0.16	15.	0.64	0.64	31.	1.60	28.		500.	No	290.	
MSC-23d	4	220-240-270	6.50	0.17	80.	0.68	1.10	51.	1.60	27.		633.	Yes	280.	
MSC-23e	4	185-204->300	6.40	0.16	30.	0.64	0.65	31.	1.56	27.		484.	No	310.	2 cooling coils
MSC-23f	4	130-175->300	6.40	0.17	65.	0.68	0.99	47.	1.56	27.		662.	Yes	310.	2 cooling coils
MSC-23g	4	240-270-465	6.80	0.21	85.	0.84	1.00	45.	1.57	26.		512.	No	490.	2 cooling coils
MSC-23h	4	105-112-137	6.50	0.15	75.	0.60	1.20	56.	1.20	16.		669.	Yes	140.	No cooling
MSC-23i	4	175-210-350	6.40	0.15	60.	0.60	0.94	45.	1.56	27.		626.	Yes	350.	2 cooling coils
MSC-23j	4	120-130-180	6.20	0.23	55.	0.68	1.05	50.	1.11	20.		635.	Yes	185.	2 cooling coils - shocked during operation
MSC-24b	4	120-138-210	6.00	0.16	30.	0.62	0.70	36.	1.42	27.		458.	No	220.	
MSC-25	4	90-90-205	4.2	0.14	15.	0.49	0.50	36.	1.35	36.		518.	No	210.	
MSC-26	4	64-70-120	4.8	0.21	50.	0.45	0.48	30.	0.82	20.		621.	Yes	135.	
MSC-26b	4	240-250-290	7.76	0.19	105.	0.76	0.95	38.	1.59	22.		618.	Yes	290.	
MSC-26c	4	120-190-228	6.80	0.18	40.	0.72	0.88	40.	1.60	26.		568.	Slight	240.	
MSC-28-29	4	112-142-225	6.30	0.25	114.	1.00	1.40	68.	1.52	28.		617.	Yes	235.	Combined test
MSC-29	4	70-75-110	6.40	0.29	55.	0.58	0.91	43.	0.79	13.		694.	Yes	120.	
MSC-32	4	>370	6.00	0.05	0.	0.20	0.20	8.	0.80	15.	LBD-CAT	258.	No	370.	0.5 mmHg never reached

TABLE 4-2
CHEMICAL ANALYSIS SUMMARY

Test No.	Canister No.	Initial O_2 Content* cc/g	Final O_2 Content* cc/gram				Final Carbon Dioxide Content* cc/gram			
			Sample 1	Sample 2	Sample 3	Average	Sample 1	Sample 2	Sample 3	Average
MSC-5	SM	244.0	101.8	99.1	—	100.5	170.0	174.7	—	172.4
MSC-6b	SM	274.5	204.8	—	—	204.8	113.8	—	—	113.8
MSC-7b	SM	232.6	56.0	—	—	56.0	182.8	—	—	182.8
MSC-8	SM	232.6	66.4	64.4	—	65.4	198.2	200.5	—	199.4
MSC-9	2	218.5	18.4	19.1	—	18.8	233.4	241.0	—	237.2
MSC-9b	2	218.5	27.8	28.1	—	28.0	175.0	188.8	—	181.9
MSC-11	1	238.2	108.0	112.5	92.6	104.4	192.8	173.2	147.2	171.1
MSC-12	1	250.7	109.8	58.2	77.7	84.9	147.8	196.2	200.5	181.5
MSC-12b	1	228.5	50.7	36.8	47.3	44.9	225.6	192.0	156.4	191.3
MSC-9C	2	218.5	39.8	32.4	15.8	29.3	239.0	235.0	212.5	228.7
MSC-10e	2	242.5	97.6	88.8	46.6	77.7	199.0	204.3	204.0	202.4
MSC-17	2	228.5	58.2	31.1	84.4	57.9	221.1	176.2	133.3	176.9
MSC-17c	2	234.7	59.5	29.8	8.73	32.7	246.0	234.0	191.0	224.0
MSC-18	2	250.7	83.9	57.1	34.4	58.5	213.8	179.5	147.2	180.2
MSC-19	2	234.7	50.0	24.2	25.2	33.0	222.0	189.2	138.4	183.0
MSC-14	3	238.2	123.0	99.4	92.5	105.0	163.8	188.0	189.8	180.5
MSC-15	3	228.5	45.6	38.3	38.5	40.8	225.5	230.0	248.5	234.7
MSC-16	3	228.5	40.5	37.0	43.1	40.2	234.0	231.0	252.0	239.0
MSC-16b	3	234.7	36.4	31.0	40.3	36.0	225.0	226.0	234.0	228.5
MSC-20	3	228.5	35.6	34.2	34.4	34.7	228.0	235.0	228.0	230.3
MSC-22b	4	238.4	91.6	56.8	27.9	58.8	120.4	157.8	174.8	151.0
MSC-22c	4	234.7	91.2	42.8	70.8	68.4	159.6	215.6	173.2	182.8
MSC-23	4	229.4	40.0	75.9	27.9	58.8	206.4	167.6	174.8	182.9
MSC-23b	4	233.3	109.8	70.6	39.6	73.3	169.2	151.4	209.0	176.5
MSC-23c	4	234.0	99.6	136.0	37.0	90.9	184.2	122.8	236.0	181.0
MSC-23d	4	234.7	52.8	29.0	49.6	43.8	142.2	164.6	145.0	150.6
MSC-23e	4	234.7	156.0	108.0	55.8	106.7	111.4	158.0	216.0	161.5
MSC-23f	4	234.7	105.0	59.2	66.4	77.0	140.0	180.0	191.0	170.2
MSC-24b	4	232.0	157.2	79.0	91.2	109.1	101.0	170.2	123.0	131.4
MSC-25	4	234.0	130.2	98.0	68.6	98.9	153.0	186.6	199.2	179.6
MSC-26c	4	234.7	157.0	68.8	54.7	93.7	114.6	145.4	168.4	142.7
MSC-16e	4	234.7	93.6	26.6	30.6	50.3	146.2	222.0	237.6	201.9

* Adjusted to 75°F & 14.7 PSIA

TABLE 4-3

COMPARISON OF CHEMICAL ANALYSIS AND TEST RESULTS

Test No.	Canister No.	Total CO_2 Removed ~ Lbs			Total O_2 Generated ~ Lbs			Final Bed Weight ~ Lbs		
		Chemical Analysis	Test Data	Ratio W_{ca}/W_{td}	Chemical Analysis	Test Data	Ratio W_{ca}/W_{td}	Measured	Calculated	Ratio W_m/W_c
MSC-5	SM	0.50	0.53	0.94	0.21	0.15	1.40	—	1.59	—
MSC-6b	SM	0.32	0.30	1.07	0.058	0.063	0.92	—	1.55	—
MSC-7b	SM	0.44	0.45	0.98	0.22	0.25	0.88	—	1.34	—
MSC-8	SM	0.58	0.60	0.97	0.23	0.27	0.85	—	1.61	—
MSC-9	2	1.96	2.03	0.97	0.82	0.71	1.15	—	4.58	—
MSC-9b	2	1.29	1.24	1.04	0.78	0.82	0.95	—	3.92	—
AVG.		----	----	1.00	----	----	1.03	----	----	—
MSC-11	1	1.36	1.30	1.05	0.46	0.46	1.00	4.40	4.26	1.03
MSC-12	1	1.33	1.37	0.97	0.57	0.49	1.16	4.07	3.90	1.04
MSC-12b	1	1.22	1.24	0.98	0.67	0.52	1.29	3.54	3.48	1.02
AVG.		----	----	1.00	----	----	1.15	----	----	1.03
MSC-9C	2	1.83	1.83	1.00	0.86	0.74	1.16	—	4.45	—
MSC-10e	2	1.98	1.75	1.13	0.58	0.55	1.06	—	5.42	—
MSC-17	2	1.33	1.30	1.02	0.673	0.66	1.02	4.18	3.63	1.15
MSC-17c	2	1.66	1.59	1.04	0.79	0.66	1.20	4.12	3.95	1.04
MSC-18	2	1.38	1.44	0.96	0.80	0.71	1.13	4.27	4.32	0.99
MSC-19	2	1.31	1.27	1.03	0.85	0.77	1.10	3.98	4.05	0.98
AVG.		----	----	1.03	----	----	1.11	----	----	1.04
MSC-14	3	1.29	1.47	0.88	0.51	0.43	1.19	3.98	4.35	0.92
MSC-15	3	1.79	1.83	0.98	0.73	0.63	1.16	4.22	4.19	1.01
MSC-16	3	1.90	1.83	1.04	0.74	0.68	1.09	4.41	4.28	1.03
MSC-16b	3	1.75	1.65	1.06	0.76	0.68	1.12	4.25	4.35	0.98
MSC-20	3	1.64	1.57	1.04	0.78	0.54	1.44	4.25	3.68	1.15
AVG.		----	----	1.00	----	----	1.20	----	----	1.02
MSC-22b	4	1.17	1.05	1.11	0.86	0.75	1.15	4.30	4.33	0.99
MSC-22c	4	1.67	1.56	1.07	0.84	0.76	1.11	5.09	5.34	0.95
MSC-23	4	2.40	2.56	0.94	1.16	1.09	1.06	7.30	7.27	1.01
MSC-23b	4	2.39	2.33	1.04	1.18	0.93	1.27	7.50	7.50	1.00
MSC-23c	4	2.43	2.00	1.21	1.12	0.77	1.46	7.47	7.85	0.95
MSC-23d	4	2.01	1.92	1.05	1.57	1.37	1.15	7.43	5.90	1.26
MSC-23e	4	2.24	2.02	1.11	0.89	0.75	1.19	7.70	7.98	0.97
MSC-23f	4	2.36	2.01	1.17	1.20	1.06	1.13	7.70	8.15	0.95
MSC-24b	4	1.60	1.44	1.11	1.09	0.70	1.56	6.75	6.97	0.97
MSC-25	4	1.62	1.35	1.20	0.64	0.50	1.28	5.02	5.28	0.95
MSC-26c	4	1.90	1.60	1.19	1.19	0.88	1.35	7.40	8.02	0.92
MSC-16e	4	1.78	1.75	1.02	0.85	0.99	0.86	4.91	5.00	0.98
AVG.		----	----	1.09	----	----	1.22	----	----	1.00

14. Evidence of the occurrence of thermal decomposition

15. Total test duration (minutes)

The test program was composed of four test series which were designed to investigate the effect on lithium perioxide performance of chemical bulk density, catalyst addition, bed geometry, bed temperature, quantity of chemical, and off-design conditions. A brief description of these test series is as follows:

1. Chemical Form Evaluation - Three chemical forms were evaluated. These were granules having high bulk density, low bulk density, and low bulk density, catalyzed with 2% nickel sulfate to promote oxygen evolution. A total of 18 tests, MSC-1 through MSC-10e, were conducted during this series. The results demonstrated that the granules catalyzed with 2% nickel sulfate showed superior performance.

2. Bed Temperature/Geometry Evaluation - Three distinct canister geometries were evaluated at varied temperature levels during this series. These canisters, defined in Section 3.6, varied in inlet face area but had nearly identical chemical volume capacities. Canister 2 had twice the inlet face area of canister 1 and canister 3 had an inlet face area three times that of canister 1. A total of 13 tests, MSC-11 through MSC-20 but not including MSC-16 tests subsequent to MSC-16b, were run for this series. Canister 3, with the largest face area (92.5 in^2) was shown to provide the best overall performance and temperature was found to be the major parameter affecting lithium peroxide performance. It is felt that canister geometry is of secondary effect on performance and canister 3 may have performed best because, with it, bed temperature control was the best.

3. Chemical Weight Evaluation - A total of 12 tests, MSC-22 through MSC-26c, were conducted for this series, using canister 4 which had the same face area as canister 3, but had a larger bed capacity (8 lb of lithium peroxide maximum). These tests again showed that the most significant parameter affecting lithium peroxide performance is the bed temperature. If allowed to exceed the lithium peroxide thermal decomposition temperature; the oxygen evolution performance improves but the carbon dioxide removal performance degrades rapidly.

4. Off-Design Performance Evaluation - An off-design evaluation test series, consisting of the 9 tests defined in Section 3.0, was planned. However, during unloading of the bed after test MSC-28-29, a void area, about 1.0-1.5 inches in diameter and 1.5-2.0 inches long was discovered. At this point, the program was redirected to use the remaining tests to investigate the cause of the void in lieu of completing the off-design test series.

As a matter of coincidence, this bed also was the first one to be vibrated during loading. It was decided to isolate the potential causes of the void and evaluate them individually. The causes considered were:

1. Vibration
2. Internal bed coolant temperature
3. Canister geometry
4. Cooling coil design
5. Inlet dew point

It is believed that the void was caused by condensate which formed on the bed interval cooling coil and subsequently dissolved granules in that area of the bed. Tests 16c and 16d were run as repeats of previous tests using canister 3 but were vibrated during loading. No void area existed after the tests and the performance was as expected. The vibration during loading was ruled out as the cause for the void and canister 3, was investigated. Tests MSC-16e, 22c, and 23e were conducted in that order using cold water cooling. No void area occurred until MSC-23e which utilized 6.4 lb of Li_2O_2. A golf ball size void was observed in the bed during unloading. The next test, MSC-23f, was run using hot water coolant (90°-100°F) and no void area occurred. A repeat of the previous test was made using cold water cooling, and this bed (MSC-23g) produced a void area. These tests showed quite conclusively that the problem was due to condensate forming on the cooling coils and subsequently destroying a portion of the bed. As further verification, MSC-23h was run with no cooling and did not have a void area.

At this point, two tests remained to be conducted. It was decided that the first test would be a repeat of a previous test (MSC-23g) that produced a void and to reverse the inlet/outlet connections to the cooling coil to see if the location of the void changed. This test, MSC-23i, did produce a void area and its location was reversed from that in MSC-23g. In each case, the void area was downstream of the coldest part of the cooling coil. The final test of this program, MSC-23j, was run to investigate the performance degradation that would occur if a void occurred during actual mission operation. For this test, the canister was subjected to random shock and vibration loading during testing. This test produced a hole and the performance was worse than for MSC-23i; but the granule bed did not settle due to being shocked. The bed appearance after testing was identical to that for MSC-23i. Based upon this test series, it is concluded that cooling with cold water causes a void downstream of the coldest area of the coil and a cooling coil redesign will be necessary to eliminate the occurrence of a void.

4.2 Chemical Analysis Data

In order to confirm the validity of the measured test results, chemical analyses were made of post-mortem samples of the test beds. These samples were analyzed to

determine the amount of carbon dioxide removed and the quantity of oxygen evolved. The results of the chemical analysis are shown in Table 4-2 and a comparison of these with the measured test results is shown in Table 4-3. These results show excellent agreement for carbon dioxide removal and good agreement with the oxygen evolution test results. It is believed that the discrepancy in the oxygen evolution results was due to past test oxygen evolution during the period that the canister was cooling prior to being unloaded.

Three samples were taken for each test bed and the locations from which these were removed is as defined as follows.

CHEMICAL SAMPLE LOCATION

Canister	Sample 1	Sample 2	Sample 3
Scale model	Random	Random	Random
Canister 1	Front of bed	Middle of bed	Rear of bed
Canister 2	Front of bed	Middle of bed	Rear of bed
Canister 3	Left side of bed	Middle of bed	Right side of bed
Canister 4	Top of bed	Middle of bed	Bottom of bed

The chemical analysis data was measured using the apparatus shown in Figure 4-65.

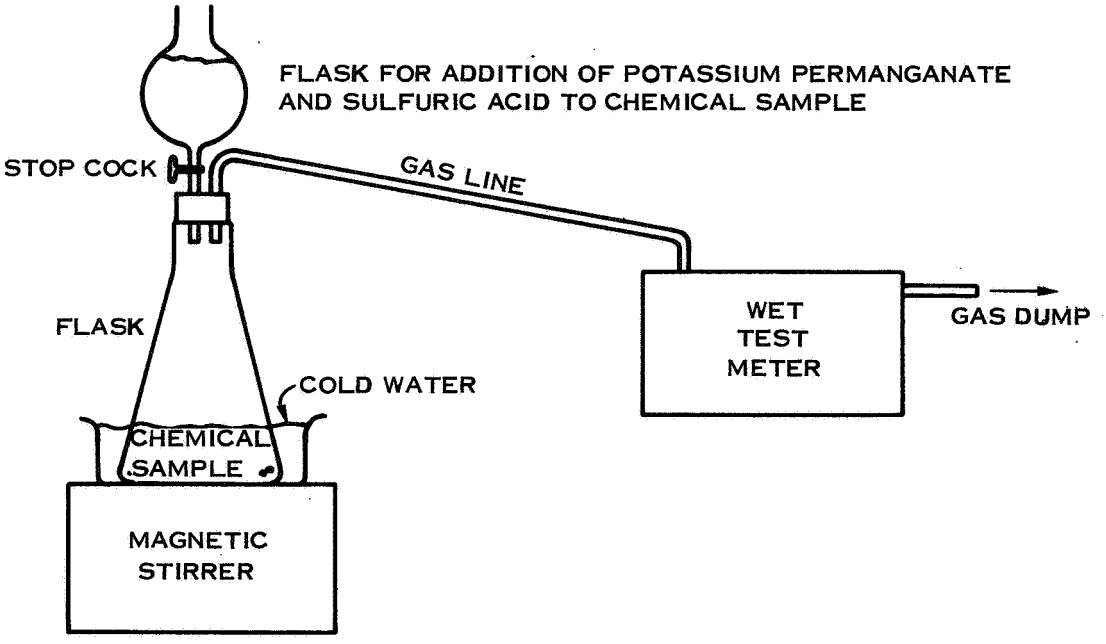

Figure 4-65. Chemical Test Apparatus

A fifty gram, homogeneous chemical sample is placed in the flash. Any oxygen in the chemical is released when a saturated potassium permanganate solution is added and is measured by the wet test meter. The carbon dioxide in the chemical is released by adding a 50% sulfuric acid solution in 100 milliliter increments. Gas evolution is complete when the addition of 100 milliliter increment of sulfuric acid increases the meter reading by only that volume.

5.0 PERFORMANCE ANALYSIS

This section presents the performance analysis results for the test data of Section 4.0.

5.1 Chemical Form Evaluation

Lithium peroxide granules of varying bulk density, with and without a nickel sulfate ($NiSO_4$) catalyst were evaluate during this phase of the program. Nickel sulfate was selected as the catalyst for evaluation based upon the work done in France by Ducros which is reported in reference 2.

The initial investigation was made for the scale model (1/3 scale) conditions described in Section 3.0. A fiberglass liner was applied to the canister walls to prevent the gas from channeling around the granule bed. The small scale test results were confirmed by the full scale tests which were conducted for the conditions specified in Section 3.0 using canister No. 2.

Due to the manufacturing process, the vendor was unable to supply catalyzed, high bulk density granules. The three chemical forms tested were high bulk density (HBD), low bulk density (LBD) and catalyzed low bulk density granules (LBD-CAT). Some properties for these materials are listed in Table 5-1.

TABLE 5-1

GRANULE PROPERTIES

Chemical Form	Bulk Density (lb/ft^3)	Catalyst	Thermal Decomposition Data*	
			Decomposition Range (°F)	Temperature of Most Rapid Decomposition (°F)
HBD	30	None	510 - 684	571
LBD	27	None	532 - 683	574
LBD-CAT	25	2% $NiSo_4$	468 - 668	528

* Test environment was pure oxygen at 3.7 psia with 8°F per minute heating.

The high bulk density material was 8 x 14 mesh granules supplied by the Foote Mineral Co. These granules were prepared by grinding them from a large block of chemical pressed from lithium peroxide powder. The low bulk density material, both with and without catalyst addition, was made by the Trans World Consulting Co. in 8 x 14 mesh granules. These were produced by making a slurry with the lithium peroxide and an inert liquid binder, forcing the mixture through a screen, cutting the granules to the desired length, and then drying the resultant granules. As is shown in Table 5-1, the addition of 2% nickel sulfate catalyst lowered the thermal decomposition temperature about 40°F.

5.1 (Continued)

A summary of the performance data for the tests conducted during this test series appears in Table 5-2. The columns of the tabulation are defined as follows:

1. The time in the test that the canister outlet partial pressure of carbon dioxide is 0.5, 1.0, and 4.0 mmHg.

2. Chemical type (eg - low bulk density, LBD)

3. Chemical weight (lb)

4. Maximum bed temperature (°F)

5. Average useable oxygen generation rate during test (lb/hr). This excludes all oxygen which would be vented overboard during peak generation periods.

6. Test duration that the required oxygen generation rate was exceeded (minutes)

TABLE 5-2

TEST SUMMARY

No.	Time (min.) to 0.5-1.0-4.0 mmHg	Chem. Type	Weight (lb)	Max. T (°F)	Avg. $\dot{m}O_2$ (lb/hr)	Time $\dot{m}O_2$> Spec. (Min)
MSC-1	120-135-190	LBD	1.32	485.	0.14	42.
MSC-2	115-130-198	HBD	1.27	541.	0.15	38.
MSC-3	75- 90-180	LBDC	1.32	526.	0.21	60.
MSC-4	96-115-205	HBDC	1.21	486.	0.18	25.
MSC-5	145-170-220	LBD	1.32	346.	0.11	12.
MSC-6a	40- 62-150	HBD	1.32	385.	0.13	0.
MSC-6b	38- 80-145	HBD	1.32	281.	0.09	0.
MSC-7a	140-150-186	LBDC	1.32	500.	0.13	14.
MSC-7b	80-100-166	LBDC	1.06	442.	0.18	34.
MSC-8	160-180-250	HBDC	1.21	326.	0.16	25.
MSC-9a	125-142-225	LBDC	3.24	350.	0.12	0.
MSC-9b	76- 95-150	LBDC	3.22	645.	0.20	45.
MSC-9c	90-125-225	LBDC	3.25	488.	0.16	25.
MSC-10a	28- 60-162	HBD	4.52	569.	0.21	52.
MSC-10b	44- 65-128	HBD	4.50	596.	0.24	45.
MSC-10c	75- 85-160	LBD	3.75	600.	0.20	35.
MSC-10d	50- 83-158	LBD	3.75	613.	0.20	36.
MSC-10e	60-100-174*	LBD	3.72	478.	0.13	3.

* Cooling water was inadvertently turned off at 180 minutes (CO_2 partial pressure dropped when the water flow stopped and remained steady at about 2.5 mmHg up to test termination at 240 minutes.

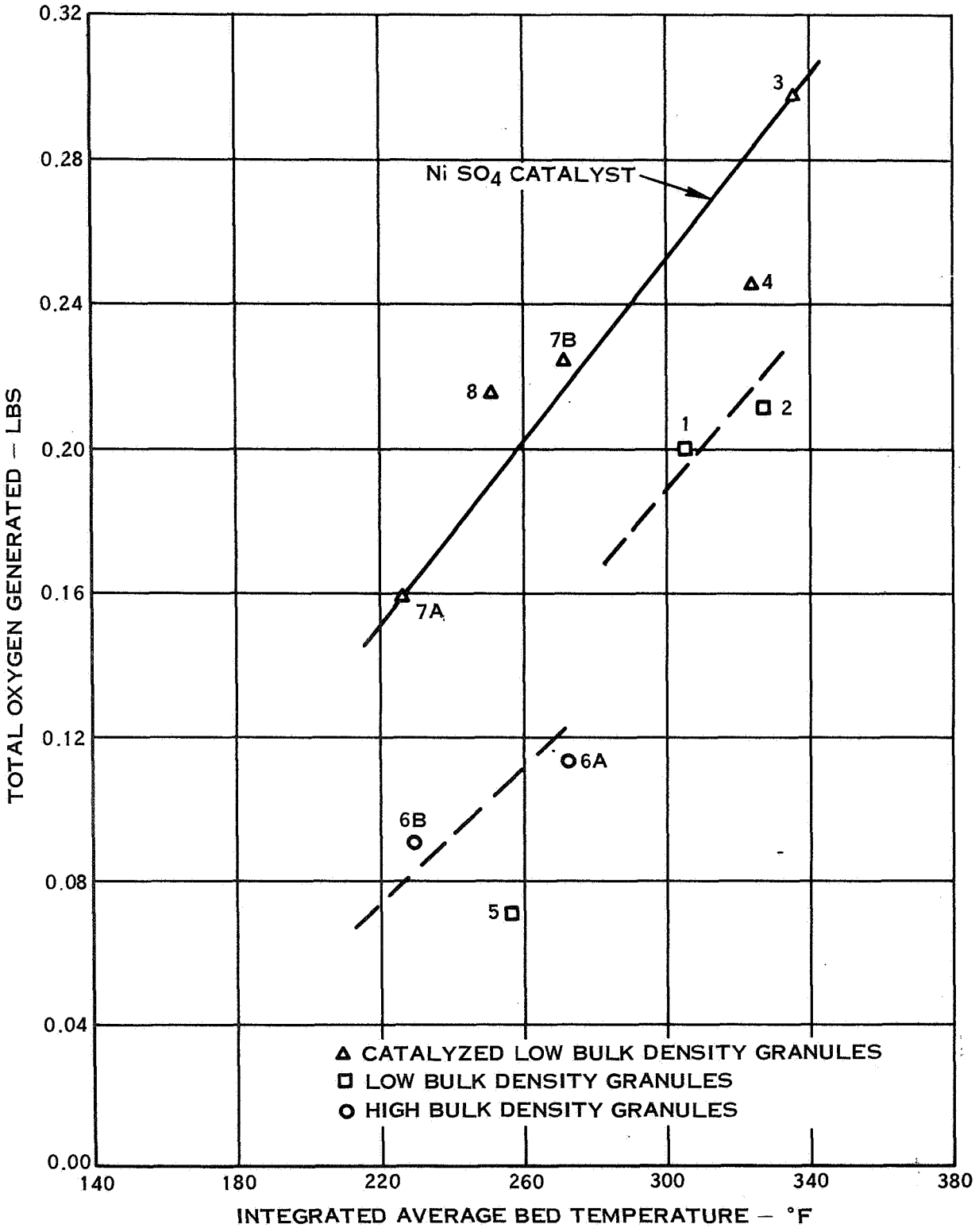

Figure 5-1. Oxygen Generated For the Scale Models Tests During 180 Minutes

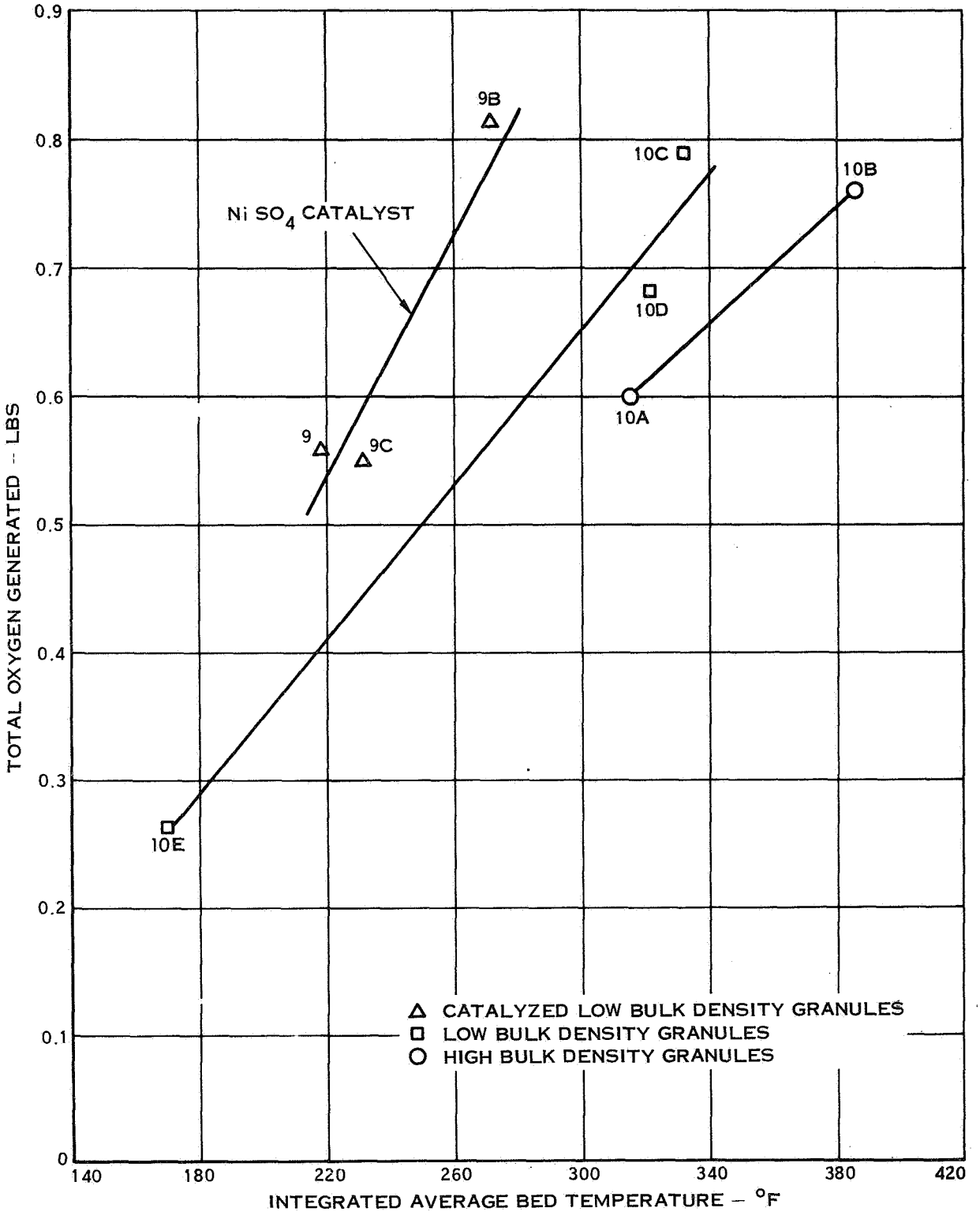

Figure 5-2. Oxygen Generated For the Full Size Tests During 180 Minutes

5.1 (Continued)

Both carbon dioxide removal and oxygen generation performance were demonstrated to be superior for the catalyzed granules. Figures 5-1 and 5-2 show the oxygen generation performance after 180 minutes of test operation for the scale model and full size tests respectively. All the data shows that superior oxygen performance is provided by the catalyzed, low bulk density granules. The integrated average bed temperature, $\overline{T}_t$, shown in Figures 5-1 and 5-2 is defined as follows. An average bed temperature, $\overline{T}$, is calculated for each time interval by averaging the readings for all the thermocouples located within the bed. The integrated average bed temperature is the time integrated average of these average bed temperatures shown in Figure 5-3 and can be represented by:

$$\overline{T}_t = \frac{\text{AREA UNDER THE CURVE TO } t_f}{t_f}$$

OR:

$$\overline{T}_t = \sum_{p=o}^{p=n} \frac{\overline{T}_p \, \Delta t}{T_f}$$

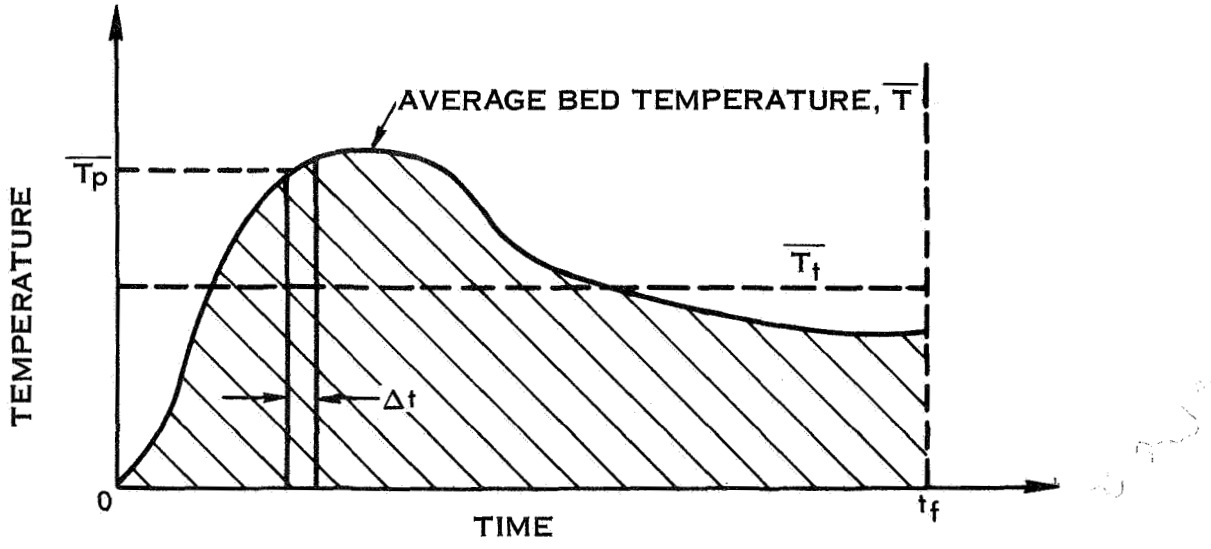

Figure 5-3. Typical Li_2O_2 Bed Temperature Profile

The catalyzed, low bulk density granules also demonstrated better carbon dioxide removal performance, as shown by Figure 5-4 for the full scale test results. In this figure, the solid lines represent the average of the test data; the dashed lines indicate the results normalized for an equivalent weight of lithium peroxide. This data extension is accomplished via the following rationale; the weight of lithium peroxide, $W_{Li_2O_2}$, of the tests performed was as shown in Table 5-3.

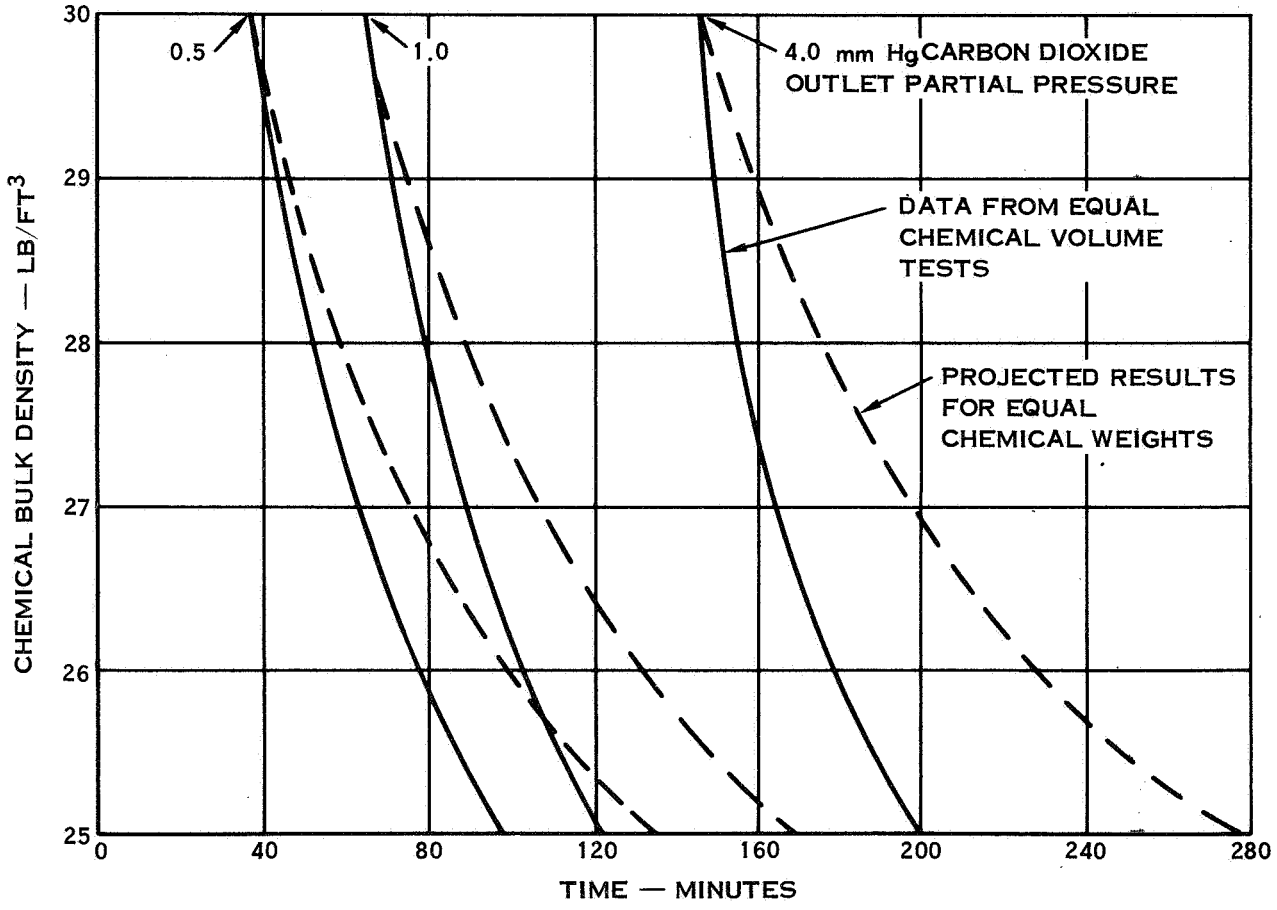

Figure 5-4. Carbon Dioxide Removal Performancs as a Function of Chemical Bulk Density

5.1 (Continued)

TABLE 5-3

CHEMICAL TEST WEIGHTS

Chemical Type	Bulk Density (lb/ft^3)	Weight of Li_2O_2 Tested (lb)
HBD	30	4.5
LBD	27	3.75
LBD-CAT	25	3.25

And:

$$\text{time)}_{\text{projected}} = \frac{4.5}{W_{Li_2O_2}} \text{ (time) actual test}$$

then; had equivalent weights of lithium peroxide been subjected to the tests, the time to reach the indicated carbon dioxide outlet partial pressures would have been as indicated by the dashed curves of Figure 5-4.

The performance improvement that resulted from the reduction in bulk density is considered to be related to the molar volume ratio (MVR). The molar volume ratio pertains to the reaction of a gas and solid where the reaction product is a solid or a solid and a gas. The definition is:

$$\text{MVR} = \frac{\text{Volume of Y modes of solid reaction product}}{\text{Volume of X modes of solid reactant}}$$

Where X and Y are determined from the balanced chemical equation, and the molar volume itself is the molecular weight divided by density. Physically, the molar volume ratio is a quantitative indication of the gas diffusion resistance created by the solid reaction product. A ratio greater than 1.0 means that, because of its larger volume, the solid reaction product will fill some of the void spaces of the reactant and will thereby increase the diffusion resistance of the gas to the unused reactant. A ratio less than 1.0 means that the diffusion resistance decreases, thus promoting further reaction. The significance of the molar volume ratio has been discussed and verified in the following references: Markowitz (1), Bach (3) and Boryta (4, 5). In work with lithium oxide (Li_2O), Boryta has shown that the relationship between bulk density and percent carbon dioxide removal is hyperbolic in nature and the results presented in Figure 5-4 show a similar tendency.

5.1 (Continued)

The catalyzed, low bulk density material, which demonstrated the best performance, was used for the remainder of the test program.

5.2 Bed Geometry Evaluation

This test series was conducted to evaluate the effect upon lithium peroxide performance of variations in the canister geometry. The tests were run in canisters of three distinct rectangular face areas. Features common to each canister included identical inlet and outlet manifold configurations and the applicant of a fiberglass liner to the canister walls to prevent the gas from channeling around the granule bed. Each of the canisters incorporated internal cooling coils to allow control of the operational bed temperature. Complete canister dimensions are as presented in Section 3.6 and Table 5-4 shows the bed face areas, bed lengths, and cooling coil lengths employed by each canister.

TABLE 5-4

CANISTER GEOMETRY

Canister No.	Flow Area (in^2)	Bed Length (in)	Cooling Coil Length (in)
1	26.3	9.0	105.
2	46.5	5.7	94.
3	92.5	2.8	149.

The tests were conducted using as nearly equivalent chemical volume as was possible. The geometric variation between canisters changed the internal bed velocity since as the flow area increases, the velocity through the bed decreases. In addition, as the flow area increases; the mass flow rate per unit area also decreases. It was expected then, that the desired degree of cooling would be easier to accomplish for the largest face area used by canister 3 and that its rate of temperature rise would be lower since the carbon dioxide and water vapor concentration, in the bed, is effectively lowered due to the larger flow area. The testing confirmed that this was correct.

Table 5-5 presents a data summary for the tests conducted during this test series to evaluate the effect of geometry on lithium peroxide performance. The columns of the tabulation are defined as follows:

1. Canister designation (per Section 3.6)

2. Time in the test that the canister outlet partial pressure of carbon dioxide reaches 0.5, 1.0, and 4.0 min Hg (minutes)

5.2 (Continued)

3. Chemical weight (lb)

4. Maximum bed temperature (°F)

5. Average useable oxygen flow rate during the test (lb/hr). This excludes all oxygen vented overboard during peak generation perriods.

6. Test duration that the required oxygen flow rate of 0.36 lb/hr was exceeded (minutes)

TABLE 5-5

TEST SUMMARY

Test No.	Canister	Time (min) to 0.5-1.0-4.0 mmHg	Weight (lb)	Max. T (°F)	Avg. $\dot{m}O_2$ (lb/hr)	Time $\dot{m}O_2 \geq$ Spec. (Min)
MSC-11	1	40-104-160	3.40	401.	0.13	22.
MSC-12	1	0- 60-168	3.10	654.	0.14	20.
MSC-12b	1	55- 62-145	2.94	594.	0.15	20.
MSC-14	3	0- 8-210	3.38	309.	0.11	0.
MSC-15	3	0- 90-210	3.18	542.	0.14	3.
MSC-16	3	25-110-240	3.26	560.	0.14	20.
MSC-16b	3	20-100-205	3.13	552.	0.15	30.
MSC-17	2	70- 85-135	3.30	563.	0.15	40.
MSC-17b	2	15- 70-185	3.14	552.	0.15	0.
MSC-17c	2	40- 70-185	3.32	570.	0.20	40.
MSC-18	2	65- 90-172	3.42	703.	0.16	38.
MSC-19	2	60- 80-148	3.32	610.	0.18	42.
MSC-20	3	70- 95-195	3.23	563.	0.13	22.

To fairly evaluate the effect of geometry upon performance, tests which exhibited nearly equivalent average bed temperatures must be compared since performance has demonstrated to be highly temperature sensitive. The tests which had nearly equivalent average bed temperatures were: test MSC-11 in canister 1; tests MSC-9, 9c, and 17c in canister 2; and tests MSC-15, 16 and 20 in canister 3. The average bed temperatures for these tests are presented in Figure 5-5. The thermal decomposition temperature of 530°F was briefly exceeded in some of these tests, but the occurrences were local and are believed not to affect the test result comparison. Average carbon dioxide removal performance is presented in Figure 5-6, based upon the averages of these tests. It can be seen that the performance of canisters 2 and 3 were distinctly better than that for cainster 1 and that canister 2. Further, Figure 5-7 shows the best performance attained for each canister configuration. In this case, the performance using canister 3 is clearly superior.

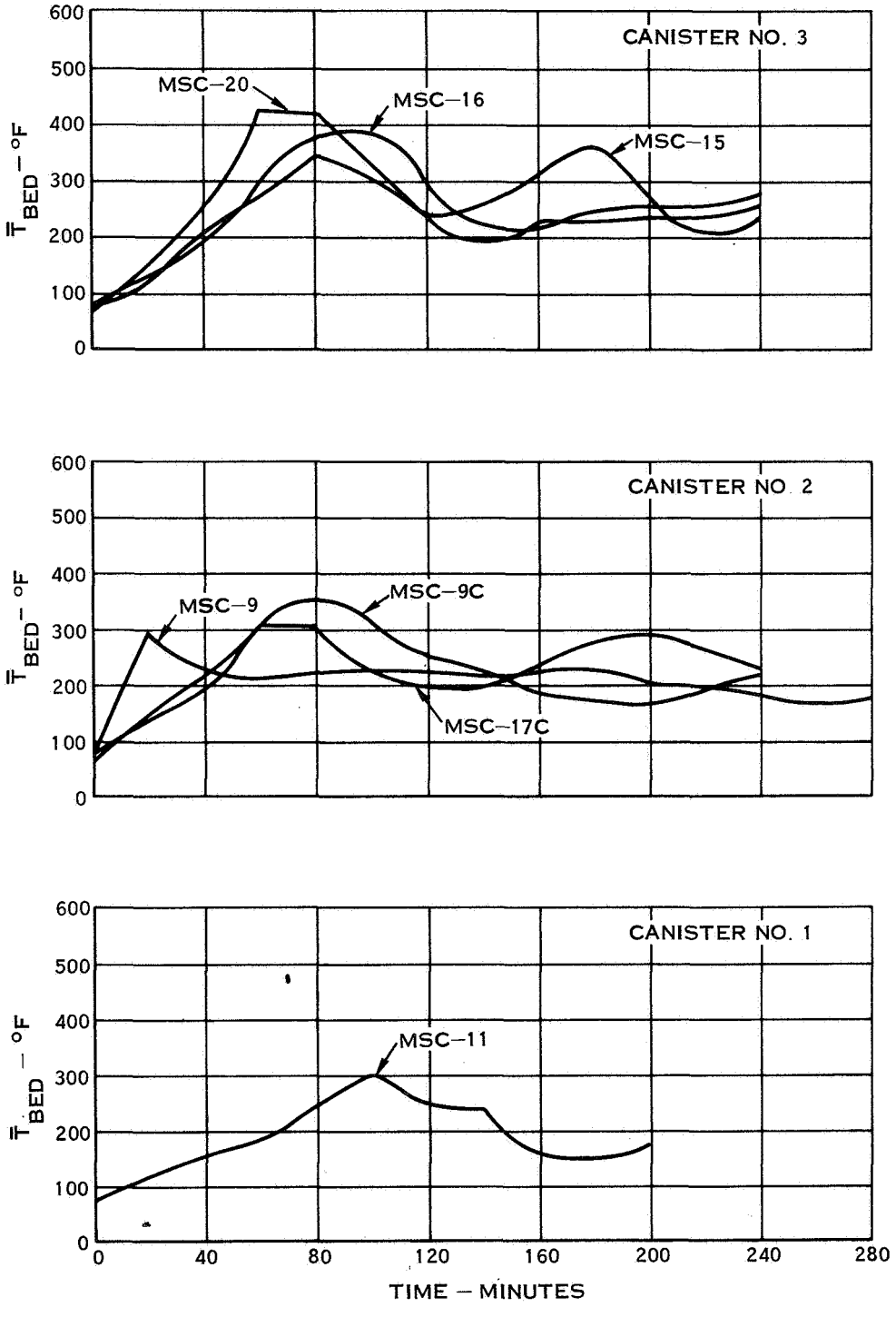

Figure 5-5. Average Bed Temperatures

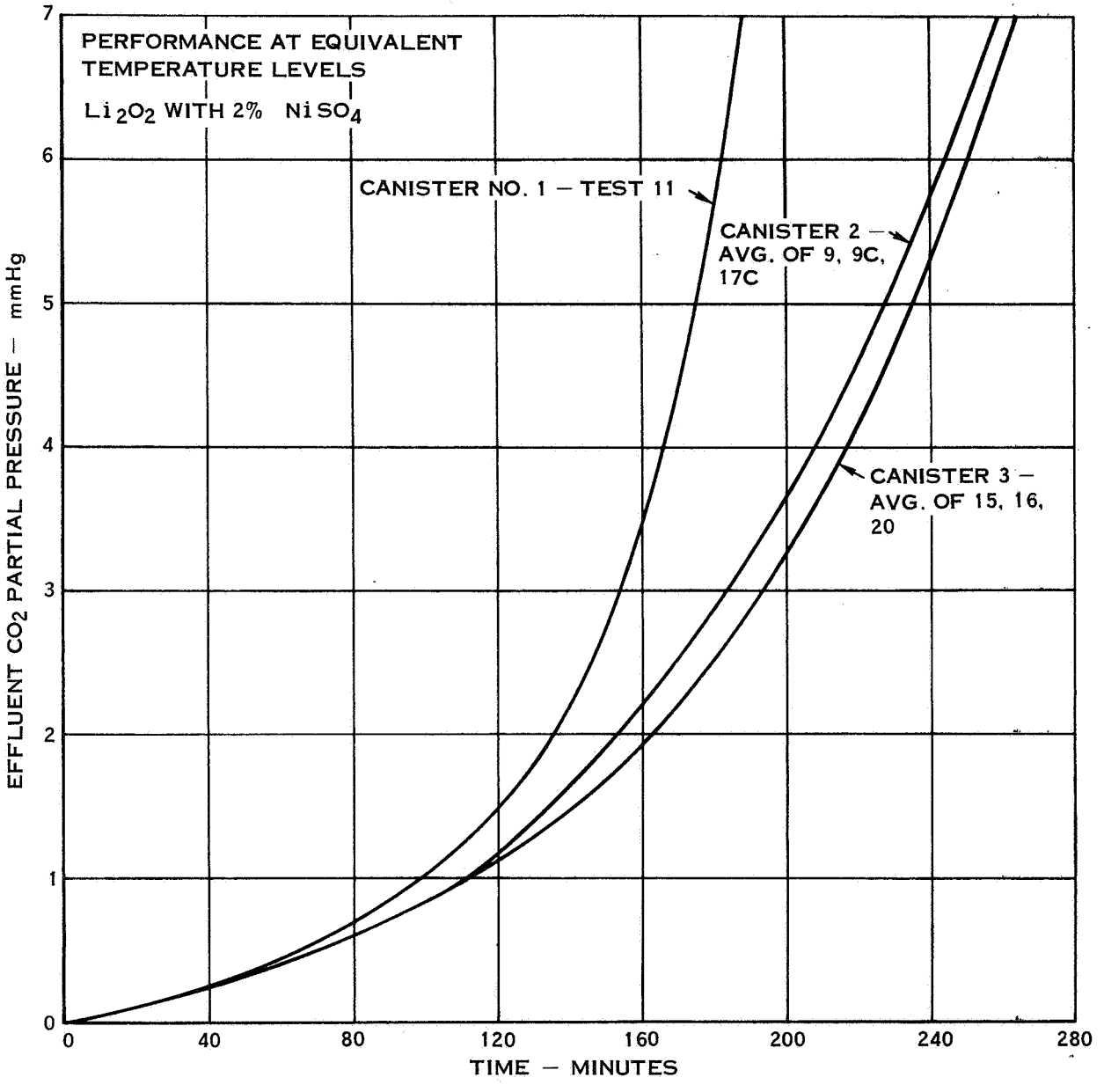

Figure 5-6. Carbon Dioxide Removal as a Function of Geometry

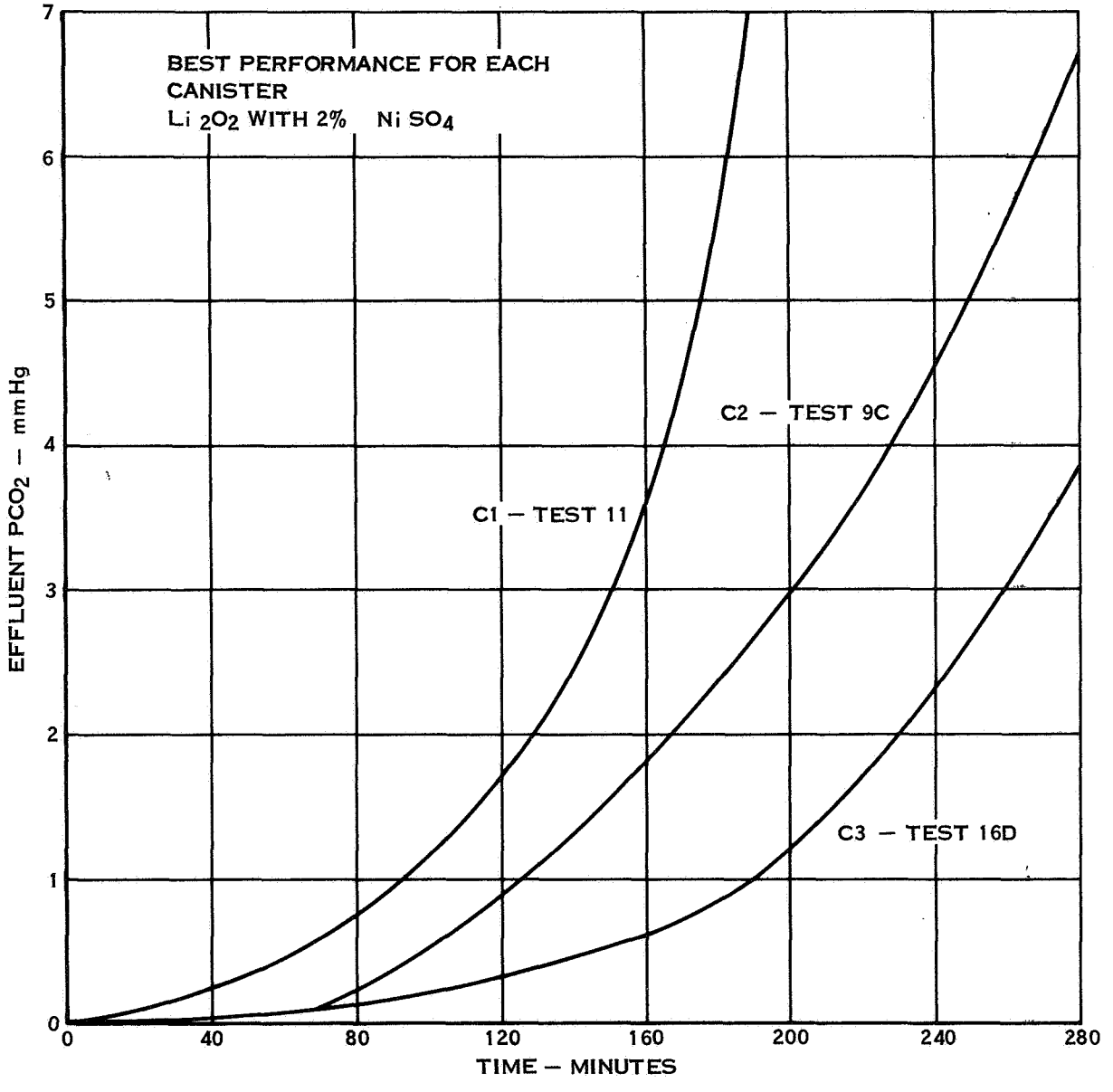

Figure 5-7. Carbon Dioxide Removal as a Function of Geometry

5.2 (Continued)

A performance comparison as a function of average bed temperature is shown in Figure 5-8 for the three canisters. The performance using canister 3 is superior over the total range of integrated average bed temperautures.

The effects of geometry on oxygen generation are shown in Figure 5-9 as a function of integrated average bed temperature. Canisters 1 and 2 generated equivalent amounts of oxygen which was significantly more than canister 3. This difference is fundamentally attributed to higher bed temperatures that occurred during tests with canister 1 and 2. This added amount of oxygen was generated through thermally decomposing the lithium peroxide during peak temperature periods. However, a high percentage of the oxygen produced in canisters 1 and 2 would have to be vented overboard during an actual mission since the oxygen requirement was exceeded. Figure 5-10 shows the percentage of the generated oxygen which could be used during a mission. This percent usable oxygen is defined as the ratio of all the oxygen generated at a rate below 0.36 lb/hr divided by the total oxygen generated. The data shows that a much higher percentage of the generated oxygen from canister 3 is usable.

The performance differences observed between the canisters are attributed to the basic differences in the canister flow areas and the efficiency of the internal bed cooling systems. Since the bed temperature and the duration that thermal decomposition occurs influence performance so significantly, it is difficult to evaluate effects due to gemetric variations. However, since canister 3 demonstrated the best carbon dioxide control performance and exhibited the best bed temperature control, this canister face area was selected to be used for the remainder of the tests.

5.3 Bed Temperature Evaluation

This test series was coupled with the bed geometry evaluation that was previously discussed. (ie - the tests for this series are the same tests as discussed in Section 5.2) A data summary for those tests is presented in that section.

The test results have shown that increasing the bed temperature produces higher oxygen yields, but impairs the carbon dioxide removal performance. To obtian good carbon dioxide performance at the 2000 Btu/hr metabolic rate level, (which is a carbon dioxide input level of 0.39 lb/hr), it was necessary to use internal bed cooling. Without the cooling the bed temperatures quickly exceed the thermal decomposition temperature releasing large quantities of oxygen, but the carbon dioxide removal performance deteriorates rapidly.

Data in previously published literature which discusses the effect of temperature on the lithium peroxide reactions have been reported by Markowitz and Selezneva in references 1 and 6 respectively. At temperatures below 250°F, Markowitz found the oxygen evolution to be less than that expected for the amount of water vapor known to have reacted with the lithium peroxide. He theorized that a reaction with water vapor could occur

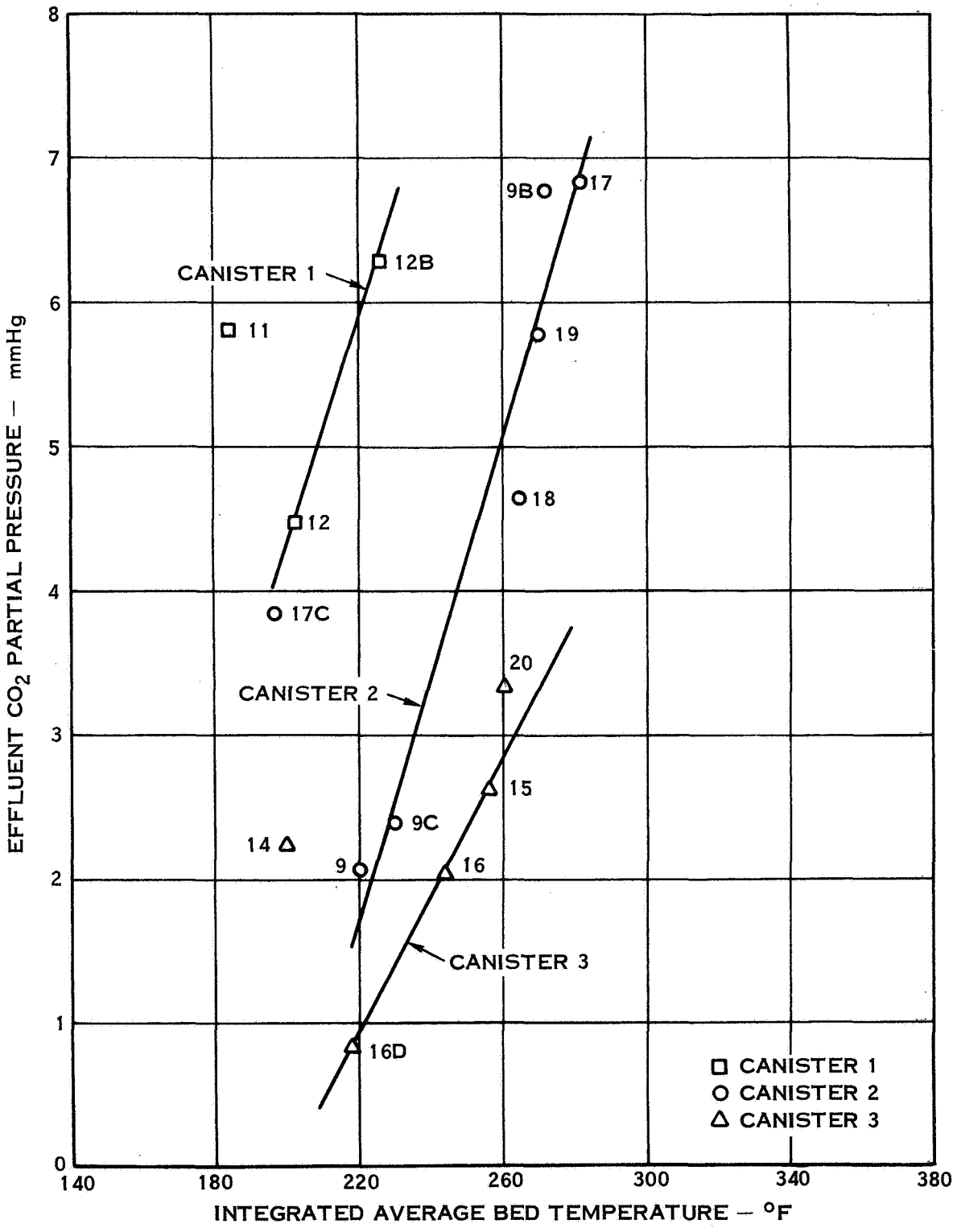

Figure 5-8. Carbon Dioxide Performance After 180 Minutes of Testing

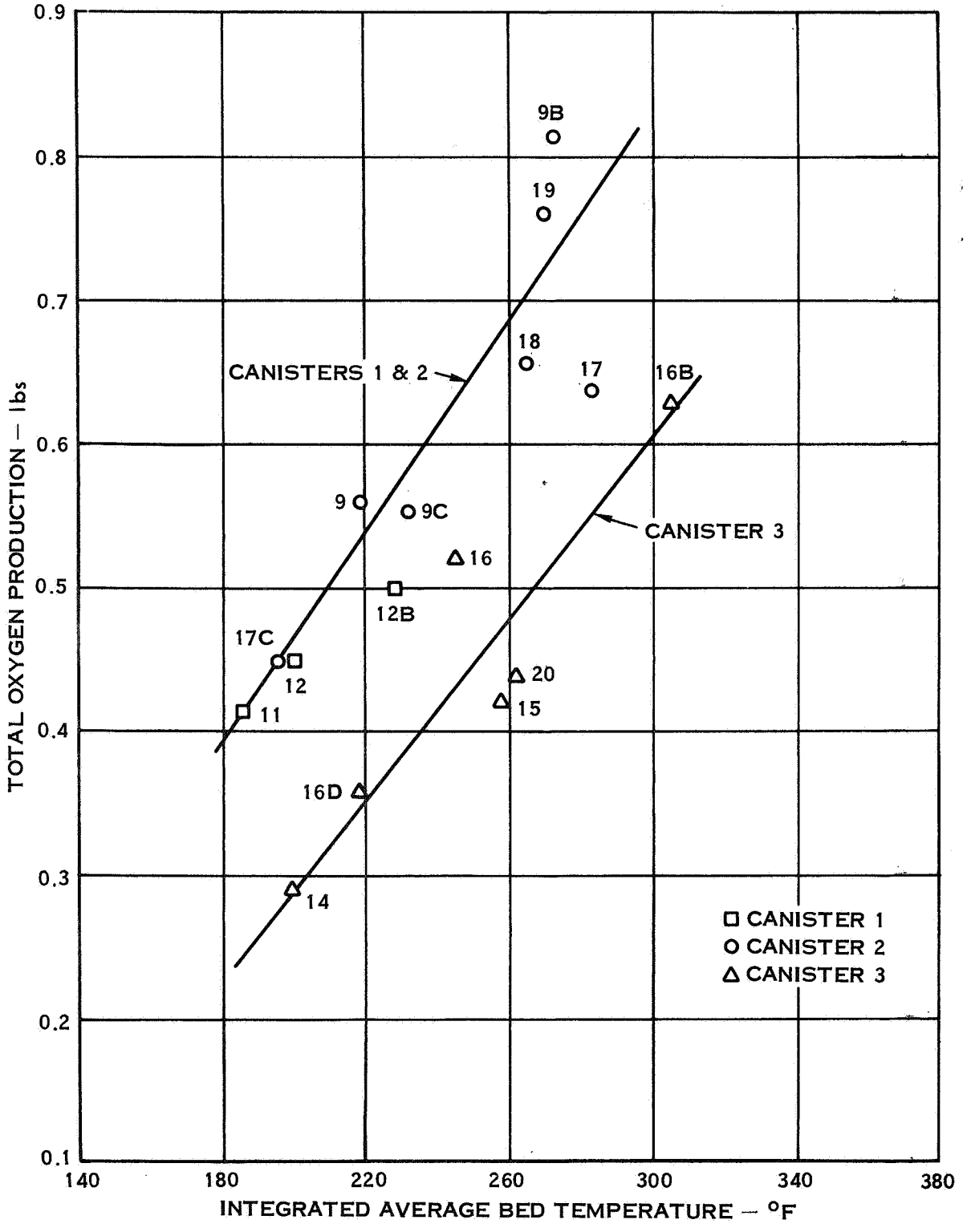

Figure 5-9. Total Oxygen Production During 180 Minutes of Testing

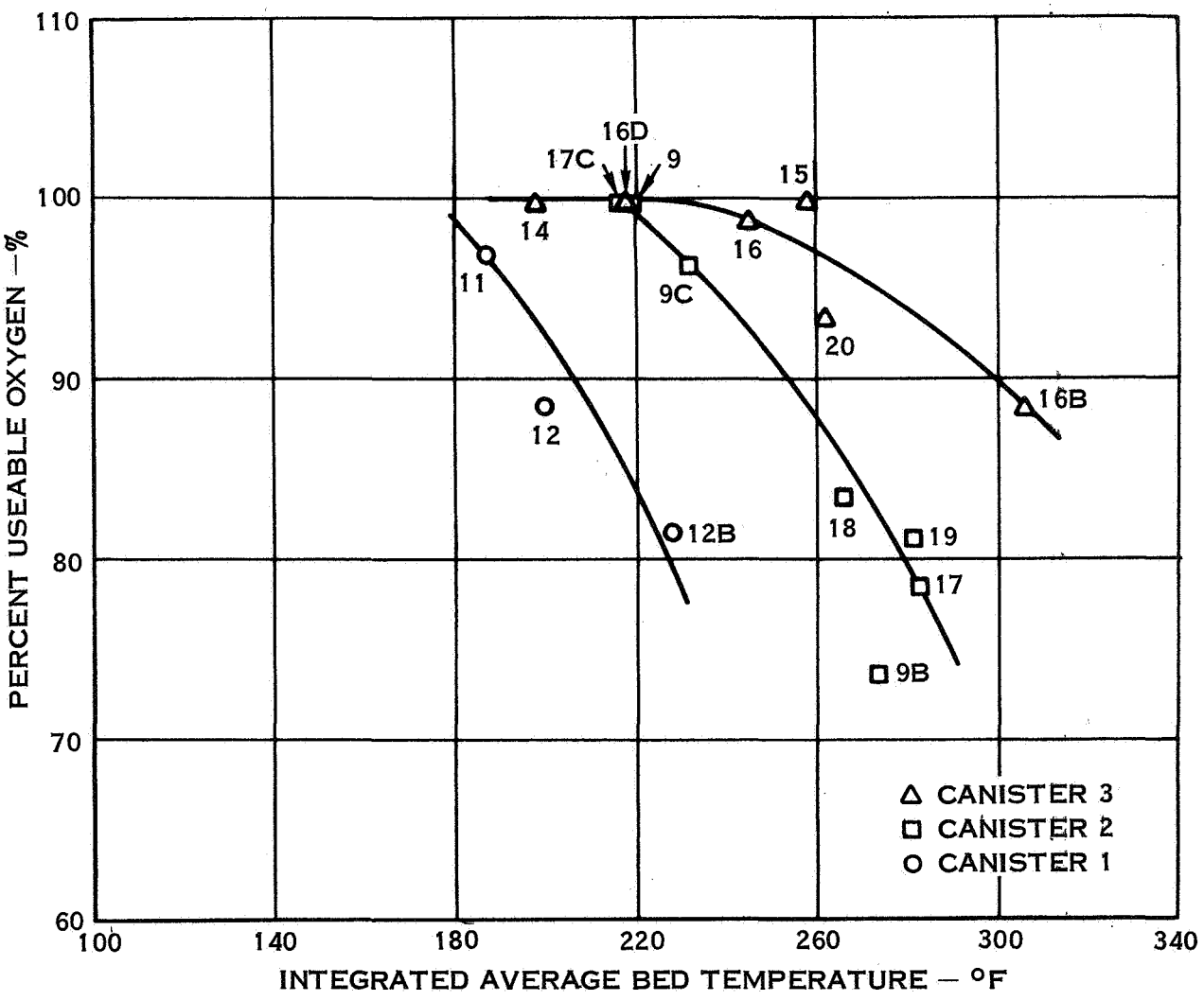

Figure 5-10. Useable Oxygen as a Function of Temperature and Geometry

5.3 (Continued)

which resulted in the formation of a solid compound containing hydrogen peroxide which would not decompose to its water vapor and oxygen constituents at these temperature levels. Consequently the expected quantity of oxygen was not released. Further heating of the chemical with dry helium caused the oxygen to be released via thermal decomposition of the hydrogen peroxide. This work suggested the use of a catalyst to promote decomposition of the hydrogen peroxide at lower temperature levels.

More complete data was obtained by Selezneva in experiments using small test beds immersed in a controlled, constant temperature bath. Tests of the reactions of lithium peroxide were conducted with the following gas mixtures: air and 4% by volume carbon dioxide, air and 2.5% by volume water vapor, and air with 4% carbon dioxide and 2.5% water vapor. Selected results of these tests are shown in Figure 5-11. No reaction with dry carbon dioxide was observed below 392°F; the reaction with water vapor was slow at room temperature, but very rapid above 392°F. Reaction with the mixture of carbon dioxide and water vapor proceeded well at much lower temperatures.

The effect of temperature on performance can be seen from Figures 5-12 and 5-13 where the average bed temperature, effluent carbon dioxide partial pressure, and oxygen generation rate are shown as a function of time for tests in canisters 2 and 3. The best performance in each canister occurs for tests MSC-9 and MSC-16d, in which neither ever exceeded the thermal decomposition temperature. The data for tests MSC-9band MSC-16c show the high oxygen yield that occurs when thermal decomposition takes place and its attendant deterioration in carbon dioxide removal performance. The data for test MSC-16 is typical of that for lithium peroxide which has briefly undergone thermal decomposition in small, localized areas.

Performance data for the total oxygen production and carbon dioxide removal performance at the end of 180 minutes are presented in Figures 5-14 and 5-15. The trend of increasing oxygen evolution as the bed temperature increases is clearly evident in Figure 5-14. The lower oxygen evolution demonstrated by canister 3 is attributed to the generally low and more uniform bed temperatures, due to better cooling, in canister 3. Virtually no thermal decomposition occurred during testing with canister 3.

The "V" shaped curves shown in Figure 5-15 indicate the existence of an optimum bed temperature for maximum carbon dioxide removal performance. Although there is only scanty data for integrated average bed temperatures below 220°F, the results are considered accurate because of the excellent test data correlation for total carbon dioxide removal and oxygen generation with the "post-morten" chemical analysis data. These data indicate that a bed temperature near 220°F may represent the optimum operating temperature from the standpoint of carbon dioxide removal performance.

Theoretical justification for an optimum temperature level for carbon dioxide removal can be rationalized in the following way. At low temperatures, the water vapor reaction

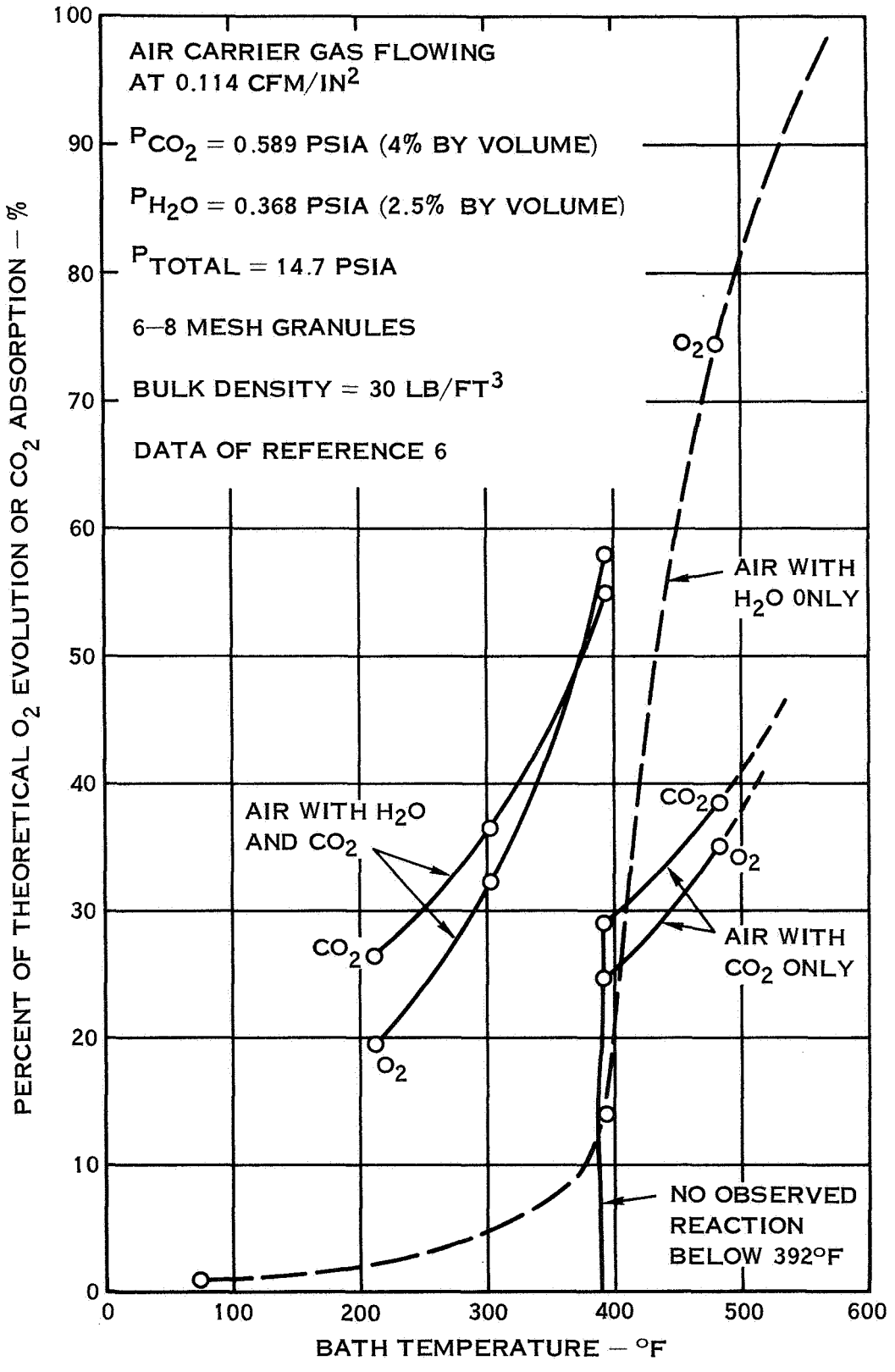

Figure 5-11. The Effect of Temperature on Lithium Peroxide Reactions

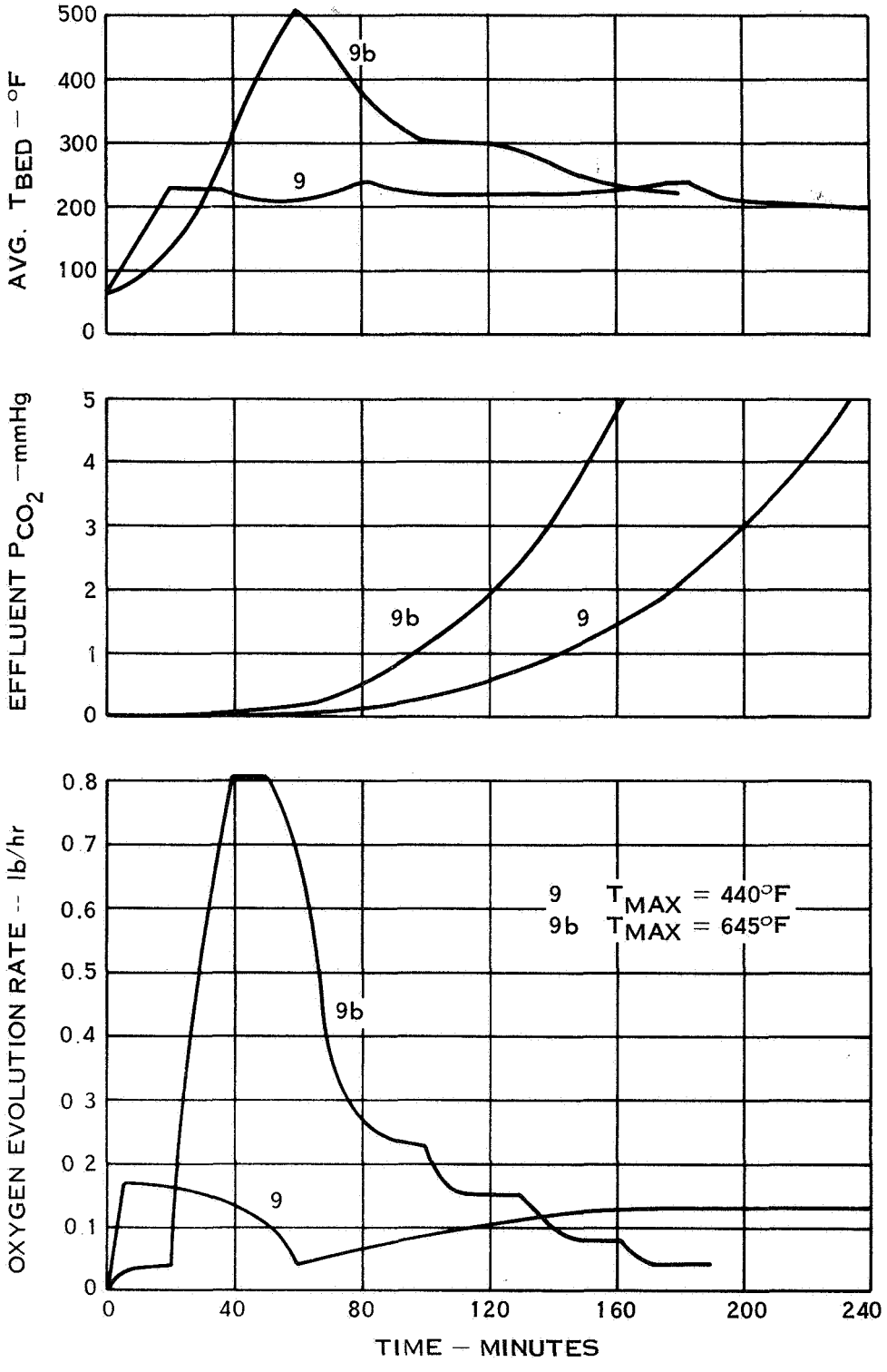

Figure 5-12. Canister 2 Performance Results

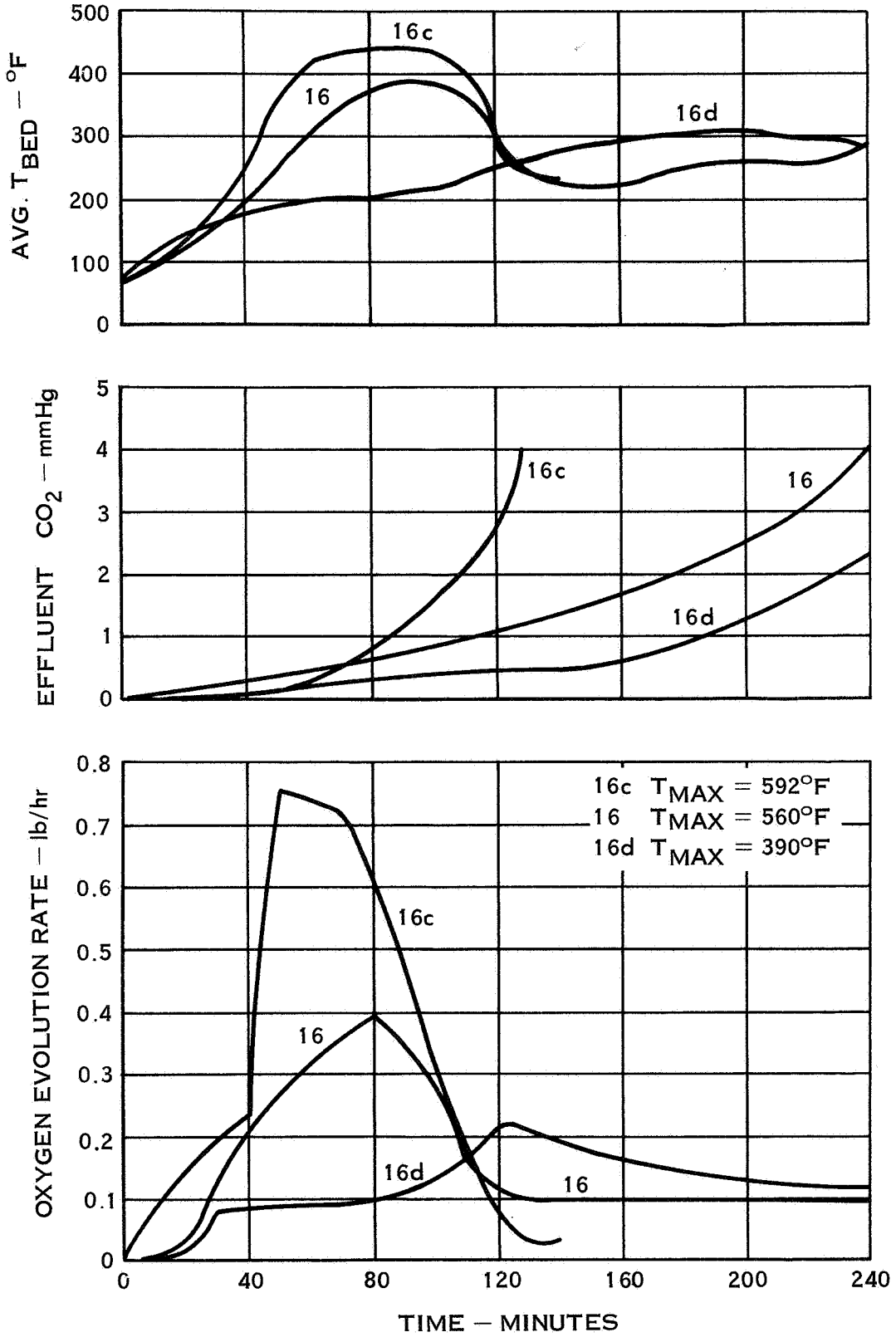

Figure 5-13. Canister 3 Performance Results

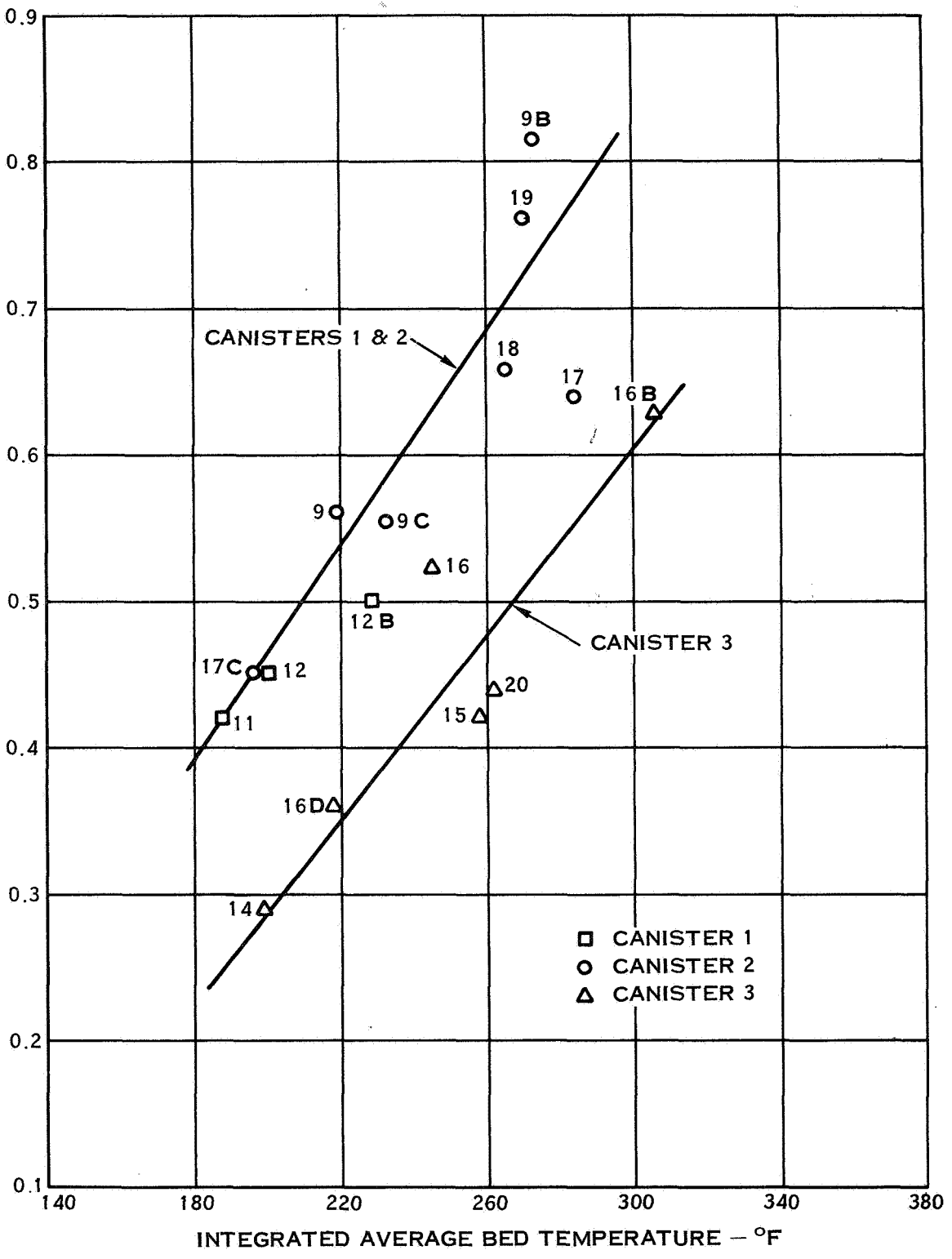

Figure 5-14. Total Oxygen Production After 180 Minutes of Testing

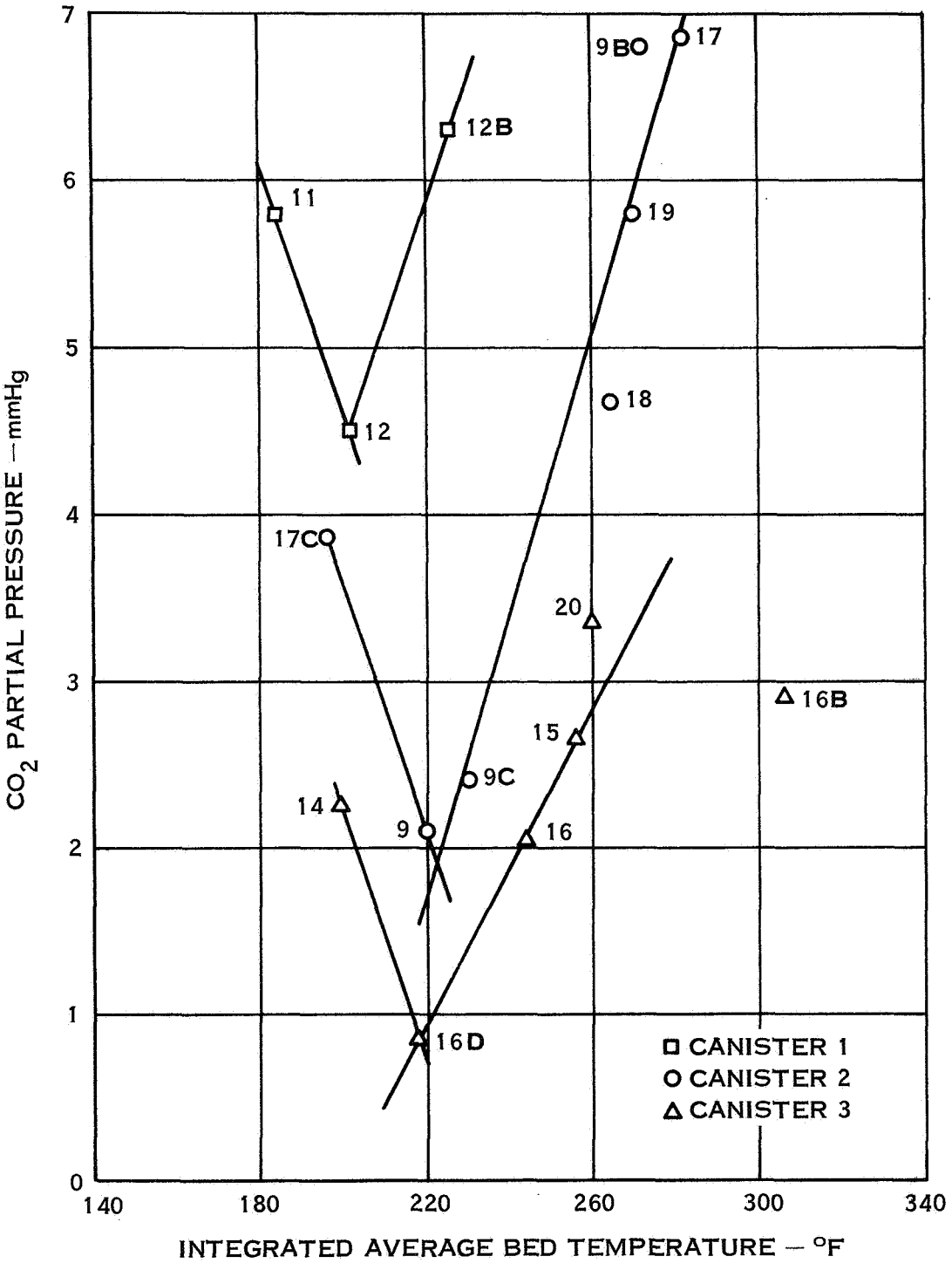

Figure 5-15. Carbon Dioxide Removal Performance After 180 Minutes of Testing

5.3 (Continued)

proceeds very slowly and for these conditions the carbon dioxide removal is accomplished by reaction with the lithium hydroxide which is formed during the water vapor reaction, and to some extent directly with the lithium peroxide. (For beds, of the size tested, extremely low utilization efficiencies are required to maintain a low outlet carbon dioxide partial pressure during the early stages of operation). As the bed temperature increases, an increasingly greater amount of lithium hydroxide is formed which provides excellent carbon dioxide removal performance, as was demonstrated by Selezneva. Further increases in bed temperature begin to slow down the reaction of carbon dioxide with the lithium hydroxide because the necessary intermediate product, lithium hydroxide monohydrate, can not exist at the higher temperatures. This was substantiated by Boryta in reference 3; the lithium hydroxide phase diagram shown in Figure 5-16 indicates the temperature - humidity requirements for the stable existence of the monohydrate. Small amounts of the monohydrate of lithium hydroxide must be able to exist in order for lithium oxide to provide the required carbon dioxide removal performance. Further temperature rise promotes thermal decomposition of the lithium peroxide resulting in the formation of lithium oxide. Carbon dioxide removal with lithium oxide also requires the intermediate formation of lithium hydroxide monohydrate, as shown by Boryta in reference 4. Since the temperature level will not allow the monohydrate to form, the lithium oxide is useless for carbon dioxide removal. The progressive thermal decomposition of the lithium peroxide at elevated temperature, although producing large quantities of oxygen, severely reduces the capability of the bed to remove carbon dioxide.

For the intended application, bed temperature has been identified as the most significant variable affecting the lithium peroxide performance. Further effort must be devoted to identifying the catalyst which will promote the decomposition of hydrogen peroxide within the range of temperatures demonstrated to be the most efficient for carbon dioxide control.

5.4 Chemical Weight Evaluation

Specifically for the chemical weight evaluation series a total of 9 tests were run using canister 4. However, for this analysis, data has been used from tests with both canister 3 and 4, both of which employed a 92.5 in^2 flow area. The basic difference between these canisters lies with cooling coil design employed. All canister 3 tests were for a 2.8 inch bed length with a cooling provided by two coils connected in series, 1.4 inches apart and centered within the bed, with gas flow perpendicular to these coils. Early canister 4 tests employed a single coil located about 1.4 inches downstream of the inlet face of the bed. However, tests with about 6 lb. of chemical showed that another identical coil was required to provide cooling for the exit end of the bed. All tests conducted in canister 4 after MSC-23d were run with the two coil cooling system, and demonstrated significantly improved performance over previous tests with the same amount of chemical.

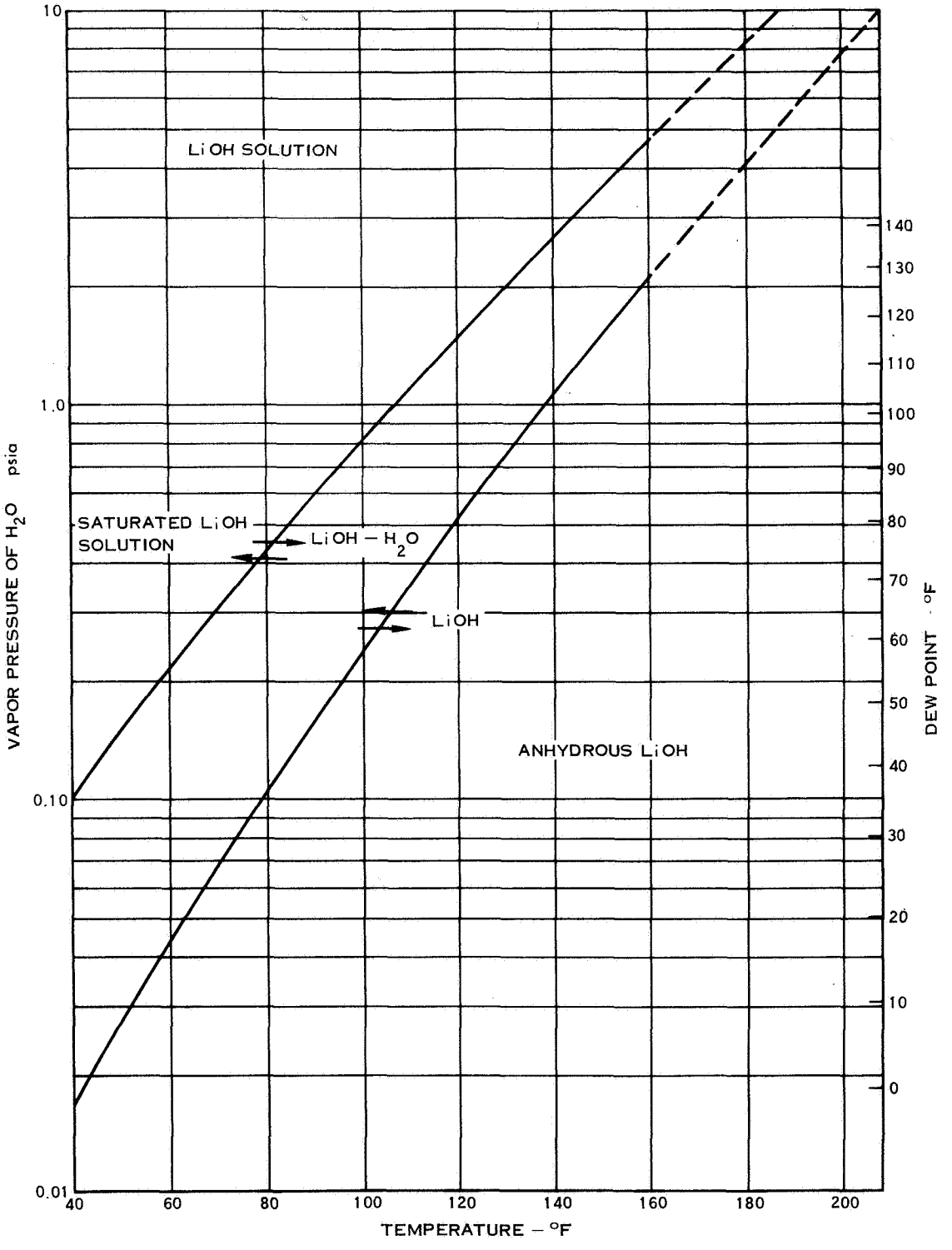

Figure 5-16. LiOH Phase Diagram

5.4 (Continued)

Table 5-6 presents a data summary for the tests run specifically for the chemical weight evaluation test series. The columns of the tabulation are defined as follows:

1. Time in the test that the canister outlet partial pressure of carbon dioxide reaches 0.5, 1.0, and 4.0 mm Hg. (minutes)

2. Chemical weight (lb)

3. Maximum bed temperature (°F)

4. Average useable oxygen generation rate during the test (lb/hr). This excludes all oxygen vented overboard during peak generation periods.

5. Test duration that the required oxygen flow rate (0.36 lb/hr) was exceeded (minutes)

TABLE 5-6

TEST SUMMARY

Test No.	Time (min) to 0.5-1.0-4.0mmHg	Weight (lb)	Max T (°F)	Avg. $\dot{m}_{O2}$ (lb/hr)	Time $\dot{m}_{O2}$ > Spec. (min)
MSC-22c	100-124-156	3.8	644.	0.28	58.
MSC-23	210-248-356	6.0	286.	0.11	0.
MSC-236	240-262-320	6.2	449.	0.13	25.
MSC-23c	180-210-277	6.29	500.	0.16	15.
MSC-24b	120-138-210	6.0	458.	0.16	30.
MSC-25	90- 90-205	4.2	518.	0.14	15.
MSC-26	64- 70-120	4.81	621.	0.22	50.
MSC-26b	240-250-290	7.76	618.	0.19	105.
MSC-26c	150-180-230	6.80	568.	0.20	40.

All of these tests were conducted for the variable metabolic profile defined in Section 3.4 for the first 240 minutes; testing after 240 minutes was conducted for a constant metabolic rate of 2500 Btu/hr.

Figures 5-17 and 5-18 show the carbon dioxide removal performance as a function of chemical weight. It can be seen that due to the improved cooling with two coils in canister 4, that the operating duration increased by about 60 minutes before the 4.0 mmHg partial pressure level was reached. The tests which employed two cooling coils were MSC-23E, MSC-23F, MSC-23G, MSC-23I, and MSC-23J. It should be noted that the difference between 0.5 mmHg and 4.0 mmHg carbon dioxide represents an accumulation of only 0.0008 lb. of carbon dioxide within the 1.5 ft^3 volume being tested. For a

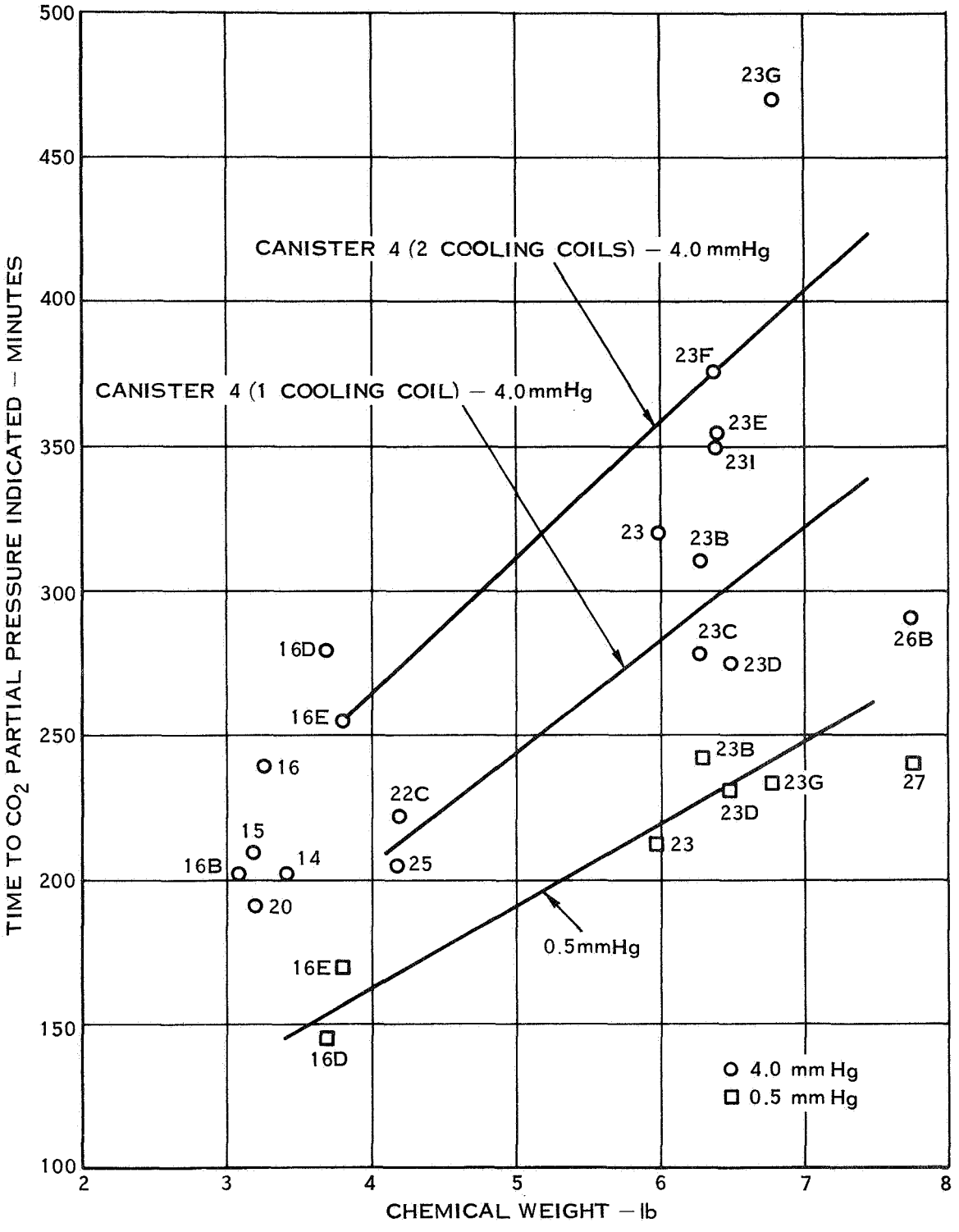

Figure 5-17. Carbon Dioxide Removal Life as a Function of Chemical Weight

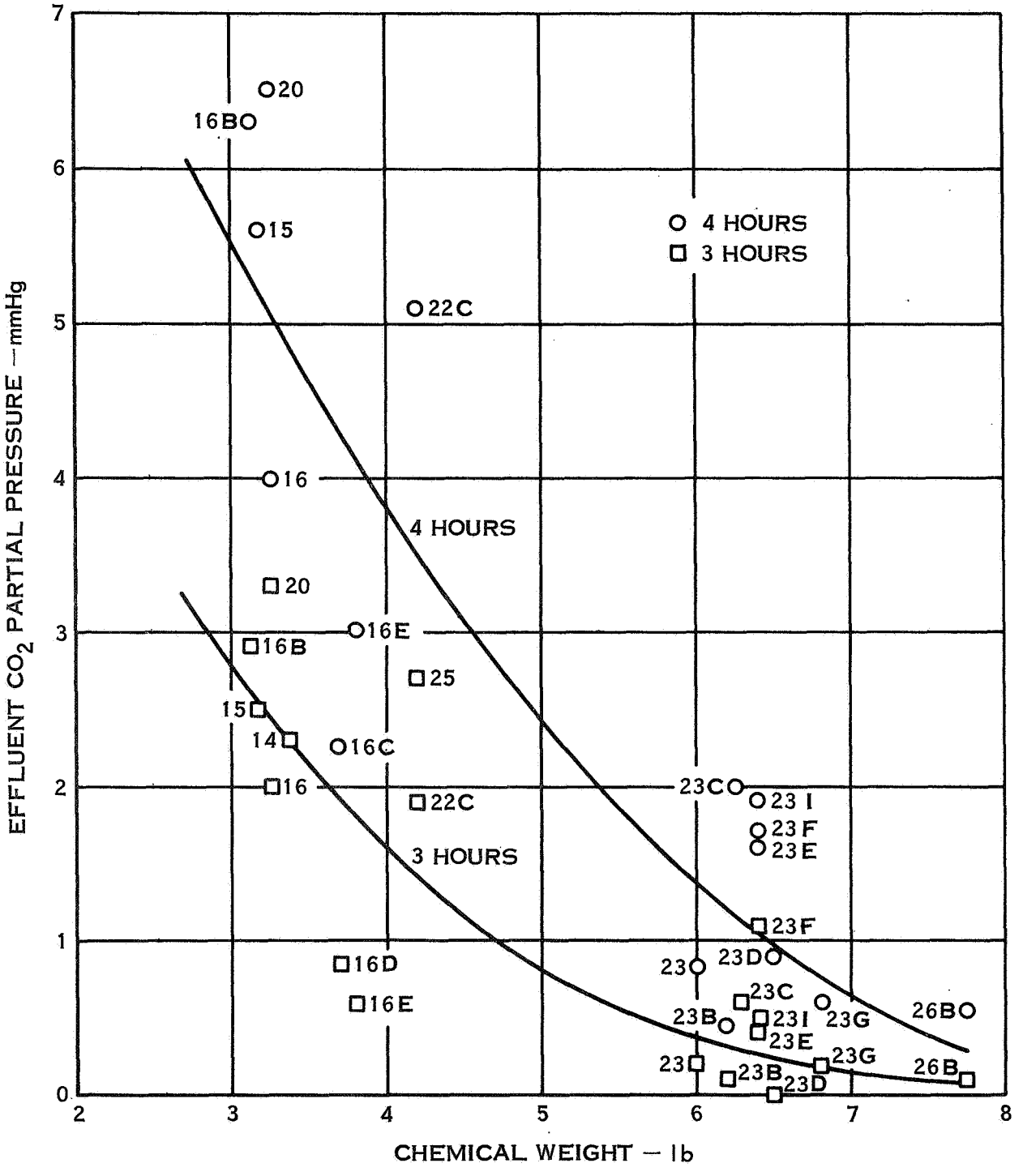

Figure 5-18. Effluent Carbon Dioxide Partial Pressure as a Function of Chemical Weight

5.4 (Continued)

removal rate of 0.39 lb/hr, this represents a removal efficiency decrease of only 0.2%. The nature of the curves in Figure 5-18 show that added chemical weight results in only slight improvement in carbon dioxide removal.

Oxygen performance curves are presented in Figures 5-19, 5-20, and 5-21. Figure 5-19 clearly shows the effect of thermal decomposition on the quantity of oxygen produced. The scatter exhibited by the test points is a consequence of the duration that thermal decomposition occured. With no thermal decomposition occurring the total oxygen is essentially independent of the total mass of chemical employed, and is a function only of the particular reactions taking place in the bed. Reaction with 0.39 lb/hr of carbon dioxide can produce 0.14 lb/hr of oxygen. Water vapor at a 70°F dew point, (0.5 lb/hr flow rate for the test conditions), can produce 0.45 lb/hr of oxygen. Therefore, the maximum oxygen evolution rate, without thermal decomposition, is 0.59 lb/hr. Since the carbon dioxide and water vapor reactions are competing, and since some of the carbon dioxide is removed by lithium hydroxide; the maximum evolution rate does not occur.

Figure 5-20 shows that a large percentage of the oxygen produced via thermal decomposition is of no value since the required rate is exceeded and the excess oxygen is vented overboard. For these tests, a far better correlation of the useable oxygen can be made with the maximum bed temperature as shown in Figure 5-22. Data variations are a function of the duration that thermal decomposition occurred and the quantity of chemical that was involved in thermal decomposition. The net result, when thermal decomposition occurs, is a greater useable generation rate than without decomposition as is shown by Figure 5-22. The data presented is for tests with canister 4 and shows that for this form of chemical the oxygen generation rate limit is around 0.15 lb/hr without thermal decomposition.

Figure 5-23 present carbon dioxide performance as a function of the maximum operating bed temperature measured during canister 4 tests. Two curves are shown. The first represents the minimum recorded performance and the other is an average of the five tests which utilized the two cooling coils in canister 4. These five tests are MSC-23E through MSC-23J, with the exception of MSC-23H which was not cooled. The data shows the importance of having good bed temperature control.

5.5 Inlet Dew Point Effect

An increase in the inlet dew point provides an additional potential for increasing the reaction rate of the lithium peroxide with water vapor. Also, a greater potential for carbon dioxide removal by the lithium hydroxide is created. However, if the thermal decomposition temperature is exceeded the latter potential will not be realized because of the instability of the lithium hydroxide monohydrate at high temperatures.

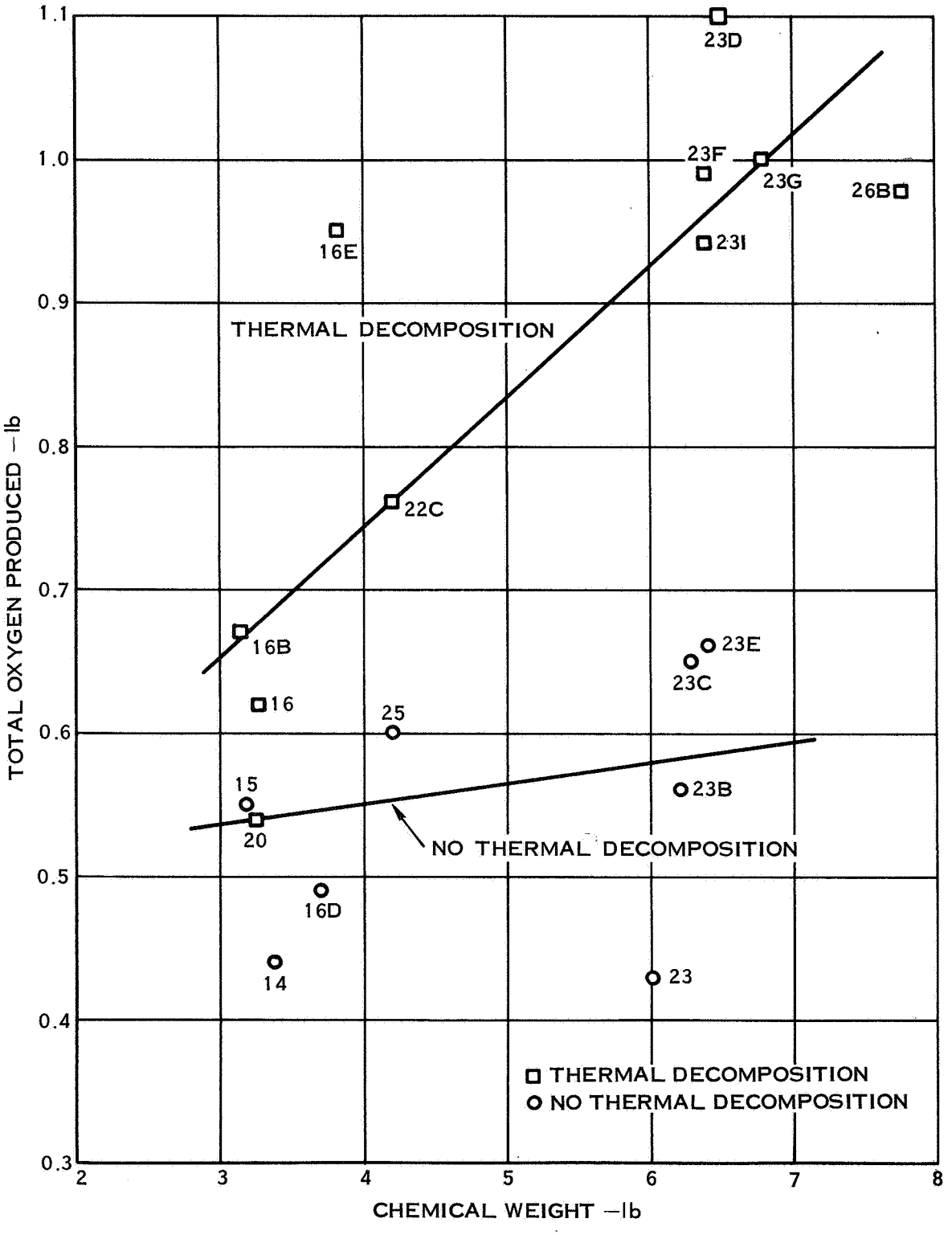

Figure 5-19. Oxygen Production as a Function of Chemical Weight

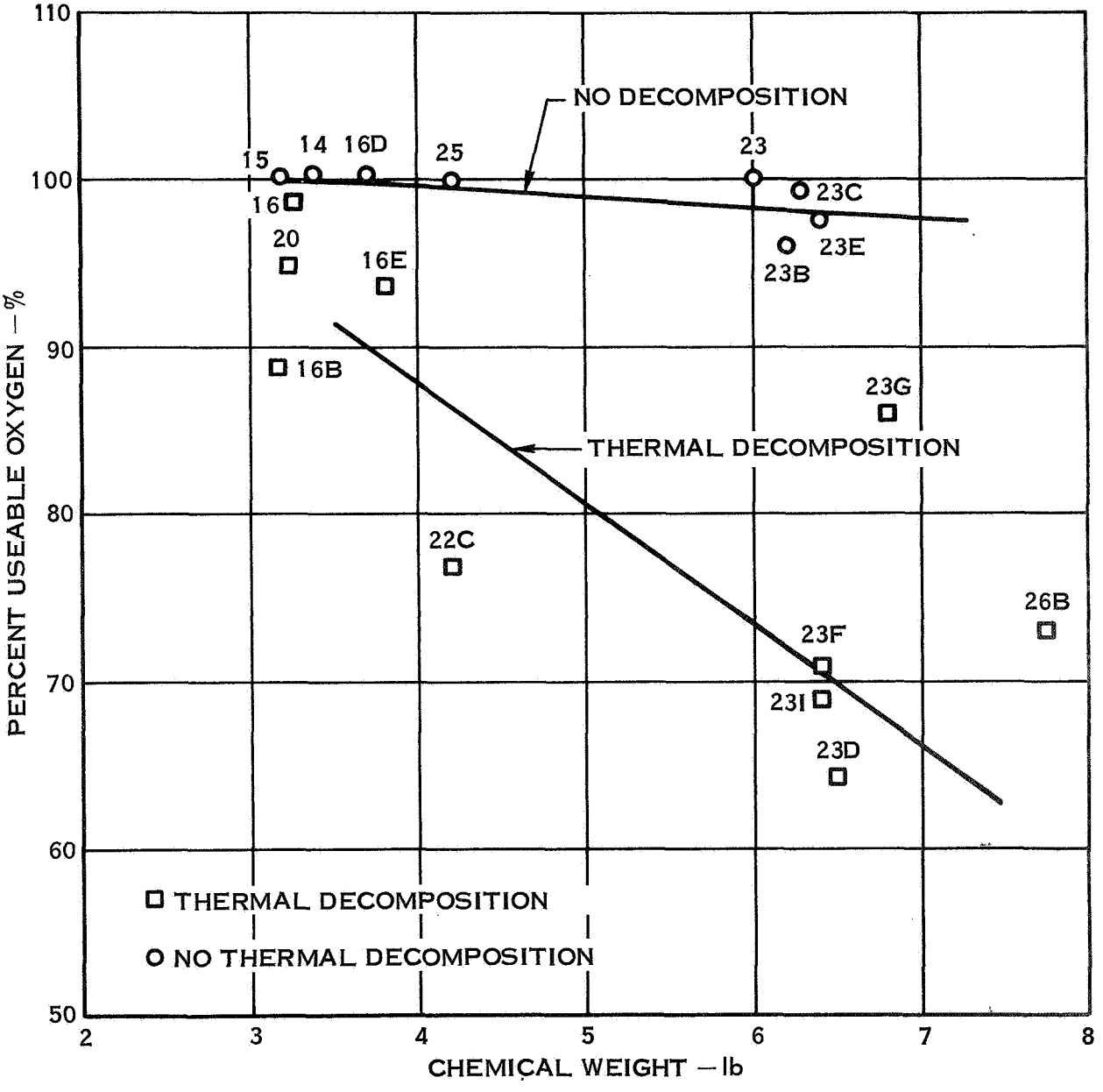

Figure 5-20. Percent Useable Oxygen as a Function of Chemical Weight

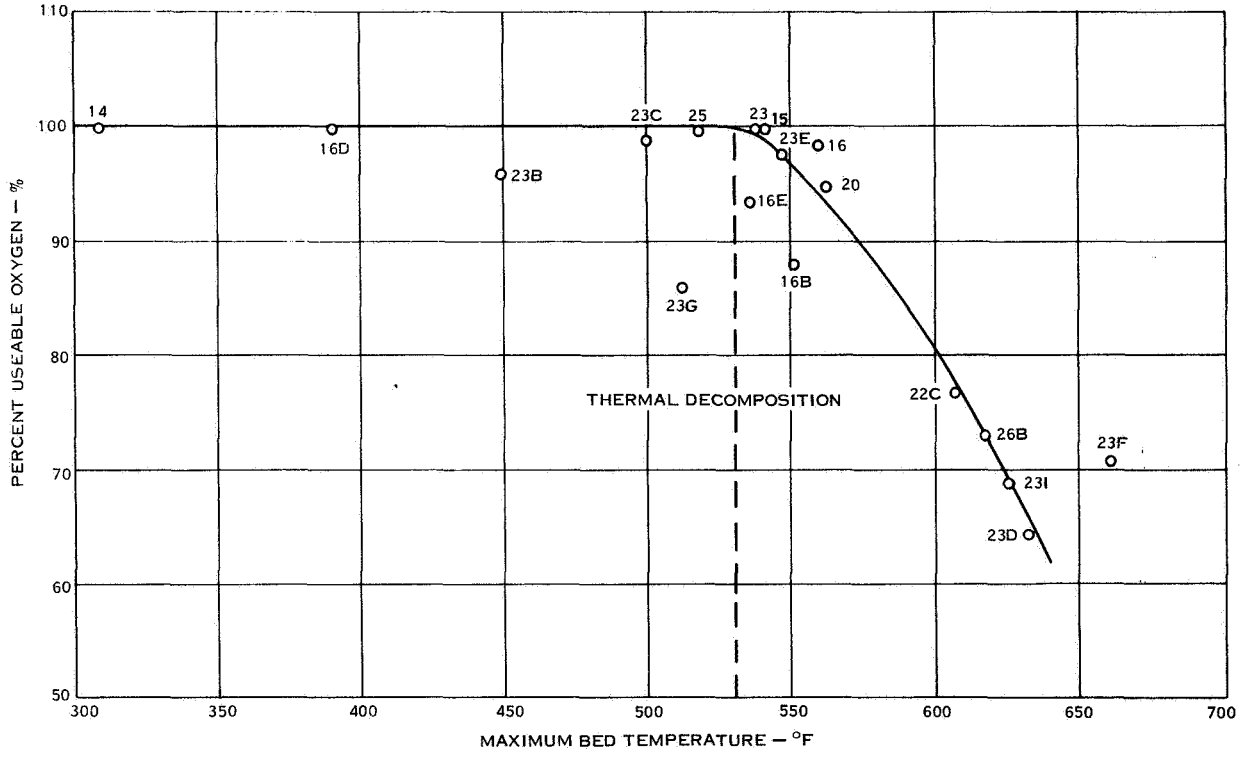

Figure 5-21. Percent Useable Oxygen Produced During 4 Hours of Testing

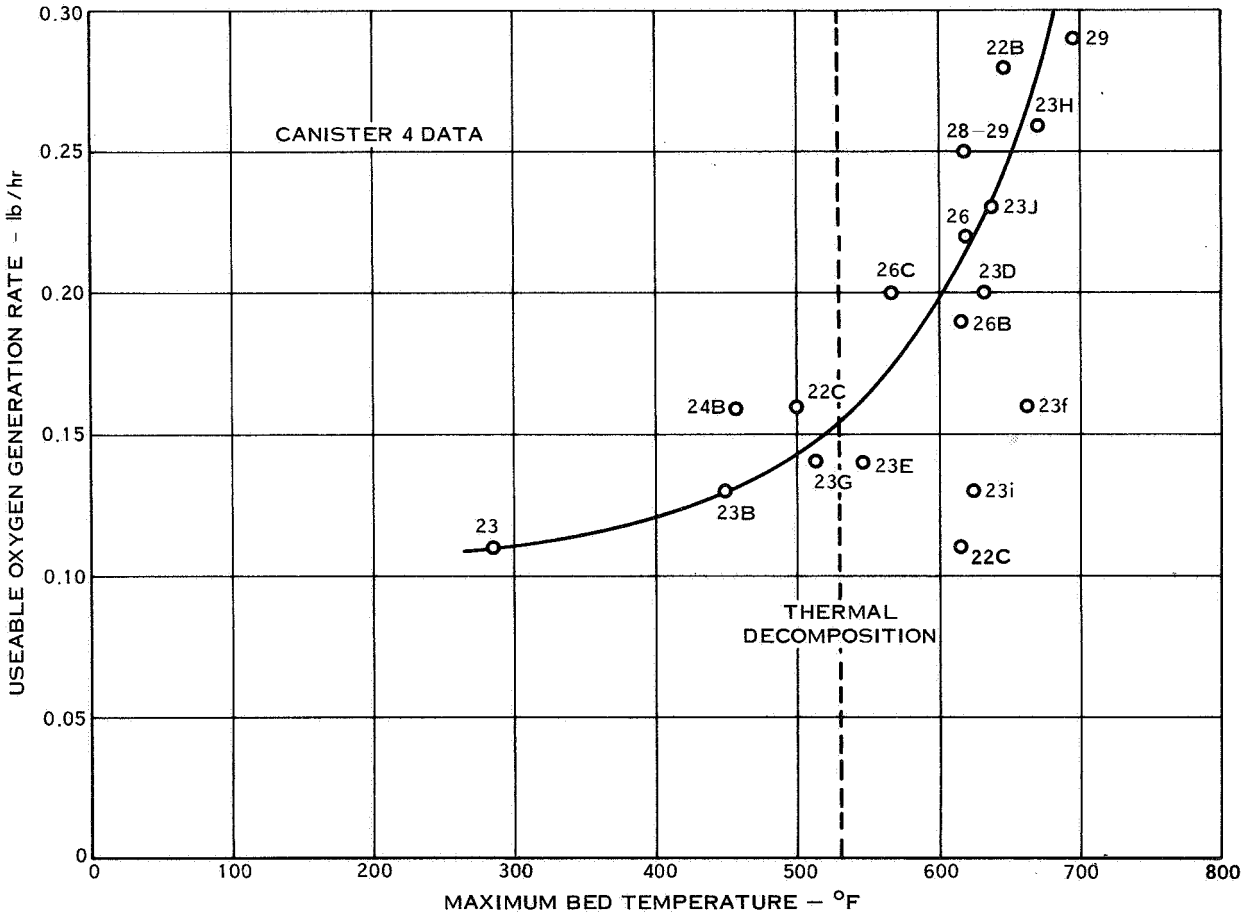

Figure 5-22. Useable Oxygen Generation Rate as a Function of Temperature

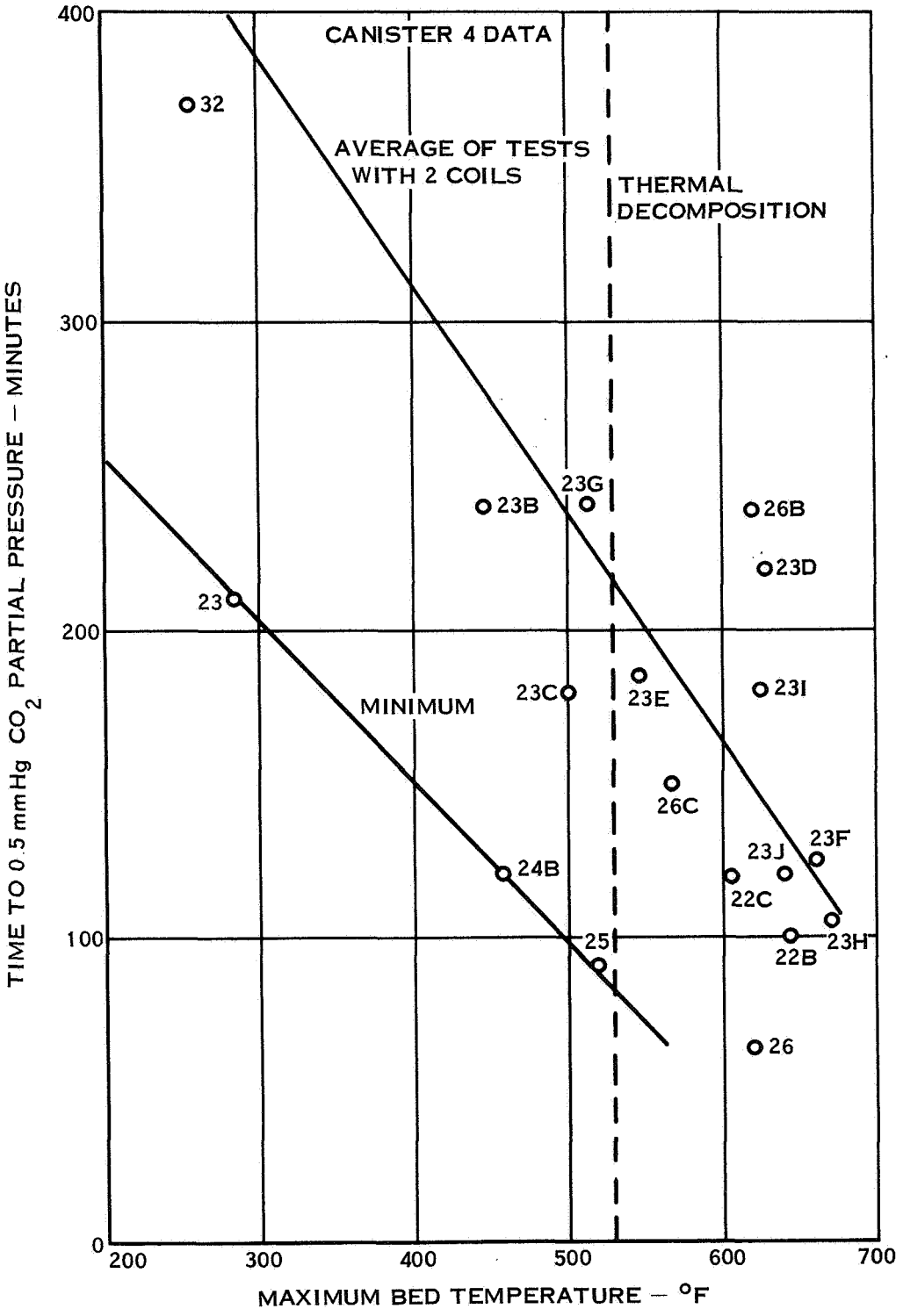

Figure 5-23. Carbon Dioxide Removal Performance as a Function of Temperature

5.5 (Continued)

Figures 5-24 and 5-25 show the oxygen generation rate, effluent carbon dioxide partial pressure, and local bed temperatures for tests MSC-28-29 and MSC-29. Both of these tests were run with an elevated dew point. For the first thirty minutes of the test shown in Figure 5-24, a 50°F dew point was used. When carbon dioxide breakthrough initiated, the dew point was raised to 85°F and the carbon dioxide level dropped.

The oxygen generation rates for both tests have two peaks which occurred when local areas of the bed exceeded the thermal decomposition temperature. Table 5-7 presents a comparison of these tests with tests having nearly equivalent bed temperatures but run with a 70°F dew point. Oxygen generation increased an average of 40 percent due to the dew point increase and the effluent carbon dioxide partial pressure increased by a factor of three.

TABLE 5-7

DEW POINT EFFECT ON PERFORMANCE

Test No.	Weight (lb)	Inlet Dew Point (°F)	Max. T. (°F)	Total O_2 After 4 Hours (lb)	Effluent P_{CO_2} After 4 Hours (mmHg)
MSC-28-29	6.29	84.	696.	1.42	4.7
MSC-29	6.40	84.	692.	-	-
MSC-23D	6.50	70.	633.	1.10	1.0
MSC-23F	6.40	70.	662.	0.99	1.8
MSC-23I	6.40	70.	626.	0.94	1.5

To maintain acceptable performance with high dew point conditions, the cooling must maintain the bed temperature below the thermal decomposition temperature.

5.6 Conclusions

The following conclusions can be reached, based upon the lithium peroxide test program:

1. Decreasing the chemical bulk density increases both the carbon dioxide removal and oxygen generation life of lithium peroxide.

2. The largest face area tested provided the best carbon dioxide performance life.

3. Thermal decomposition of the chemical provides optimum oxygen yields.

4. Thermal decomposition of the chemical deters carbon dioxide removal via a combination of producing lithium oxide which is too dense to efficiently remove carbon dioxide or by heating the lithium hydroxide monohydrate above its temperature for stable operation.

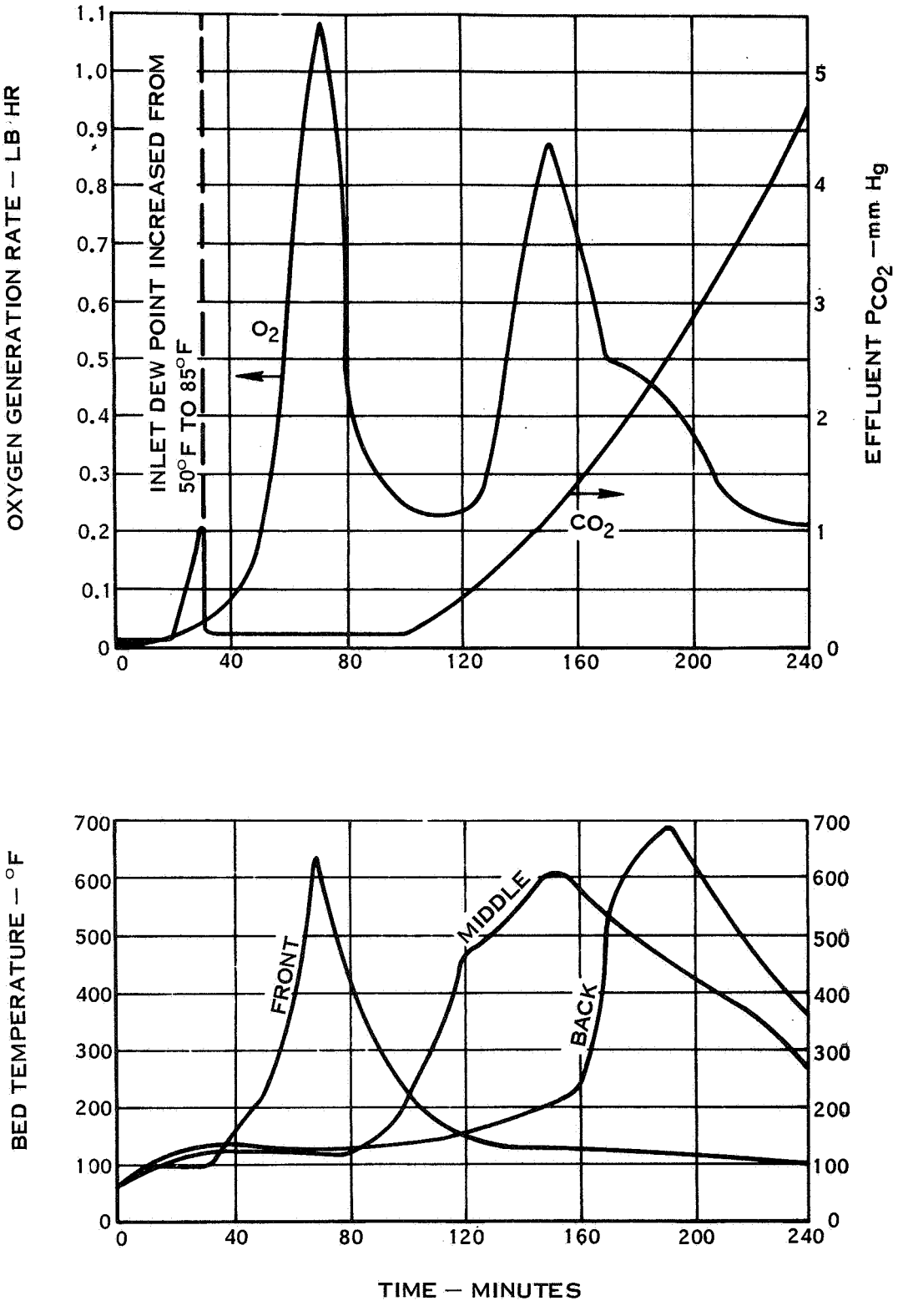

Figure 5-24. High Dew Point Results (Test MSC-28-29)

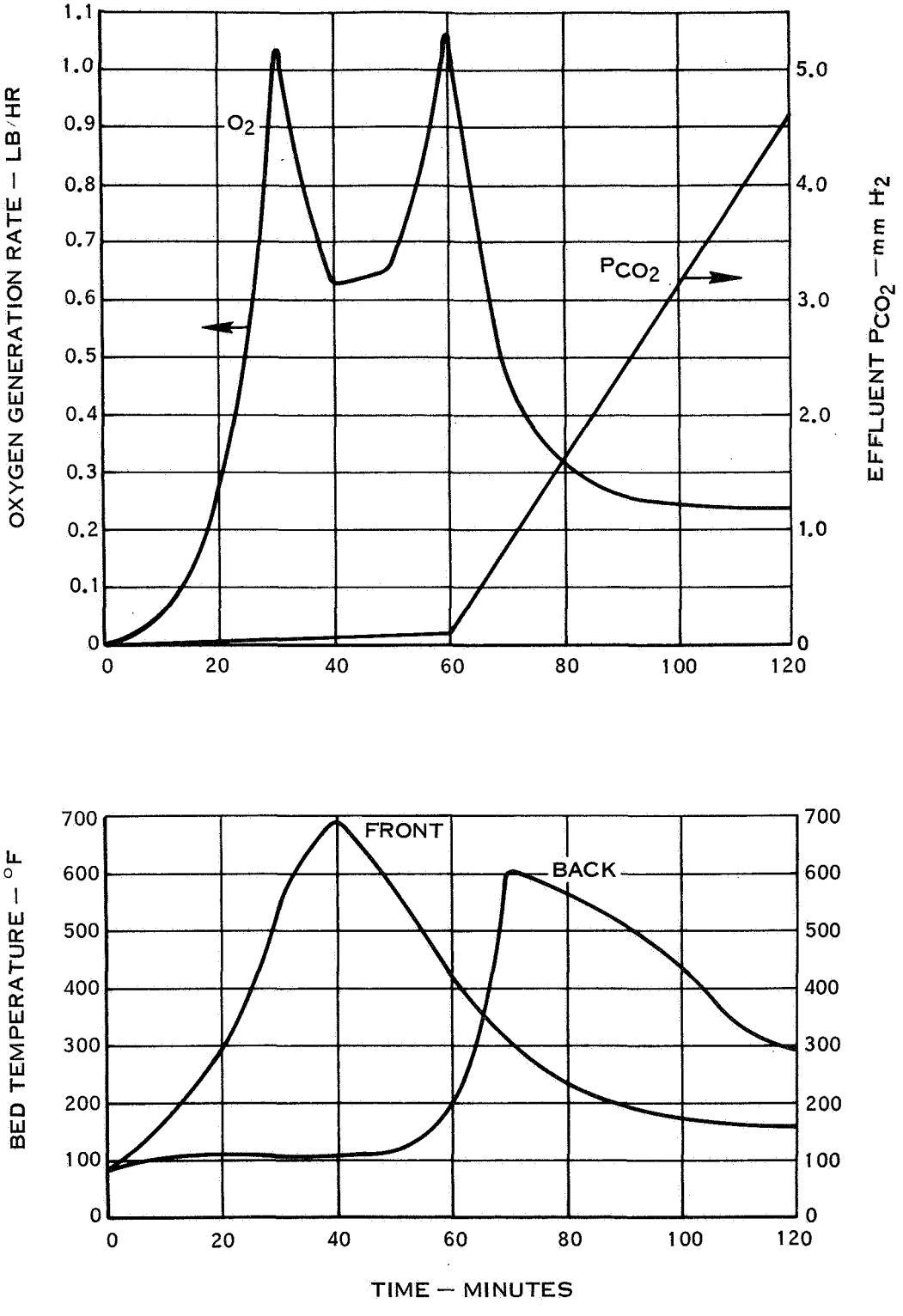

Figure 5-25. High Dew Point Test Results (Test MSC-29)

5.6 (Continued)

5. The addition of 2% nickel sulfate catalyst lowers the thermal decomposition temperature from 570°F to 530°F.

6. The lithium peroxide bed must be maintained below 550°F for maximum performance.

7. Increases in the quantity of lithium peroxide provide a slight increase in carbon dioxide removal performance but virtually no increase in oxygen evolution.

8. The most significant parameter for lithium peroxide operation is bed temperature. Control of this parameter is required to maintain performance.

9. Further development of a lithium peroxide system for application to a portable life support system is warranted.

5.7 System Comparison

The most promising candidate systems to provide oxygen supply and carbon dioxide control for the next generation portable life support system are the lithium hydroxide/oxygen and lithium peroxide/oxygen systems. In both cases, gaseous oxygen is stored at 7500 psia.

These systems have been sized for a four (4) hour EVA mission at an average metabolic rate of 2000 BTU/hr. with the outlet partial pressure of carbon dioxide maintained below 0.5 mm Hg. Sizing of the lithium hydroxide/oxygen system includes a 20% penalty for performance degradation after a hot soak which is based on Apollo EMU PLSS test data.

Figures 5-26 and 5-27 depict the effect of EVA mission duration upon candidate system volume and weight while Figures 5-28 and 5-29 present vehicle weight and volume penalty imposed by these systems as a function of the number of EVA missions planned. These figures illustrate the following: the combined oxygen supply/carbon dioxide control system utilizing lithium peroxide has a decided volume and weight advantage (11% volume and 23% weight advantage for a four hour mission), on a system basis, over the system utilizing lighium hydroxide; on a space vehicle basis, the system utilizing lithium peroxide also has a weight and volume advantage over the system utilizing lithium hydroxide which becomes increasingly more significant as the number of EVA missions increase.

The dotted curves in Figure 5-26 through 5-29 indicate Hamilton Standard's best estimates for potential improvements to system volume and weight which can be accomplished through further development of lithium peroxide.

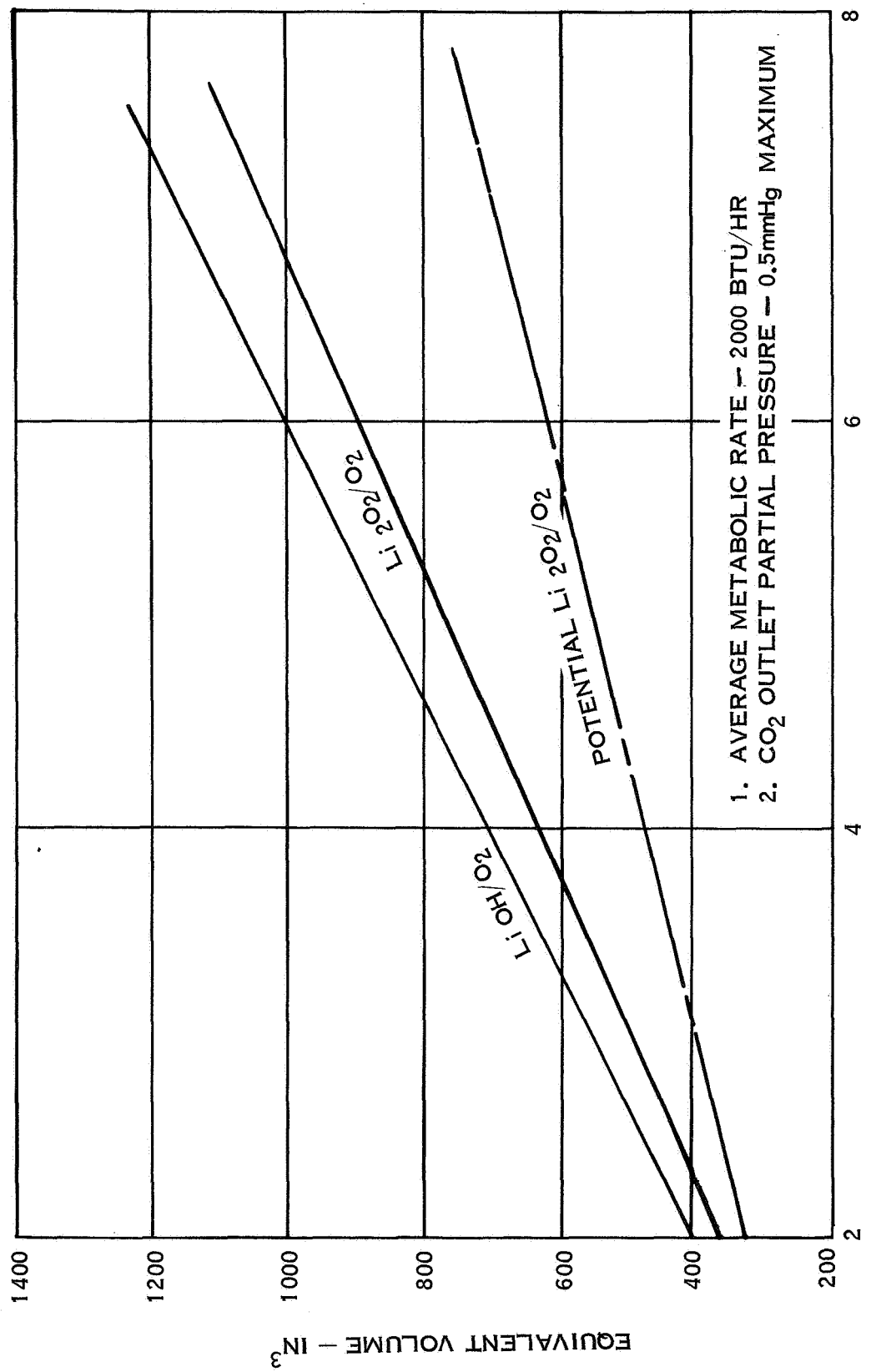

Figure 5-26. System Equivalent Volume vs Mission Duration

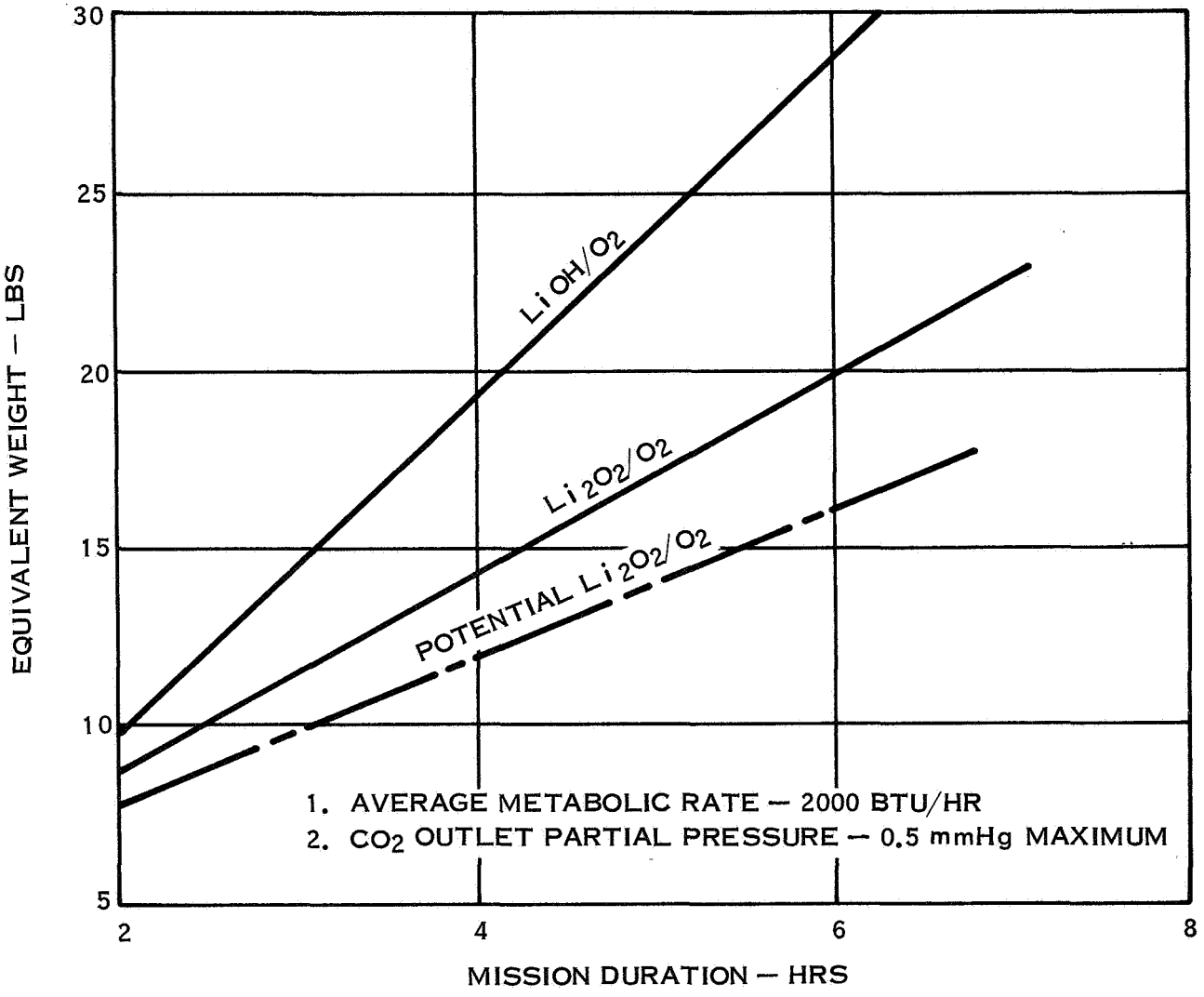

Figure 5-27. System Equivalent Weight vs Mission Duration

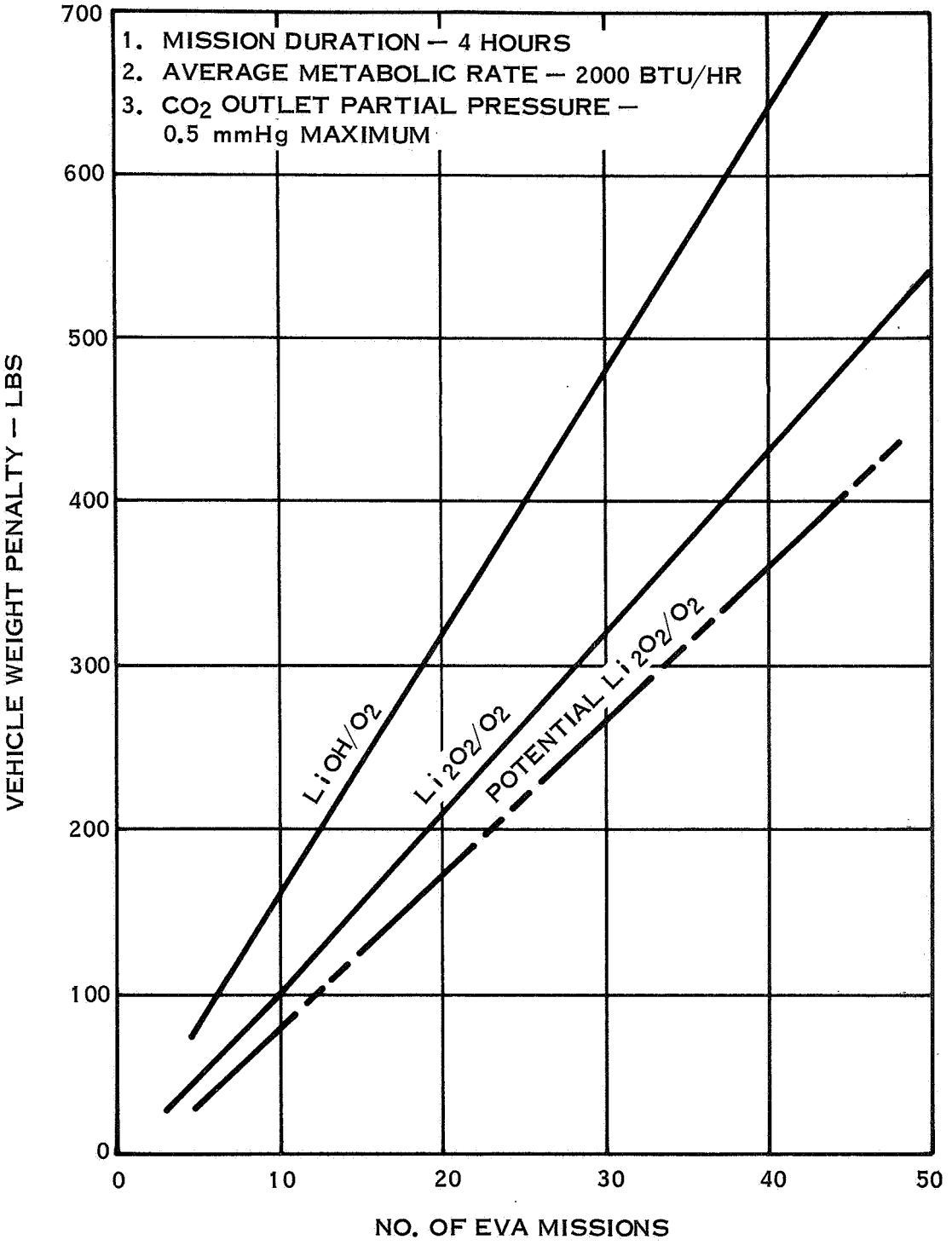

Figure 5-28. Vehicle Weight Penalty vs No. of EVA Missions

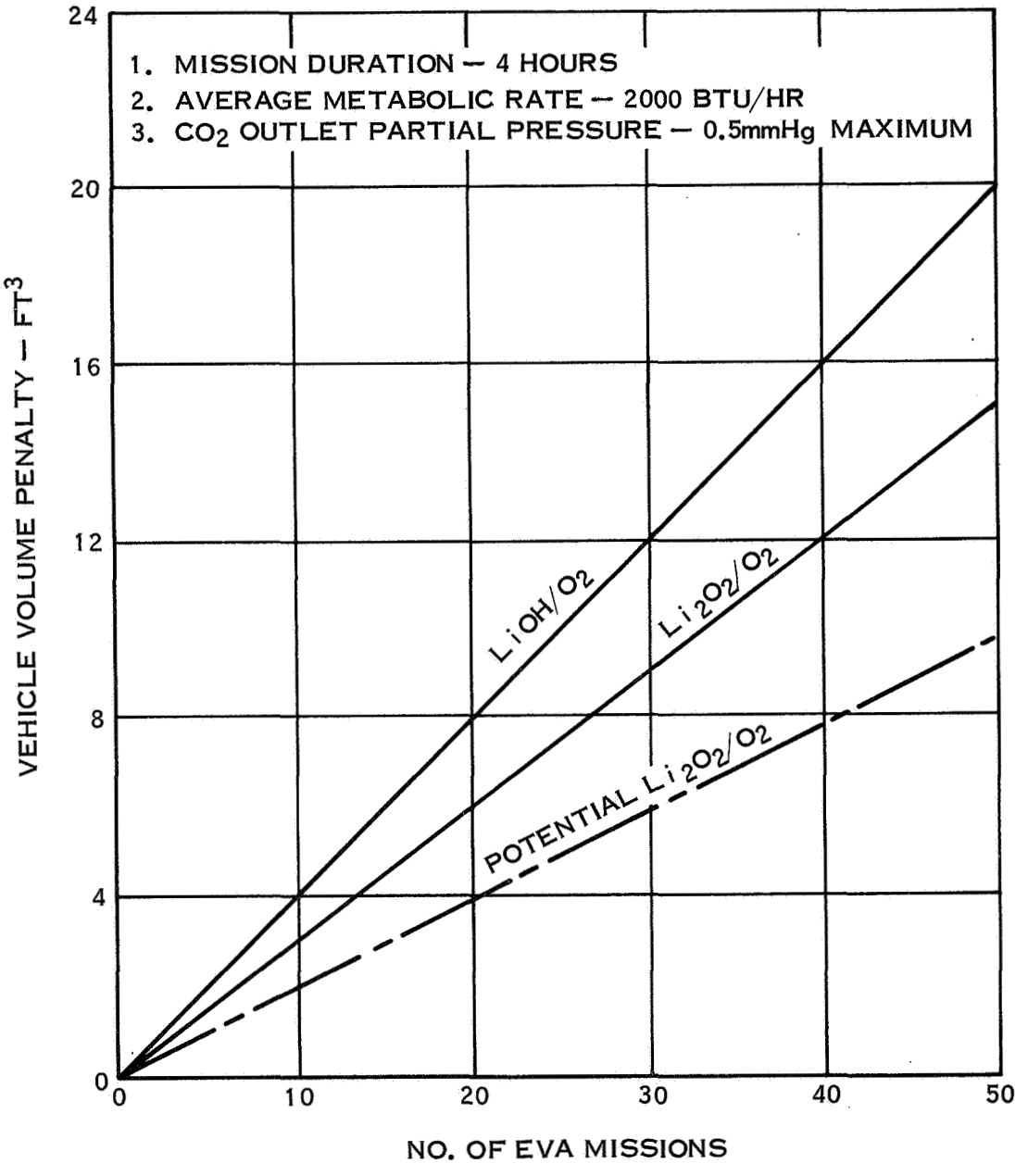

Figure 5-29. Vehicle Volume Penalty vs No. of EVA Missions

6.0 RECOMMENDED FUTURE EFFORT

This program has demonstrated that the operational bed temperature is the most significant parameter affecting lithium peroxide performance. The program recommended for future effort responds to the further investigation of the effect of bed temperature in the following two ways:

1. By performing further catalyst investigations in an effort to identify a catalyst which will cause a high rate of oxygen evolution at lower bed temperatures (250 - 400°F).

2. By performing an evaluation to identify the optimum technique for controlling the operating bed temperature.

The following test program is recommended for future lithium peroxide development effort.

6.1 Test Program

The test program, which has a total of 84 tests, is composed of the following set of test series.

a. Catalyst Evaluation - Tests will be conducted to evaluate lithium peroxide performance when catalyzed with manganese oxide (MnO), iron sulfate ($FeSO_4$), and manganese dioxide (MnO_2). The performance of these catalyzed forms will be compared with the previously generated data using the nickel sulfate ($NiSO_4$) catalyst to determine the best catalyst. Composite beds using various combinations of the catalyzed granules will also be tested if complementing performance differences are observed. Fundamentally, the purpose of catalyst addition is to promote oxygen evolution and an ideal catalyst would provide this function far below the thermal decomposition temperature of the lithium peroxide. IR&D tests with lithium peroxide catalyzed with manganese oxide and iron sulfate have shown encouraging oxygen evolution rates and appear to be attractive candidates for a composite bed. Recent work reported in AMRL-TR-68-57 showed that lithium peroxide catalyzed with manganese dioxide produced 5.5 times the oxygen evolution rate of uncatalyzed lithium peroxide. At the higher temperatures that occur in an advanced portable life support system application, the oxygen generation rate improvement should be substantially better.

   A total of 25 tests maximum will be run for this series. All tests will be run at the 2000 BTU/hr condition, except for the last three tests which will be conducted with the best chemical at the variable profile condition. The effluent gas from three tests using the best chemical will be sampled periodically and analyzed to assure that its composition is pure. The best chemical evaluated during this test series will be used for all subsequent testing.

6.1 (Continued)

This test series is broken down as follows:

1. Four tests will be conducted with each catalyzed form (MnO, $FeSO_4$, and MnO_2) at a constant metabolic rate of 2,000 Btu/hr for a total of 12 tests. For these tests two different degrees of cooling will be employed for two tests each to establish an optimum region of operating bed temperature for each type of catalyst and to obtain cooling requirement data which will be used to design heat transfer devices employed in the bed cooling evaluation test series.

2. Two sets of composite beds using combinations of the catalyzed material (e.g. 50% MnO/50% $FeSO_4$) will be tested twice for each mixture. During one test for each composite a high degree of cooling will be employed; during the other a low degree of cooling. A repeat of the test with each mixture which shows the best performance will be made. A total of six tests will be run with composite beds.

3. Three variable metabolic profile tests will be run with the catalyzed chemical or composite bed which demonstrated the best performance. During these tests the effluent gas will be sampled at 30 minute intervals and analyzed to assure that it is pure and contains no toxic or noxious constituents.

b. Bed Cooling Evaluation - Tests will be conducted to establish an optimum technique for maintaining the bed temperature within the desired range. Both passive and dynamic methods will be employed and evaluated. A total of 20 tests maximum will be run during this series. Tests will be run at baseline conditions, except the last three which will employ the variable profile with the best control technique. A thorough analysis will be made of each cooling system tested to assure that it is feasible from the total system standpoint and that it is compatible with both the system and crewman interfaces. The best cooling technique will be used for all subsequent tests.

This test series is composed of the following tests.

1. Passive Cooling - For these, the canister will be mounted on a heat sink device which simulates the Apollo EMU PLSS sublimator in operation. The tests will be performed both with and without internal conductive members with two tests conducted for each type and a total of four tests for this series.

6.1 (Continued)

2. Passive/Dynamic Cooling - For these tests, one or more surfaces of the canister will perform the function of a heat exchanger to remove the generated heat. As with the solely passive system, beds will be tested both with and without internal conductive members for two tests each and a total of four tests for the series.

3. Dynamic Cooling - The canister tested for these tests will have internal cooling coils through which the coolant flows. The coils will be tested in both the perpendicular to gas flow and parallel to gas flow attitudes and two distinct levels of coolant inlet temperature will be employed. A total of eight tests will be conducted; two for each combination of cooling coil attitude and coolant inlet temperature.

4. One repeat test will be conducted for the cooling technique which has shown the best performance and has been judged to be compatible with all system and crewman interfaces.

5. Three variable metabolic profile tests will be run using the optimum cooling concept to verify its performance under variable operating conditions.

c. Procedural Tests - Tests will be conducted to establish the criteria for and verify the validity of specifications which will be formalized for material handling, canister loading, granule manufacturing, and quality control. The sum total for this test series will be 22 tests, all at baseline conditions, and will be made up of the following tests.

1. Manufacturing Process - The granule manufacturing process will be closely monitored to accumulate the information needed to generate a formal procedure. Two distinct granule sizes, each made with an appropriate percentage of two different binders, will be procured and tested twice for each combination of granule size and binder for a total of eight tests. These tests are to verify the performance repeatability of granules manufactured per the process specification.

2. Canister Loading Process - Canisters will be loaded, one-third of a bed at a time, and vibrated at three distinct vibration levels. Two tests will be run for canisters loaded at each distinct vibration level to determine the optimum loading technique. A total of six tests will be performed and a formal loading procedure will be generated based upon these test results.

6.1 (Continued)

3. Quality Control - A formal procedure will be generated to specify the required lithium peroxide powder and granule purity, the level of inspection required, and the handling and storage requirements. Five tests will be run on material which has been accepted per the specification to verify its adequacy. For all of these tests the effluent gas will be sampled and analyzed to verify that no toxic or noxious constituents are present. Further, for two of these tests, charcoal (0.36 lb) will be loaded into the lithium peroxide canister and a dacron filter (as used in the PLSS lithium hydroxide canister) will be employed to evaluate its adequacy to prevent migration of lithium peroxide or lithium hydroxide dust downstream. Particular attention will be paid, during the gas analysis, to determine the presence of any lithium peroxide or lithium hydroxide dust and to determine if the charcoal is being oxidized. Three tests will be performed on lithium peroxide material which has been stored for three months per the storage specification to verify its adequacy. A total of eight tests will be conducted to establish the level of quality control needed.

d. Hot/Cold Soak Evaluation - Two tests each for lithium peroxide which has undergone hot and cold soak conditions per the Apollo EMU PLSS specification requirements will be run at baseline conditions to verify that these conditions do not degrade lithium peroxide performance. This series has a total of four tests.

e. Composite Bed Evaluation - A total of eight tests will be conducted during this evaluation. Three distinct percentages (5, 7.5, 10%) of potassium superoxide (KO_2) will be added to the lithium peroxide bed to establish the optimum percentage of potassium superoxide to provide the oxygen needed during the early portion of the mission. Each percentage of potassium superoxide will be tested twice. Two tests will be conducted with the best potassium superoxide percentage and 0.36 lb of charcoal in the lithium peroxide bed. Filtration will again be employed for these tests and this effluent gas will be sampled and analyzed.

f. Off-Design Evaluation - The following off-design tests, with potassium superoxide present if its benefit has been verified, will be conducted to obtain additional operational information. A total of nine tests will be run during this series.

1. Inlet Water Vapor Variation - A total of three tests at baseline conditions will be conducted with the following levels of water vapor flow rate: no water vapor present, 50°F and 85°F dew points.

2. Inlet Carbon Dioxide Variation - A total of four tests at baseline conditions will be run for the following levels of carbon dioxide flow rate: no carbon dioxide, carbon dioxide corresponding to metabolic rates of 500, 1000, and 3000 Btu/hr.

6.1 (Continued)

3. Total Flow Rate Variation - A total of two tests will be run, using the variable metabolic profile, with the system flow rate at five cfm for one test and nine cfm for the other.

REFERENCES

1. A Study of The Application of Lithium Chemicals to Air Regeneration Techniques in Manned, Sealed Environments, AMRL-TDR-64-1, M. M. Markowitz and E.W. Dezmelyk, Foote Mineral Co., February, 1964.

2. Use of Lithium Peroxide as an Agent for Purification of Tainted Air (French Translation), H. Ducros and S. Berranger, Foreign Technology Division, Wright Patterson Air Force Base, January, 1966.

3. Application of Lithium Chemicals For Air Regeneration of Manned Spacecraft, AMRL-TR-65-106, R.O. Bach, W.W. Boardman, Jr., and J.W. Robinson, Jr., Lithium Corp. of America, June, 1965.

4. Configuration Investigation For Lithium Oxide Carbon Dioxide Control Systems, AMRL-TR-67-62, D.A. Boryta and E.W. Dezmelyk, Foote Mineral Co., October, 1967.

5. Contribution of Water To The Kinetics of CO2 Absorption By LiOH, D.A. Boryta, Project No. 105-37-210, Report No. 37-4-67, Foote Mineral Co., September 22, 1967.

6. Interaction of Lithium Peroxide With Water Vapour And Carbon Dioxide, K.I. Selezneva, Russion Journal of Inorganic Chemistry, (820-823), August, 1960.